Evaluation of the activity of antibiotics and adjuvant strategies against dual species biofilms in the context of cystic fibrosis

Zhifen Wang

Supervisor: Françoise Van Bambeke

Cellular and molecular pharmacology, Louvain Drug Research Institute

Université catholique de Louvain

Jury

Prof. Anne des Rieux (Chair)

Advanced Drug Delivery and Biomaterials, Louvain Drug Research Institute, Catholic University of Louvain, Belgium

Prof. Rita Vanbever (Secretary)

Advanced Drug Delivery and Biomaterials, Louvain Drug Research Institute, Université catholique de Louvain, Brussels, Belgium

Prof. Françoise Van Bambeke (Supervisor)

Cellular and Molecular Pharmacology Laboratory, Louvain Drug Research Institute, Université catholique de Louvain, Belgium

Prof. Aurelie Crabbe

Laboratory of Pharmaceutical Microbiology, Universiteit Gent, Gent, Belgium

Prof. Barbara Kahl

Institute of Medical Microbiology, Universitätsklinikum Münster, Münste,r Germany

Prof. Christiane Knoop

Erasme Hospital, Université libre de Bruxelles, Brussels, Belgium

Prof. Hector Rodriguez-Villalobos

Department of Microbiology, Cliniques universitaires Saint-Luc, Brussels, Belgium

Acknowledgements

Life's journey spans countless chapters, and the pursuit of a PhD is merely one among them. Along this path, I've crossed paths with kind-hearted individuals whose support, alongside that of a wonderful team and an inspiring boss, has rendered even the most formidable challenges inconsequential. As this journey comes to an end, I am deeply grateful to all these kind people, as well as the financial support provided by the Chinese Scholarship Council (CSC) PhD grant, a grant from the King Baudouin Foundation (Fonds Forton), and the Belgian Mucovereniging/Association Muco.

Firstly, I would like to express my heartfelt gratitude to my supervisor, **Françoise Van Bambeke**. She provided me with the opportunity to embark on the journey of pursuing a PhD and has been my guiding light throughout these four years. Her unwavering encouragement, support, and belief in me have been invaluable along this path. Additionally, I am grateful for her patience at the beginning of this journey, and for her friendly and kind demeanor.

I extend my sincere gratitude to the members of my thesis committee: **Prof. Anne des Rieux**, **Prof. Rita Vanbever**, **Prof. Hector Rodriguez-Villalobos**, and **Prof. Christiane Knoop**. You were not just members of the jury; your support and encouragement were instrumental in guiding me to the culmination of this journey. Without your invaluable assistance, I wouldn't have reached this point.

I would also like to express my gratitude to the external members of the jury, **Prof. Barbara Kahl** and **Prof. Aurélie Crabbe**. I am very thankful that you agreed to review my thesis. I appreciate Prof. Barbara Kahl for making the considerable journey to be present at my defense.

As I step into the lab, I feel compelled to express my deepest gratitude to my esteemed office colleagues. The memories we've shared are truly precious, and I am immensely thankful for each one. Foremost among them, I extend my heartfelt appreciation to **Dr. Hélène Thirot** and **Audrey Comein**, my esteemed initial colleagues. Your generosity, unwavering assistance, constant encouragement, and steadfast support have been indispensable to me. I am particularly grateful to **Gwenaëlle Mahieu** for her prompt responses whenever I needed assistance. My profound appreciation extends to **Jad Atrissi** and **Randy Buzisa Mbuku** for their unwavering encouragement and support, as well as to **Paria Rasouli**, **Ahmad Sleiman**, **Dr. Perrin Ngougni**, **Dr. Tiep Nguyen**, **Perrine Evrard**, **Aline Lardinois**, **Alexandra Degraeve**, **Emilia Hoste**, **Steven De Soir**, **and Jessica Solis** for their camaraderie and assistance. I would also like to thank **Dr Albert Ruiz Sorribas**, **Dr Negar Mozaheb** and **Dr Gang Wang** for their invaluable help with the experiments. To **Dr Gert-Jan Wijnant** for correcting the pronunciation of the University of Louvain and the University of Leuven, and for his beer. To Dr. **Frédéric Goormaghtigh** for his invaluable advice. Furthermore, I express my sincere appreciation for the technical support provided by **Virginie Mohymont**, **Murielle Callier**, **Vasileios Yfantis**, and **Michael Socpa Yongkeck**. Your contributions have been instrumental to the success of my endeavors, and I am immensely grateful for your unwavering support.

I extend my heartfelt gratitude to **Prof. Joseph Lorent** and **Prof. Weidong Pan** for their unwavering assistance and unconditional support. Additionally, I am thankful to **Prof. Marie-Paule Mingeot-Leclercq** for her warm smile and constant encouragement each day. My appreciation also goes to **Prof. Paul M. Tulkens** for his encouragement and support. Furthermore, I would like to **thank Prof. Maria Veiga da Cunha** and **Prof. Patrick Van Der Smissen** for their friendly assistance during my work.

Going to my daily life, I am grateful for the presence of my friends**: Mandeep Kaur**, **Harsh Goyal**, **Hafiz Abdul Khaliq, Yonghua Tan, Yuxiang Duan, Tianjiao Wei, Luyao Xu, Ying Liu, Qiqi Dong, Hafsa Ameraoui, Manjitha Parambath, Lei Hu, Qian Gao, YaZhou Liu, JunJie Lan, Jiaqi Fang, Cristina Gan Oria, and Wunan Zhang**. They have made Belgium feel like home to me, providing unwavering support and companionship whenever I need it. I would also like to extend my heartfelt thanks to my neighbors, **Weiwei Wang** and **Ioana Timofte**, for their warmth and kindness.

Finally, I am profoundly grateful to my family. Their unconditional love, constant encouragement, and unwavering support have been the cornerstone of my journey. I would also like to extend special thanks to Ying Liu, a remarkable individual, for his steadfast support, encouragement, and love.

Table of contents

Abstract

Cystic fibrosis, a genetic disorder, causes stick mucus stagnation in patients' airways, promoting bacterial colonization and biofilm formation. The primary pathogens, *Staphylococcus aureus* (*S. aureus*) and *Pseudomonas aeruginosa* (*P. aeruginosa*), exhibit a sequential colonization pattern, with the former often preceding the latter. Notably, both species are frequently co-isolated from the same patients.

Our objective was to establish a dual-species biofilm applicable to clinical isolates and to evaluate antibiotic activity in combination with enzymes or phages against biofilms.

We demonstrated the stability of *S. aureus* and *P. aeruginosa* over time in biofilms developed by reference strains or clinical isolates if *S. aureus* is inoculated before *P. aeruginosa*. We observed a symbiotic relationship between co-isolated *S. aureus* and *P. aeruginosa*, which was attributable to reduced *P. aeruginosa* virulence and increased *S. aureus* tolerance.

We then showed that these dual species antibiotics are particularly reluctant to antibiotic activity. We therefore tested the potential interest of combining them with enzymes acting on the constituents of the matrix of the biofilms or with phages. We found that DNase I (already administered to patients with CF to fluidify mucus) and alginate lyase significantly enhanced antibiotic activity against the dual-species biofilm compared to antibiotics alone but that they need to be used at high concentrations. We also found that a cocktail containing one phage active on *S. aureus* and one phage active on *P. aeruginosa* (phage ISP and phage PSP3) showed additive effect to antibiotics against dual species biofilm formed by reference strains.

Collectively, these results demonstrate that cross-adaptation in coisolated *S. aureus* and *P. aeruginosa* enhances bacterial survival in challenging environments. Additionally, enzymes or phages can serve as effective adjuvants, boosting antibiotic activity against biofilms in the context of cystic fibrosis, although further work is needed to optimize their conditions of use in order to maximize their activity.

List of abbreviations

AgNPs	Silver Nanoparticles
agr	accessory gene regulator
AI-2	autoinducer 2
AprA	alkaline protease
ASM+	Artificial sputum medium
ATP	adenosine triphosphate
BHL	N-butanoyl-L-homoserine lactone
CF	Cystic fibrosis
CFTR	Cystic fibrosis transmembrane conductance regulator
ClfA	clumping factor A
ClfB	clumping factor B
cyclic-di-GMP	cyclic diguanylate monophosphate
DNase I	Deoxyribonuclease I
eDNA	extracellular DNA
ENaC	epithelial sodium channel
EPS	extracellular polymeric substances
FnbpA and FnbpB	fibronectin-binding proteins A and B
HCO_3^-	bicarbonate
HHQ	2-heptyl-4-quinolone

Hla	alpha-toxin
Hlg	gamma-hemolysin
HQNO	2-heptyl-4-hydroxyquinoline N-oxide
HSLs	homoserine lactones
ICUs	intensive care units
IQS	2-(2-hydroxyphenyl) -thiazole-4-carbaldehyde
LasB	elastase B
LB	lysogeny broth
LPS	lipopolysaccharide
MDR-PA	Multiple-drug resistant P. aeruginosa
MHB-Ca	cation-adjusted Mueller Hinton Broth MHB-Ca
MIC	Minimal inhibitory concentrations
MOI	multiplicities of infection
MSA	Mannitol Salt Agar
MSCRAMMs	microbial surface component recognizing adhesive matrix molecules
NHQ	2-nonyl-4-quinolone
NQNO	2-nonyl-4-hydroxyquinoline N-oxide
NTM	nontuberculous mycobacteria
OdDHL	N-(3-oxododecanoyl)-L-homoserine lactone
PBS	phosphate buffer saline
PCA	phenazine-1-carboxylic acid
PCH	pyochelin
PCN	phenazine-1-carboxamide
PIA	polysaccharide intercellular adhesin
PMN	phagocytosis and neutrophil
PNAG	poly-β-1,6-N-acetylglucosamine

PQS	2-heptyl-3-hydroxy-4-quinolone
PQS	Pseudomonas quinolone signal
PSMs	phenol-soluble modulins
PVD	pyoverdine
PVL	Panton-Valentine leucocidin
PYO	pyocyanin
QS	Quorum sensing
T1SS, T2SS, T3SS, T4SS, T5SS and T6SS	The Type I, II, III, IV, V and VI Secretion System
TMP/SMX	Trimethoprim/Sulfamethoxazole
TSA	Trypticase soy agar
TSST-1	toxic shock syndrome toxin-1
SCV	small colony variants
SpA	Staphylococcal protein A
RC10C10	Mono-rhamnolipids
rhlA	rhamnolipid synthesis
RRC10C10	di-rhamnolipids
1-HP	1-hydroxyphenazine

Chapter I: Introduction

I.1. Cystic fibrosis- Inherited and Multisystem disease

I.1.a. Global overview

Cystic fibrosis (CF) is a monogenetically inherited disease that affects multiple organs, with lung damage being a major contributor to morbidity and mortality in CF patients. The disease is caused by variants in a gene that codes for a chloride channel, specifically the CF transmembrane conductance regulator (CFTR) proteins. These gene variants disrupt the synthesis and function of CFTR protein at the apical membrane of epithelial cells in various organs, leading to ion imbalance and dehydration of the epithelial cell surfaces. This dehydration results in the production of thick and difficult-to-evacuate mucus in the affected tissues [1, 2].

CF is the most prevalent lethal genetic recessive disease mainly affecting Caucasian individuals, with approximately 37,000 cases in North America (32,100 cases in the US), 54,043 in Europe (including 10,907 in the UK and 1,387 patients in Belgium) for the year 2021 [3, 4]. The remaining cases are distributed in Asia, Africa, Australia, and South America [5], totaling 105,000 people worldwide today [4]. Europe has the highest prevalence of CF, particularly in Northern, Northwest, and Central Europe. Of European countries, the highest birth rate is 1 to 1353 in Ireland, and the lowest, 1 to 25000 birth in Finland [6].

Today, 75% of individuals with CF are diagnosed by the age of 31.9 months or earlier, and 54% of the CF population is aged 18 or older. In terms of age distribution,

the ECFSPR 2021 Annual Data Report indicates that slightly more men (53.3%) are affected than women (47.7%).

The therapeutic advancements achieved over the past few decades have substantially heightened the life expectancy of patients, transitioning from a risk of over 70% mortality at birth in the 1930s to a current survival rate surpassing 95%, with an estimated life expectancy of 53 years [7].

Despite CF being a multi-systemic disease, the primary morbidity and mortality stem from lung function failure associated with bacterial infection. Even with interdisciplinary cooperation and treatment advancements, the situation did not significantly change. The lungs of CF patients are colonized by multiple bacteria due to the sticky and thick mucus in the airway, with *Pseudomonas aeruginosa* (*P. aeruginosa*) and *Staphylococcus aureus* (*S. aureus*) consistently being the most prevalent. According to the 2021 Cystic Fibrosis Foundation Patient Registry highlights, the collection of respiratory cultures for each bacterial species decreased compared to 2019. This decline could be associated with decreased in-person clinic attendance and the inability to produce sputum for some individuals, given that 2021 marked the second year of the COVID-19 pandemic and the third year since elexacaftor/tezacaftor/ivacaftor became available for people with CF [4]. Notably, *S. aureus* and *P. aeruginosa* continue to dominate lung infections dramatically (Figure 1).

Bacteria	2019 Percent With Infection	2021 Percent With Infection
 *Pseudomonas aeruginosa*	43%	28%
 *Stenotrophomonas maltophilia*	12%	6%
 Methicillin-resistant *Staphylococcus aureus*	25%	18%
 *Achromobacter xylosoxidans*	6%	3%
 *Burkholderia cepacia* complex	3%	1%
 Nontuberculous mycobacteria	14%	10%
 *Staphylococcus aureus*	70%	64%

Figure 1. Collections of respiratory microbial cultures in 2019 and 2021 (Image adopted from [4])

I.1.b. Historical overview

Some symptom associated CF can be traced back to around 3000 B.C.E., with origins in a folklore ritual tradition involving the cross-licking of newborns and children to detect a salty taste [8]. However, the disease was not well understood until the late of 1930s when a large clinical and pathological study with 49 children with pancreatic fibrosis was conducted by Dorothy H Andersen, a pathologist in Babies' and Children's Hospital in New York.

In her work, she conducted a comprehensive, detailed, and clear pathophysiological study involving 49 autopsies of children, including 22 new cases from her hospital. She also analysed family occurrence (36 cases presenting family history), as well as race and geographic distribution (wide distribution) for this disease. In the microscopic examination of multiple organs, the significant affected organs included the lungs (with bronchitis, peribronchitis, and the bronchial lumen filled with purulent exudate), trachea (purulent tracheitis), liver (fatty liver), gallbladder (presence of mucus), and pancreas (cystic fibrosis). Moreover, in 25 cases, the cause of death was attributed to lung infection with a predominant presence of *S. aureus*. Following this comprehensive study, the disease was regarded as an independent entity thereafter.

It's worth mentioning that Guido Fanconi, a Swiss professor of Pediatrics at the University Children's Hospital in Zurich, published autopsy results of two children, where he described for the first time the association of congenital bronchiectasis, cyst formation, and fibromatosis of the pancreas [9]. Dorothy H. Andersen is often considered the first person to have discovered this disease. The possible reasons for this recognition disparity might stem from the fact that Andersen's paper was published in English, garnering more general recognition, while Guido Fanconi published his work in German, leading to lesser visibility. Additionally, Andersen's paper included a larger sample size (49 cases) compared to Fanconi's study (2 cases), providing a clearer and more comprehensive description of the pathophysiology of this disease [9].

In the late 1940s, Andersen and Hodges established, for the first time, that CF is a recessive genetic disease through clinical evidence [10]. During the decade, available antibiotics were used for cystic fibrosis and demonstrated an obvious beneficial effect in prolonging the survival of CF infants. In the 1950s, Andersen and Paul di Sant'Agnese recognized that elevated salt content in sweat could be

indicative of cystic fibrosis [11]. This pivotal discovery laid the groundwork for the subsequent development of the sweat test. Six years later, in 1959, Gibson and Cooke established the pilocarpine iontophoresis sweat test for diagnosing cystic fibrosis, a method still utilized in contemporary diagnostics. Pilocarpine, acting as an agonist of muscarinic acetylcholine receptors present in sweat glands, stimulates sweat production, thereby facilitating sample collection for the determination of its salt concentration [12]. Additionally, between 1957 and 1960, a comprehensive prophylactic therapy program significantly improved survival rate. This program included early diagnosis through sweat tests, physiotherapy, antibiotics, nebulized treatments with phenylephrine and propylene glycol, as well as the introduction of nocturnal mist tents.1970s, antibiotics treatment impressively improved the survival rate, which is first time reported patients with CF exceeded 18 years rather than only infant before this period [13]. At the same time, nutrition treatment also brought up big change, such as beef serum protein hydrolase. The 1980s marked significant progress in understanding the biomolecular basis of chloride and sodium ion transport deregulation [14]. A pivotal milestone was achieved with the cloning of the CFTR gene in 1989 [15]. The well-recognized and studied mechanism of this disease paved the way for later CFTR modulator treatments.

I.1.c. Cystic Fibrosis Transmembrane Conductance Regulator

I.1.c-1. Function of the CFTR protein and CFTR gene

The CFTR protein, a glycoprotein consisting of 1480 amino acids, is a member of the adenosine triphosphate (ATP)-binding cassette (ABC) transporter superfamily, overseeing the transmembrane transport of small molecules. Its primary function is to serve as a chloride channel in the apical membrane of epithelial cells located in

multiple organs such as the lungs, upper respiratory tract, pancreas, liver, gallbladder, intestines, sweat glands, and reproductive tract. Structurally, it consists of two transmembrane domains allowing the passage of chloride ions, two cytosolic nucleotide-binding domains interacting with ATP, and a single regulatory R-domain that can be phosphorylated by protein kinase A (Figure 2). The opening of the channel enables the transport of chloride ions from intracellular to extracellular when the R-domain is phosphorylated and ATP binds to the nucleotide domain. Its closure can be triggered by ATP hydrolysis [16].

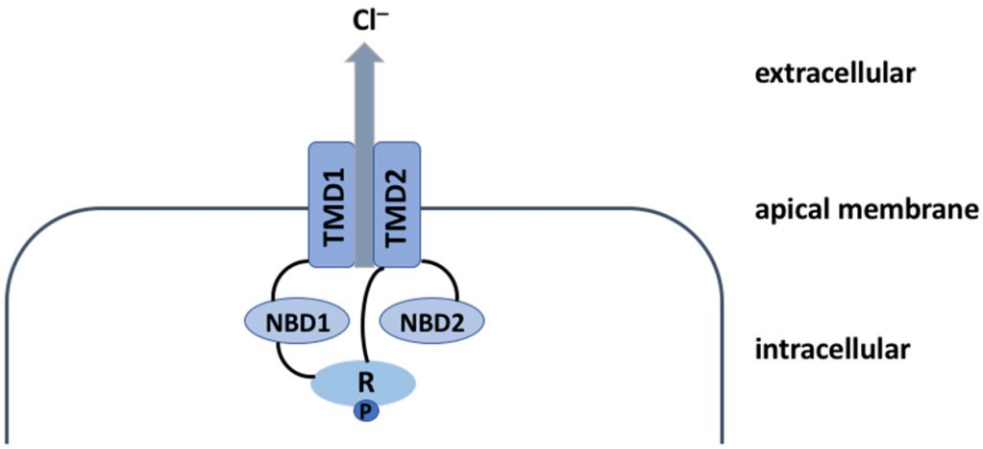

Figure 2. schematic representation of CFTR protein, comprising two transmembrane domains (TMD1 and TMD2), two cytosolic nucleotide-binding domains (NBD1 and NBD2), and a regulatory R-domain. TMD1 connects to NBD1, and TMD2 connects to NBD2, creating two TMD-NBD complexes joined by the R-domain, primarily facilitating the transport of chloride ions (Cl-) (image from [16]).

The CFTR protein is also involved in the regulation of the epithelial sodium (Na^+) channel (ENaC), which plays a central role in salt absorption, as well as bicarbonate (HCO_3^-), influencing the pH in mucus. More recently, the chloride channel has been implicated in the transport of glutathione, thiocyanate, immune cells, and the metabolism of lipids [16]. However, the transport of chloride and the regulation of ENaC continue to play a dominant role in the pathology of CF.

The gene encoding CFTR protein is situated on chromosome 7 (7q31.2) and spans approximately 189,000 base pairs of DNA [17]. Nearly 2100 variants in CFTR genes have been identified, and the list is continually growing [18]. These variants are broadly categorized into six classes based on the CFTR protein function (Figure 3) [19]. The F508del variant in class II, is the most frequent overworld. This variant corresponds to the loss of a phenylalanine amino acid at position 508 of the CFTR protein resulting from the deletion of three nucleotides (codon deletion) [20].

Mutations in the CFTR gene, such as missense, nonsense, and frameshift mutations, disrupt CFTR protein synthesis, function, and stability located in the apical membrane of epithelial cells in multiple organs. The dysfunctional chloride channels restrict chloride exit from epithelial cells and reabsorb Na^+, increasing the concentration of chloride and sodium inside cells. The higher concentration of these ions leads to passive water absorption from the respiratory epithelial surface through aquaporins and the paracellular pathway, resulting in the production of thick and sticky mucus in exocrine ducts.

Moreover, the sticky and thick mucus traps inhaled pathogens and particles and impairs the cilia responsible for cleaning them, contributing to airway obstruction, bronchitis, and lung infections. These lung diseases remain a primary cause of morbidity and mortality. Additionally, owing to the widespread distribution of CFTR protein in multiple organs, cystic fibrosis is a multiple system disease.

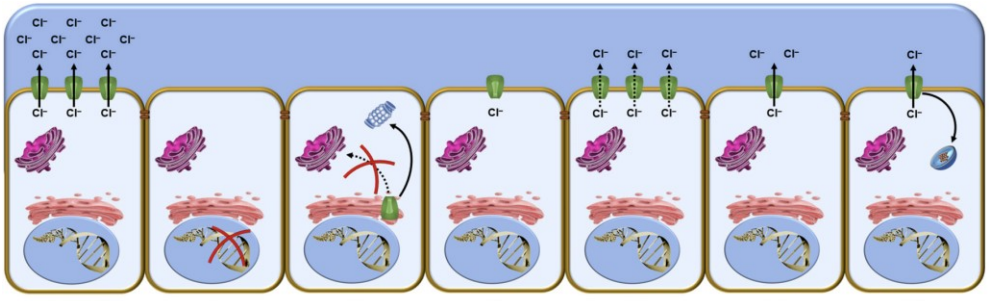

	wt-CFTR	I	II	III	IV	V	VI
Defect types		**No protein**	**No traffic**	**No function**	**Less function**	**Less protein**	**Less stable**
Mutation examples		G542X R553X W1282X	G85E ΔI507 **ΔF508** N1303K	V520F S549R G551D	R117H R334W S1235R	A455E 1680-886A>G 2657+5G>A	**rΔF508** Q1412X
Required approaches		Rescue protein synthesis	Correct protein folding	Restore channel conductance	Restore channel conductance	Maturation / Correct misplicing	Promote protein stability

Figure 3. Categorization of CFTR mutations according to CFTR protein function (image from [21]).

I.1.d. Clinical manifestations

The individually specific manifestations of cystic fibrosis and the rates of disease progression differ due to a range of protein dysfunctions caused by mutations in CFTR genes [19]. However, there are some classic manifestations in cystic fibrosis patients, including lung infections and recurrent sinusitis associated with the respiratory system, as well as steatorrhea and malnutrition resulting from pancreatic insufficiency [22]. Moreover, the damages to the lungs of patients with CF are those that will most threaten their quality of life.

The initial manifestation for CF patients typically involves meconium ileus, resulting from stick mucus secreted by abnormal intestinal glands, abnormal concentrating processes in the proximal small intestine, and pancreatic enzyme insufficiency, occurring in approximately 20% of individuals with CF [23, 24]. Even prenatally,

foetuses with cystic fibrosis exhibit more pronounced echogenic bowel than normal foetuses, with the additional risk of intrauterine bowel perforation and meconium ileus [25].

In addition to meconium ileus, nearly 85% of infants born with CF experience exocrine pancreatic insufficiency, marked by symptoms such as steatorrhea, flatulence, poor weight gain, and low absorption of fat-soluble vitamins (A, D, E, and K), leading to malnutrition [26]. Furthermore, there is a potential for impaired gallbladder function due to obstructed intrahepatic bile ducts, which may result in liver damage [27].

As age of infant, the persistent cough, wheezing and earlier respiratory infection frequently occur. Throughout the infancy and earlier childhood, the salt depletion electrolyte disturbances may also be present, including hypochloraemia, hypokalaemia, and metabolic alkalosis.

As individuals with CF progress into adulthood, respiratory symptoms become more prominent, marked by chronic cough, heightened sputum production, and persistent lung infections that can result in bronchiectasis and respiratory failure. Gastrointestinal challenges persist, characterized by ongoing issues with malabsorption and digestive problems. Additionally, adults may encounter CF-related diabetes, concerns regarding bone health, and related to reproductive health. 95% of men with CF often experience congenital bilateral absence of the vas deferens, the duct responsible for transporting sperm from the epididymis to the prostate. This condition results in azoospermia, rendering men with CF infertile (though not sterile) [28]. In contrast, women are less affected, with up to 50% able to conceive children. However, they may face challenges due to thicker cervical mucus, which can impede sperm penetration and reduce the likelihood of fertilization [29].

I.1.e. Microbiology of CF lung disease

The microbiome of the CF lung is different from that of the healthy lung. In terms of bacteria, healthy lungs have lower bacterial abundance, higher diversity and the most common genera are *Streptococcus*, *Veillonella* and *Prevotella*. Conversely, CF lungs have abundant pathogens, less diversity, while *S. aureus* and *P. aeruginosa* are the most common pathogens [30-32].

Airway Pathogen Prevalence Overview

Various abundant pathogens can be detected in the airways of CF patients through sputum or throat swab cultures. Among these pathogens, *S. aureus* and *P. aeruginosa* consistently emerge as the most predominant in microbial detection every year, based on a 16-year collection spanning from 1992 to 2022. The second highest is *Haemophilus influenzae* (*H. influenzae*), ranging between 10% and 20%. Other pathogens include *nontuberculous mycobacteria* (NTM) (10% to 13%) [33], *Stenotrophomonas maltophilia* (*S. maltophilia*) (approximately 10%), while *Achromobacter xylosoxidans* (*A. xylosoxidans*) ,and *Burkholderia cepacian* (*B. cepacia*) both fall below 10% (Figure 4).

Pathogen Prevalence Over Time: 1992-2022

In the evolution of prevalence over the years, *S. aureus* continued its upward trend until 2020, and the prevalence of MRSA in individuals with CF also increased from 2000 to 2010, displaying signs of plateauing thereafter. In contrast, *P. aeruginosa* shows a consistent decrease over time. Multiple-drug resistant *P. aeruginosa* (MDR-PA) has also consistently declined, with the most notable decrease observed among individuals younger than 18 years (43.8% had a positive culture in 2002 compared to 13.5% in 2022). The increase in *S. aureus* over time is believed to be linked to

improved microbiologic practices for the detection and reporting of Gram-positive organisms. Additionally, the observed decrease in *P. aeruginosa* is thought to be associated with the eradication of earlier infections and infection control measures. The prevalence of NTM, despite a decline post-2019 (13.9% in 2019, 10% in 2020 and 2021, 10.3% in 2022), remains higher than levels from decades ago [34]. Additionally, *S. maltophilia* showed a slight increase before 2019, while the *B. cepacia* complex remained stable. Interestingly, all species in positive sputum cultures exhibited a decreasing trend after 2019, except for *H. influenzae*, which demonstrated a slight increase between 2021 and 2022, likely influenced by the prevalence of pathogens.

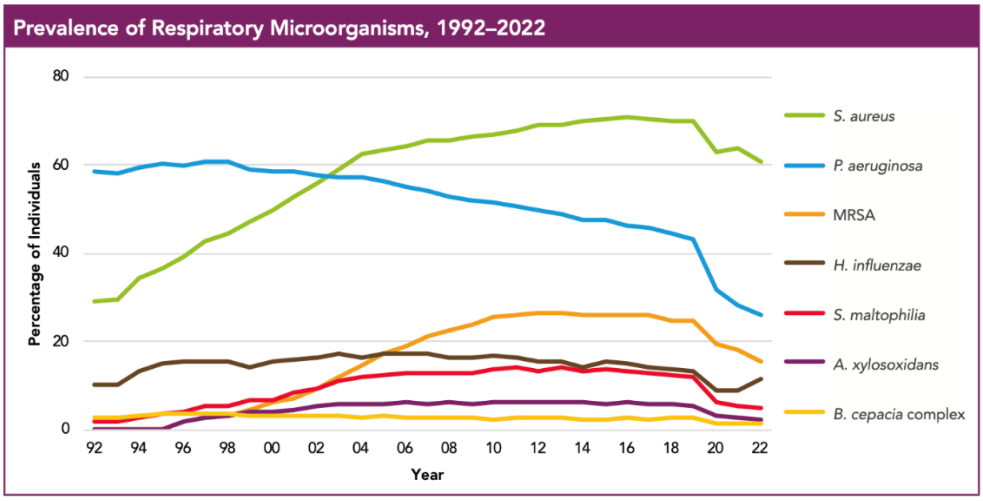

Figure 4: Temporal evolution of respiratory microorganisms prevalence in CF patients' airways (Adapted from [35]).

Age-Related Prevalence Trends

Although *S. aureus* and *P. aeruginosa* are the most prevalent among all pathogens isolated from the airways of CF patients, their prevalence varies with the age of CF patients. *S. aureus* is most prevalent in children and adolescents, reaching its highest

prevalence in those younger than 15, constituting around 80% of all bacteria [35]. However, after the age of 15, *S. aureus* exhibits a decreasing trend over time. As for MRSA, the highest prevalence occurs between the ages of 10 and 20 (Figure 5).

P. aeruginosa is predominantly present in patients who are older adults, with a prevalence close to 50% observed after the age of 35, and its occurrence increases over time starting from 10 years old. The rates of MDR-PA infection are highest among older adolescents and adults with CF, likely indicative of cumulative exposure to antibiotics. The rising prevalence of *P. aeruginosa* and the declining prevalence of *S. aureus* with age, beyond the impact of the immune system and antibiotics, could be linked to the interaction between *S. aureus* and *P. aeruginosa*. *P. aeruginosa* secretes virulence factors that can counter or eliminate *S. aureus*, while *S. aureus*, upon lysis, may serve as a nutrient source for *P. aeruginosa*. It's worth noting that *S. aureus* and *P. aeruginosa* are co-isolated from the same patients, comprising approximately 30% of the patient population.

In addition to the highest prevalence of *S. aureus* in children, *H. influenzae* follows as the second most prevalent, reaching approximately 20% until the age of 10. After the age of 10, the prevalence of *H. influenzae* decreases over time and falls below 10%.

For NTM, its acquisition is strongly associated with age in individuals with CF [36]. Detection of NTM can be challenging and insufficient through a swab culture. Therefore, it is commonly identified in individuals with CF who can produce sputum.

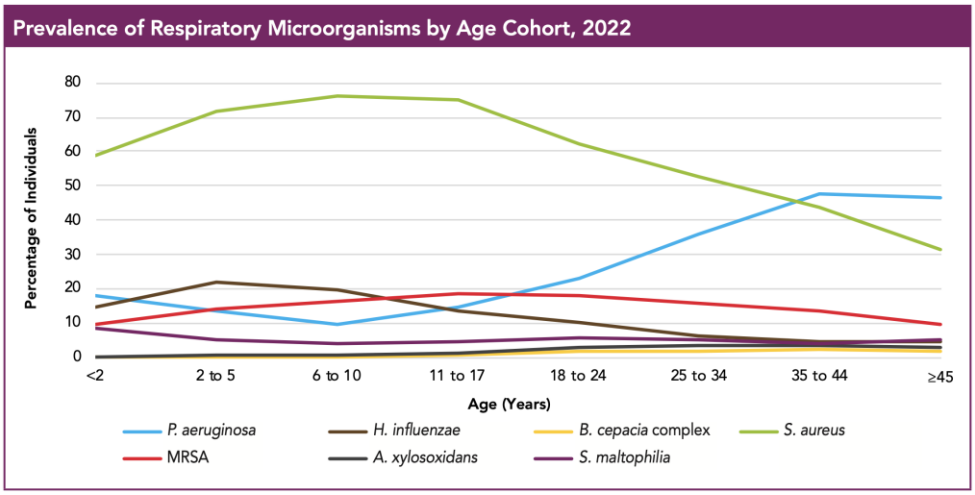

Figure 5. Prevalence of respiratory microorganisms found in lungs of patients with CF (From [35]).

I.1.f. Treatment strategies

The widespread distribution of the CFTR protein across various organs contributes to diverse clinical manifestations in individuals with CF. Addressing these manifestations requires tailored treatment strategies, including gastrointestinal care with pancreatic enzymes and nutritional supplements to manage malabsorption. Respiratory treatment incorporates improvement of mucociliary clearance to promote effective mucus movement, along with anti-inflammatory and anti-infective therapies aimed at addressing inflammation and combating respiratory infections. Additionally, emerging CFTR modulators are employed to restore the protein's ion transport function. In severe cases, lung transplantation may be considered.

In addressing gastrointestinal problems, Pancreatic Enzyme Replacement Therapy (PERT) is essential for aiding digestion and managing pancreatic insufficiency. Alongside PERT, incorporating fat-soluble vitamins (A/D/E/K) and adopting high-

calorie, high-fat diets become necessary to meet the heightened nutritional demands associated with CF.

The restoration of lung mucociliary clearance can be achieved by targeting mucus. These strategies include mechanically removing mucus and reducing mucus viscoelasticity. Mechanical mucus removal methods encompass chest physiotherapy, oscillating devices, and breathing exercises [37]. Inhaled hypertonic saline, mannitol, and Dornase alfa can thin mucus by reducing its viscoelasticity [38-40]. It's worth noting that Dornase alfa thins mucus by degrading DNA in the mucus [38], while the other two facilitate direct rehydration on the surface of the airway.

Alongside respiratory inflammation, individuals with CF frequently contend with other inflammatory conditions, such as pancreatitis and sinusitis, among others. Therefore, anti-inflammatory interventions are also crucial. Ibuprofen, recommended by the American Cystic Fibrosis Foundation, has been shown to mitigate the decline in lung function, particularly in younger patients [41, 42]. Another agent, the macrolide antibiotic azithromycin, operates by diminishing IL-4 and IL-8, suppressing neutrophil activity, and reducing the production of tumor necrosis factor [43, 44].

Anti-infective therapies

Antibiotics can be employed in four distinct ways to address bacterial infections in patients with CF: prophylaxis to prevent infections, eradication of early infections, control of chronic infections, and treatment of exacerbations.

Prophylaxis

The use of prophylaxis for *S. aureus* is currently a subject of debate regarding whether preventing bacterial colonization can lead to improved clinical outcomes. The UK guidelines recommend, as of 2017, initiating anti-*staphylococcus*

prophylaxis with antibiotics characterized by a narrow spectrum of action, such as flucloxacillin and cephalexin, to reduce the risk of *S. aureus* infection [45, 46].

Contrary findings from separate studies in Germany and the United States could not demonstrate the efficacy of prophylaxis with oral cephalosporins. Although patients in these studies had a reduced number of sputum cultures positive for *S. aureus*, there was an elevated number of cultures positive for *P. aeruginosa* [47, 48]. This controversial issue prompted the UK's National Institute for Health Research to initiate a randomized trial in 2016, assessing the use of flucloxacillin as a prophylactic agent for children with CF. The study is currently ongoing, and updates on its progress can be accessed through the following website.

http://www.cfstart.org.uk/.

Eradication of early infection

Eradication therapy typically focuses on early or acute infections, aiming to reduce or delay the onset of chronic infection. This treatment approach is characterized by its specificity, as it aggressively targets identified pathogens over a shorter duration to prevent the establishment of chronic infection. In cases where prophylaxis for *Staphylococcus aureus* is ineffective, guidelines recommend continuing flucloxacillin treatment and introducing a second anti-staphylococcal antibiotic, such as fusidic acid or rifampicin, for a duration of two to four weeks. In addition to floxacillin, cephalexin, a cephalosporin is often used to eradicate *S. aureus* infection [49].

The early eradication of *P. aeruginosa* is crucial, as it becomes highly resistant to antibiotic treatment once it progresses into chronic infection, especially with the formation of biofilms. The CF Foundation in the United States recommends inhaled tobramycin (300 mg twice daily) for treating the initial or new growth of *P.*

aeruginosa from an airway culture [50] whereas in the UK and Europe, the primary therapy involves a regimen of nebulized colistin and oral ciprofloxacin as the first-line treatment [51].

Chronic infection of control

In contrast to eradication therapy, the management of chronic infections often entails prolonged or intermittent antibiotic treatment. For the chronic suppression of *P. aeruginosa*, antibiotics are primarily administered via inhalation. Recommended inhaled antibiotics include tobramycin, endorsed by US guidelines, aztreonam lysine, recommended as an alternative by both European and US guidelines, and colistimethate [52]. Colistimethate, widely utilized in Europe, is now available in dry powder form [52]. For chronic *S. aureus* infections, evidence supporting prolonged maintenance therapy is currently lacking. However, oral antibiotics such as Trimethoprim/Sulfamethoxazole (TMP/SMX) linezolid (both intravenous and oral formulations), and intravenous vancomycin are employed for managing exacerbations in cases of MRSA chronic infection [53].

Pulmonary exacerbation therapy

A pulmonary exacerbation is characterized by an escalation in respiratory symptoms, such as increased cough, sputum production, and shortness of breath, along with an acute decrease in lung function [54]. Patients experiencing these symptoms indicative of a pulmonary exacerbation should have prompt access to a specialized centre. Treatment typically includes antibiotics, physiotherapy, and dietary adjustments. Antibiotics may be administered orally, via inhalation, and/or intravenously. For *P. aeruginosa* infections, a combination of two or more antibiotics is recommended, with a standard duration of 14 days of intravenous therapy, although optimal antibiotic selection and treatment duration are still under investigation. Intravenous antibiotic therapy can be administered either at home or

in the hospital, with hospital-based treatment being the standard of care for most patients. Physiotherapy primarily focuses on airway clearance technique. Regular review by a specialist physiotherapist is essential to tailor airway clearance and optimize aerosol regimens as needed. Dietary adjustments are crucial, as patients often experience a reduced appetite and require increased caloric intake during a pulmonary exacerbation due to higher metabolic demands.

CFTR modulator therapies

CFTR modulators are compounds that interact with malfunctioning CFTR proteins, aiming to partially reinstate their functionality [55]. The restoration of CFTR protein function involves two mechanisms. One mechanism increases the probability of the protein channel being open, allowing the passage of chloride or bicarbonate. CFTR modulators using this mechanism, known as potentiators, incorporate ivacaftor. The other mechanism improves the quantity of channels at the cell surface by assisting the protein in folding properly, enabling transport to the cell surface. Molecules with this function, known as correctors, include lumacaftor, tezacaftor, and elexacafrtor.

Ivacaftor, the first developed, is now approved for patients aged 4 months and older. The promising results of Ivacaftor have spurred the development of other CFTR modulators. Current regimens of CFTR modulators include: (1) individual therapy with Ivacaftor; (2) lumacaftor and Ivacaftor combination; (3) tezacaftor and ivacaftor combination; (4) ivacaftor, tezacaftor, and elexacaftor combination [56].

CFTR modulator therapy has shown improved health outcomes with effective use, like increased lung function and reduced need for intravenous antibiotics.

Additionally, the latter therapy (elexacaftor/tezacaftor/ivacaftor [ETI]) has been associated with a reduction in the frequency of detection of *S. aureus* and *P. aeruginosa* from samples of sputum and throat swabs [57]. However, it remains

uncertain whether this is associated with the reduced production of sputum as a result of this new therapy and the need to rather collect throat swabs yielding lower detection in culture-based analyses, or whether it indeed indicates reductions in pathogen abundance in the lower airways [57]. Of note, CFTR modulator therapy also comes with some adverse reactions, such as headache, upper respiratory tract infection, abdominal pain, diarrhea, etc [58].

Lung transplantation

As the lung disease progresses towards the end stage, a lung transplant may be considered. Typically, a double lung transplant is preferred, as leaving the other, more affected lung in place increases the risk of infection and damage. It's important to note that not everyone is eligible for a lung transplant.

I.2. *S. aureus* & *P. aeruginosa*-from planktonic cells to biofilm

I.2.a. *Staphylococcus aureus*

I.2.a-1. Commensalism and Pathogenicity Overview

S. aureus is a Gram-positive, cocci-shaped bacterium with a diameter ranging from 0.5 to 1 µm. As a facultative bacterium, it possesses the ability to lyse red blood cells and is characterized by being coagulase-positive and catalase-positive, distinguishing it from coagulase-negative *staphylococci* like *Staphylococcus epidermidis*.

This versatile microorganism serves both as a commensal and a potential pathogen. Approximately 30% of the human population carries this bacterium, commonly found in the skin, nasal passages, and mucous membranes of both humans and animals. When these tissues experience breaks, *S. aureus* can transition into a pathogenic state, leading to infection and disease. In addition to residing in human and animal hosts, healthcare settings, contaminated surfaces, medical equipment, and healthcare facilities can serve as reservoirs for *S. aureus*.

As a member of the "ESKAPE" pathogens, *S. aureus* is recognized for its ability to evade conventional treatment measures. These pathogens, including *Enterococcus faecium*, *Klebsiella pneumoniae*, *Acinetobacter baumannii*, *P. aeruginosa*, and *Enterobacter* species, are notorious for developing significant antibiotic resistance and withstanding immune attacks, primarily through diverse mechanisms, including genetic mutations. *S. aureus*, as a pathogen, is implicated in various infections, including device-related infections (catheters, prosthetic heart valves, joint replacements, etc.), osteomyelitis, infective endocarditis, skin and soft tissue infections, pneumonia, toxic shock syndrome, and is a significant cause of infections in young people with CF.

I.2.a-2. Virulence factors

S. aureus itself not only triggers inflammation, compromising health, but also releases virulent factors that directly target organs, tissues, and cells, thereby contributing to its pathogenicity. Key virulence factors involve proteins covalently anchored to the cell wall peptidoglycan, playing critical roles in adhesion to host cells, evasion of the host immune response, and the production of exotoxins.

Adhesins

Adhesins play a pivotal role in initiating the colonization process. Classical adhesins, known as microbial surface component recognizing adhesive matrix molecules (MSCRAMMs), include clumping factor (Clf) A and B proteins, fibronectin-binding proteins A and B (FnbpA and FnbpB), collagen-binding protein, and bone sialoprotein-binding protein. ClfA exhibits the capability to adhere to immobilized fibrinogen, contributing to immune evasion by binding soluble fibrinogen, while ClfB adheres to desquamated epithelial cells. FnBPA/B and bone sialoprotein facilitate adhesion to the extracellular matrix (ECM), whereas collagen adhesion occurs in collagen-rich tissues, thereby enhancing the processes of colonization and infection [59]. In addition to the MSCRAMMs, *S. aureus* surface proteins G (SasG) and X (SasX) also serve as adhesins [60].

Escape the host immunity

S. aureus employs a variety of strategies to evade host immunity effectively. These mechanisms include developing resistance to phagocytosis and neutrophil (PMN) killing, thwarting opsonization, and secreting proteins that form pores in the host cell membrane, leading to cell leakage and death. This primarily impacts immune cells such as neutrophils and other cell types, including epithelial cells. The polysaccharide capsule and staphyloxanthin play pivotal roles in resisting phagocytosis and neutralizing reactive oxygen species (ROS) produced by phagocytes [61, 62].

Staphylococcal protein A (SpA), a significant virulence factor in pneumonia, enhances immune evasion by binding to immunoglobulins, thereby preventing opsonization [63]. Furthermore, the extracellular fibrinogen binding protein (Efb) potently blocks phagocytic uptake by creating a fibrinogen shield around the bacteria. This shield is formed through simultaneous binding to complement C3b and

fibrinogen at the bacterial surface [64]. Additionally, *S. aureus* produces proteins such as alpha hemolysin and Panton-Valentine leucocidin (PVL), inducing pore formation in the plasma membrane, leading to cytolysis [65]. Complementing these strategies, the bacterium generates proteases, including staphopains A and B, V8 protease, and aureolysin. These proteases interact with the immune system, cleaving surface proteins of neutrophils, plasma proteins, and antimicrobial peptides [66]. Collectively, these multifaceted approaches contribute to the effective evasion of the host's immune defences by *S. aureus*.

Exotoxins

At the core of *S. aureus* pathogenicity is the production of a diverse array of exotoxins, each playing a crucial role in the bacterium's virulence. Apart from evading host immunity mentioned, alpha-toxin (α-hemolysin), and PVL are also regarded as exotoxins. Other exotoxins include beta-toxin (β-hemolysin), gamma-toxin (γ-hemolysin), leukocidins and phenol-soluble modulins (PSMs) [67]. Notably, α-hemolysin, β-hemolysin, and PVL play pivotal roles in pneumonia and lung injury by exerting cytolytic activity on host cells. PVL, encoded by two co-transcribed genes located on a lysogenized bacteriophage, is also implicated in severe skin and soft tissue infections [68, 69]. Additionally, toxic shock syndrome toxin-1 (TSST-1), Staphylococcal Enterotoxins (SEA, SEB, SECn, SED, SEE, SEG, SHE, and SEI), and the exfoliative toxins (ETA and ETB) contribute to conditions such as toxic shock syndrome and staphylococcal scalded skin syndrome (SSSS), respectively [59].

Exopolysaccharide

The main exopolysaccharide produced by *S. aureus* is poly-β-1,6-*N*-acetylglucosamine (PNAG), which functions as the polysaccharide intercellular adhesin (PIA). PNAG (Figure 6), a positively charged polysaccharide, facilitates

intercellular adhesion among bacterial cells and plays a crucial role in the structural integrity of the biofilm matrix. Additionally, PNAG is implicated in evading the host immune response.

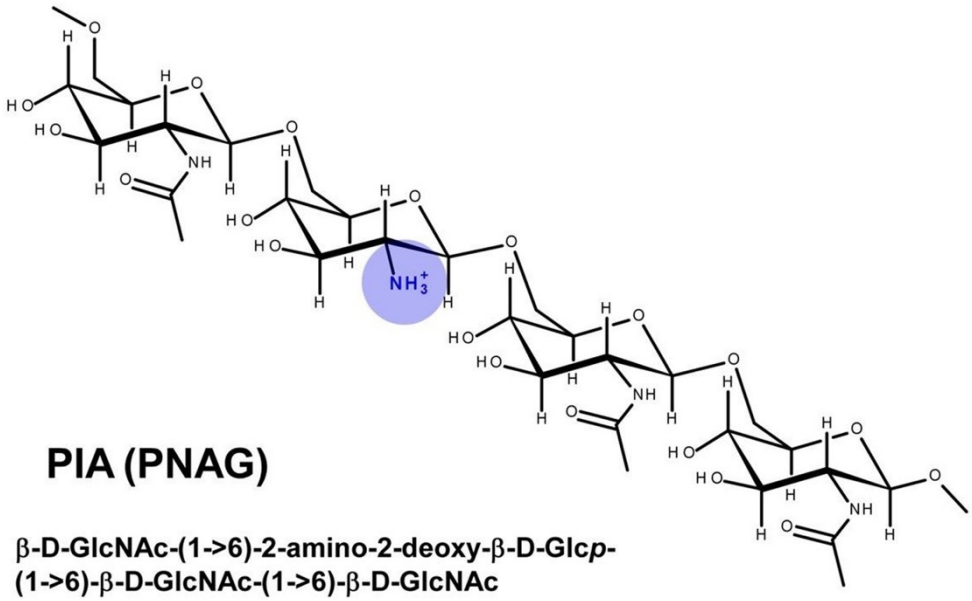

Figure 6. The primary exopolysaccharide synthesized by *S. aureus* consists of poly-β-1,6-*N*-acetylglucosamine (PNAG), with around one-fourth of it undergoing deacetylation, resulting in the generation of a free amino group. This amino group imparts a positive charge (depicted in blue) under acidic pH conditions (adapted from [70]).

Among these virulence factors, the adhesion protein ClfB, exfoliative toxins (such as ETA, ETB), and enterotoxins (such as SED and SHE), showed increased expression in isolates from CF patients compared to healthy individuals [71]. However, the pathogenicity of *S. aureus* in CF patients does not solely depend on individual or a few virulence factors. Instead, it is primarily associated with the phylogenetic background (genetic lineage or evolutionary history of the bacteria) and its adaptation to CF patients (as described in I.2.a-4) [71].

I.2.a-3. Quorum Sensing

Quorum sensing (QS) is an intercellular communication system employed by bacteria. QS systems comprise an enzyme responsible for synthesizing the signal molecule, known as autoinducer, and a receptor that binds to this signal molecule. This binding event triggers the reprogramming of gene expression, including those responsible for autoinducer production, establishing a positive feedback loop [72]. As the bacterial population reaches a specific threshold, the concentration of autoinducers increases, activating the QS system. Consequently, this activation stimulates the expression of various virulence-related genes, allowing coordinated and synchronized actions within the bacterial population.

S. aureus possesses two systems: the accessory gene regulator (agr) system and the LuxS/AI-2 system. The *agr* locus was first described by Hwei-Ling Peng and colleagues in 1988 [73, 74]. It is now a well-studied system in *S. aureus* and serves as a critical mechanism for quorum sensing. Conversely, the LuxS/AI-2 system requires further investigation, as there is no genomic evidence of established AI-2 receptors in *S. aureus* [75, 76].

The Agr system comprises two adjacent transcripts (Figure 7), called RNAII and RNAIII, which are controlled by P2 and P3 promoters, respectively. The autoinducer peptide, comprising 7-9 amino acids in length, is synthesized by the ribosomal peptide AgrD, which is encoded by the *agrD* gene. AgrD, the precursor of AIP, is proteolytically processed by an integral membrane-bound peptidase AgrB encoded by *agrB* gene and is transported outside the cell by AgrB with the assistance of signal peptidase SpsB. Once the concentration of AIP reaches a threshold, the signal AIP is detected by the histidine kinase AgrC encoded by *agrC*, which undergoes

autophosphorylation. Then the phosphate is relayed to AgrA encoded by *agrA*, which, in turn, binds the P2 and P3 promoters, driving the expression of RNAII and RNAIII transcripts, respectively. Phosphorylated AgrA also binds the promoters for the phenol-soluble modulin (PSM) genes, inducing their expression. The system exhibits increased expression of additional toxins, including alpha-toxin (Hla) and gamma-hemolysin (Hlg).

The LuxS/AI-2 system consists of the autoinducer 2 (AI-2), a furanosyl borate diester. The role of the LuxS/AI-2 system as a quorum-sensing regulatory system in staphylococci remains debated due to the absence of a recognized receptor, with its primary function being associated with metabolic activity. Despite this, it has been established that AI-2 regulates capsule synthesis, biofilm formation (through the production of IcaR), antibiotic susceptibility, and virulence [77].

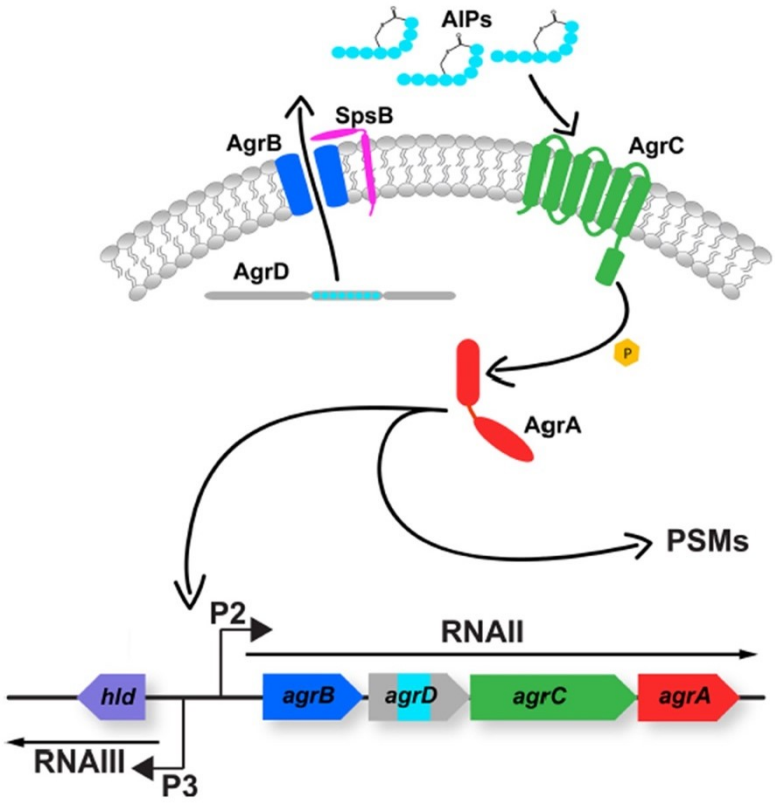

Figure 7. Schematic of *agr* quorum-sensing system regulation. AgrD, after maturation, is transported into the extracellular environment by AgrB with the assistance of SpsB, releasing the autoinducing peptide (AIP). As the concentration of AIP reaches a critical level, it binds to AgrC, leading to the phosphorylation of AgrA. Phosphorylated AgrA then binds to the P2 and P3 promoters, initiating the expression of RNAII and RNAIII transcripts, respectively. Additionally, phosphorylated AgrA interacts with the promoters of phenol-soluble modulin (PSM) genes, inducing their expression (image from [78]).

I.2.a-4. Adaptation to cystic fibrosis lung

In exceedingly challenging environments marked by factors such as thick mucus, antibiotic exposure, host immune response, and competition with other strains

(particularly *P. aeruginosa*), *S. aureus* is compelled to adapt within the CF lung milieu, ensuring its prolonged survival in vivo. This adaptation is characterized by alterations in both genes and phenotype. Compared to health individuals, *S. aureus* exhibits a higher mutation frequency when isolated from CF patients [79]. Dysfunction of *agr*-type genes is a typical representative example [80]. The overall number of expressible virulence genes significantly decreases over time [71]. The downregulation of virulence gene expression in *S. aureus* allows it to evade antibiotic treatment and immune system responses, as certain virulent factors act as receptors for immune cells. Notably, the deterioration of the lungs in CF patients is not directly associated with a decrease in the expression of virulence genes but is linked to this adaptive process [71].

Genetic changes commonly result in alterations in phenotype, but phenotypic changes are not solely dependent on genes. Changes in gene expression and phenotypes occur in a time-dependent manner and accumulate [81, 82]. In addition to genetic factors, environmental stress can directly contribute to changes in phenotypes. Small colony variants (SCVs) represent the most distinctive characteristic of *S. aureus* isolated from CF patients. They exhibit slow growth rates, lower metabolic activity, intracellular persistence, increased resistance against antibiotics, and are associated with more severe lung disease. Furthermore, SCVs often appear in CF patients with chronic infection, especially in those who are significantly older and have poorer lung function compared to patients without SCVs [83, 84]. The presence of SCVs reflects the long-term adaptation of microorganisms to the host environment [85]. Most *S. aureus* SCVs in CF patients are thymidine-auxotrophic, displaying resistance to trimethoprim-sulphomethoxazole treatment [79]. Beyond SCVs, phenotypic variations also include pigmentation (e.g., yellow, grey, and white), mucoid and nonmucoid traits, as well as haemolytic and non-haemolytic characteristics (Figure 8).

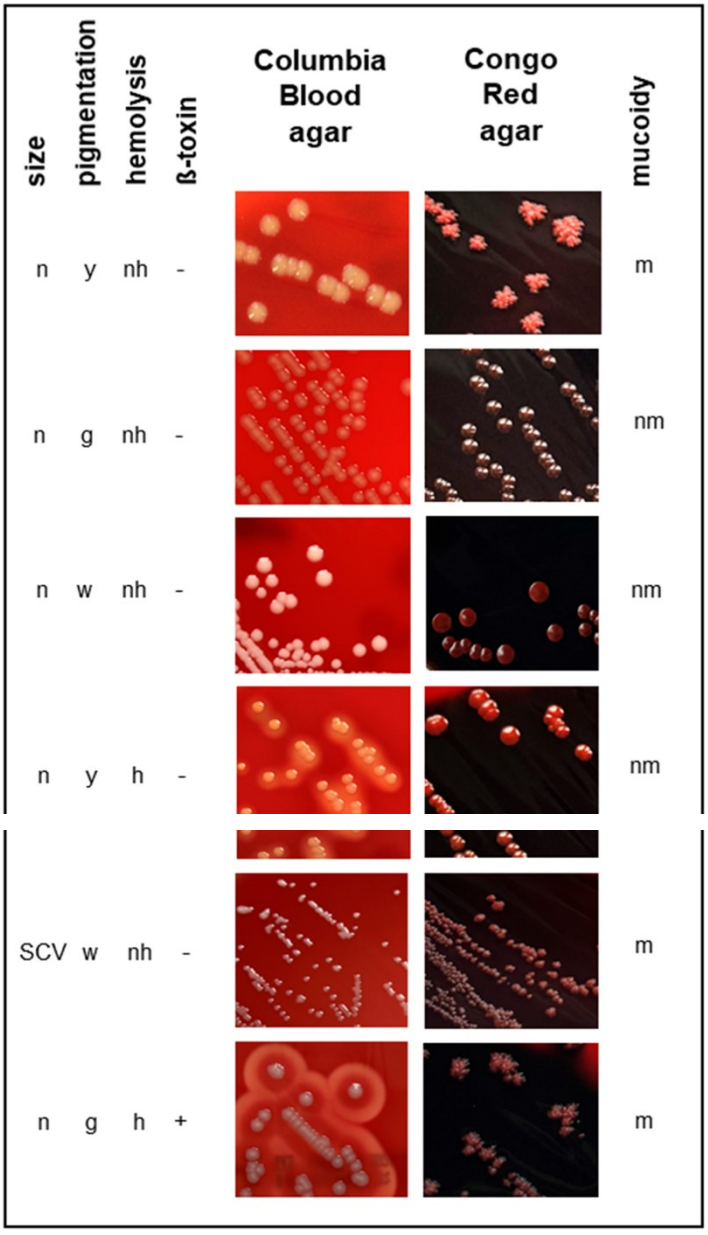

Figure 8. Shared phenotypical diversity in CF isolates of *S. aureus*, encompassing size (normal [n] and small colony variants [SCV]), pigmentation (yellow [y], grey [g] and white [w], haemolysis (haemolytic [h] and non-haemolytic [nh]) and β-toxin (negative [-] and positive [+]). Image from [86].

I.2.b. *P. aeruginosa*

I.2.b-1. Versatile Opportunistic Pathogen

Pseudomonas aeruginosa, a rod-shaped, motile Gram-negative bacterium, typically measures between 0.5 to 0.8 μm in width and 1.5 to 3.0 μm in length. Demonstrating adaptability, this bacterium primarily utilizes aerobic respiration but can switch to anaerobic respiration using nitrate in low oxygen environments [87].

Widespread in nature, *P. aeruginosa* is commonly found in diverse environments such as soil, water, and plants. It also colonizes medical equipment, including catheters and endotracheal tubes. It is not a commensal microorganism, such as *S. aureus,* in the human body, but *P. aeruginosa* is recognized as an opportunistic pathogen. It can infect individuals with compromised immune systems (e.g., HIV, neutropenic patients), burn-wound patients, and those in intensive care units (ICUs) [88, 89].

Beyond hospital-acquired infections, *P. aeruginosa* is a significant pathogen in chronic lung infections among adult cystic fibrosis patients. With its large genome (5.5 - 7.4 Mbp), extensive array of virulence factors, and metabolic flexibility, it can quickly adapt to external stress conditions, including antimicrobial treatments and changes in nutrient availability. This adaptability enables *P. aeruginosa* to not only survive but thrive in a wide range of environments [89-91].

Notably, *P. aeruginosa* is also classified as one of the "ESKAPE" pathogens, akin to *S. aureus*.

I.2.b-2. Virulence factors

P. aeruginosa harbors a diverse array of virulence factors that play pivotal roles in facilitating bacterial adhesion, colonization, invasion, inhibition of the host immune response, and depletion of host nutrients. These virulence factors can be categorized into two main groups: surface structure virulence factors, including flagella, type IV pili, lipopolysaccharide (LPS), and the type 1-6 secretion systems; and secreted virulence factors, primarily associated with QS products and factors secreted by various secretion systems (Figure 9).

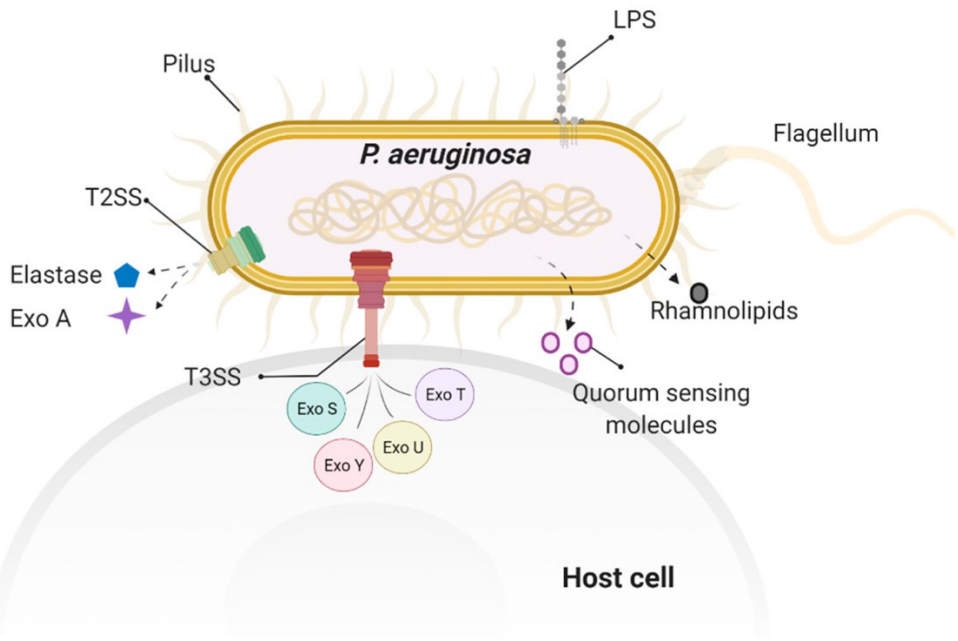

Figure 9: Surface structure virulence factors (polar flagellum, pilus, LPS, and T3SS) and secretion virulence factors (main QS products and factors secreted by T2SS and T3SS) (adapted from [92]).

Surface Structure Virulence Factors

Flagellum

The flagellum is a complex apparatus assembled from more than 20 different proteins and is located on the bacterial cell surface [93]. *P. aeruginosa* possesses a single polar flagellum, playing a crucial role in controlling swimming, swarming motilities, and chemotaxis. Swimming motility involves the movement of individual cells in liquid, while swarming motility refers to the collective movement of bacteria in semi-solid liquid [94]. While the flagellum itself is not directly toxic to host cells, it serves as a delivery system for virulence factors to host cells and other species. Wild *P. aeruginosa* strains with flagella demonstrate increased virulence compared to mutants lacking flagella [95]. Additionally, the flagellum aids *P. aeruginosa* in adhesion and invasion of host immunity [96].

Type IV pili

Type IV pili constitute another vital structure surface virulence factor for *P. aeruginosa*. These hair-like appendages, situated on the bacterial cell surface, govern twitching motility—an intricate form of bacterial movement characterized by the extension and retraction of type IV pili, driven by cytoplasmic ATPases. This type of movement allows the bacterium to crawl along surfaces. Meanwhile, type IV pili directly impact host cells through twitching motility, facilitating physical interactions and movement across host cell surfaces. This contributes to the bacterium's ability to adhere, breach barriers, and establish infection, ultimately enhancing overall virulence [97].

Lipopolysaccharide

Lipopolysaccharide (LPS) is a glycolipid situated on the outer face of the outer membrane and integrated into the cell wall of *P. aeruginosa*. Comprising lipid A

(endotoxin), core oligosaccharides, and O-antigen [98], the variably penta-, hexa-, or hepta-acylated forms of lipid A exhibit differing potencies in activating host innate immunity through Toll-like receptor 4 (TLR4)-MD-2 complex binding [99]. Specifically, the TLR4-MD-2 complex recognizes and transmits robust proinflammatory signals (such as IL-8) in response to hexa-acylated LPS but not penta-acylated LPS [100]. The O-antigen is a primary target for protective immunity, shielding bacteria from phagocytosis and contributing to bacterial survival by delaying immune receptor recognition [101]. During chronic infection, LPS undergoes adaptive changes, such as specific modifications to lipid A, conferring resistance to host antimicrobials, or the loss of O - antigen, promoting immune evasion [101-103].

Secretion systems

The final set of surface structure factors is the secretion system. *P. aeruginosa* possesses six secretion systems: Type I (T1SS), Type II (T2SS), Type III (T3SS), Type IV (T4SS), Type V(T5SS) and Type VI (T6SS), playing a crucial role in bacterial adhesion and virulence [104]. These molecular nanomachines can inject toxins and exoenzymes into both eukaryotic and prokaryotic cells or secrete them into the environment. Among them, T1SS, T6SS, and T5SS are involved in metal ion acquisition. For instance, the T1SS-secreted protein HasAp, a haemophore, binds heme from haemoglobin to capture iron ions, while T6SS is involved in a Cu^{2+}-scavenging pathway [105]. T4SS is associated with horizontal genetic transfer between diverse microorganisms and is potentially implicated in pathogenesis. Linked with T2SS, T4SS plays a role in the assembly and disassembly of pili, with fewer studies conducted compared to other secretion systems [106, 107]. It's worth noting that T2SS and T3SS are the most critical virulence appendages. T2SS secretes Elastase, degrading elastin, a major component of lung tissue critical for its elasticity.

It also cleaves surfactant protein D (SP-D), influencing bacterial aggregation, altering alveolar macrophage function, and regulating bacterial clearance [108]. Additionally, the needle of T3SS can inject toxin proteins, called effectors, directly into the cytosol of host cells, helping invade host immunity and cause infection [109, 110].

Secreted virulence factors

Secreted virulence factors contribute to impairing the function of body cells and tissues. These factors are primarily produced and by secretion systems (T1SS-T6SS) and QS systems, as well as other sources, mainly including exopolysaccharides, toxic proteins, enzymes, and organic small molecules.

Exopolysaccharides

P. aeruginosa produces three exopolysaccharides, namely alginate, polysaccharides synthesis locus (Psl), and pellicle (Pel). Alginate, the first reported polysaccharide, is composed of D-mannuronic acid residues interspersed with L-guluronic acid residues (Figure 10A). It forms a pseudocapsule that protects bacteria against phagocytosis and antibiotics, and it also decreases ROS damage by lowering PMN chemotaxis and inhibiting complement factors [111, 112]. Alginate is produced by mucoid *P. aeruginosa*, often isolated from chronically infected patients, and it serves as a main component of biofilms formed by mucoid strains.

Non-mucoid *P. aeruginosa* produce two distinct polysaccharides: Psl, a neutrally charged polysaccharide, composed of a repeating pentamer containing D-mannose, L-rhamnose, and D-glucose residues (Figure 10B); and Pel, primarily composed of a linear polymer of α-1,4-*N*-acetylgalactosamine, with a significant presence of dimeric repeats consisting of galactosamine and N-acetylgalactosamine, and it is partially de-N-acetylated [113]. The drawn chemical structure of Pel is currently

unavailable. Like alginate, both Psl and Pel contribute to the formation of biofilms, but these biofilms are produced by non-mucoid *P. aeruginosa.*

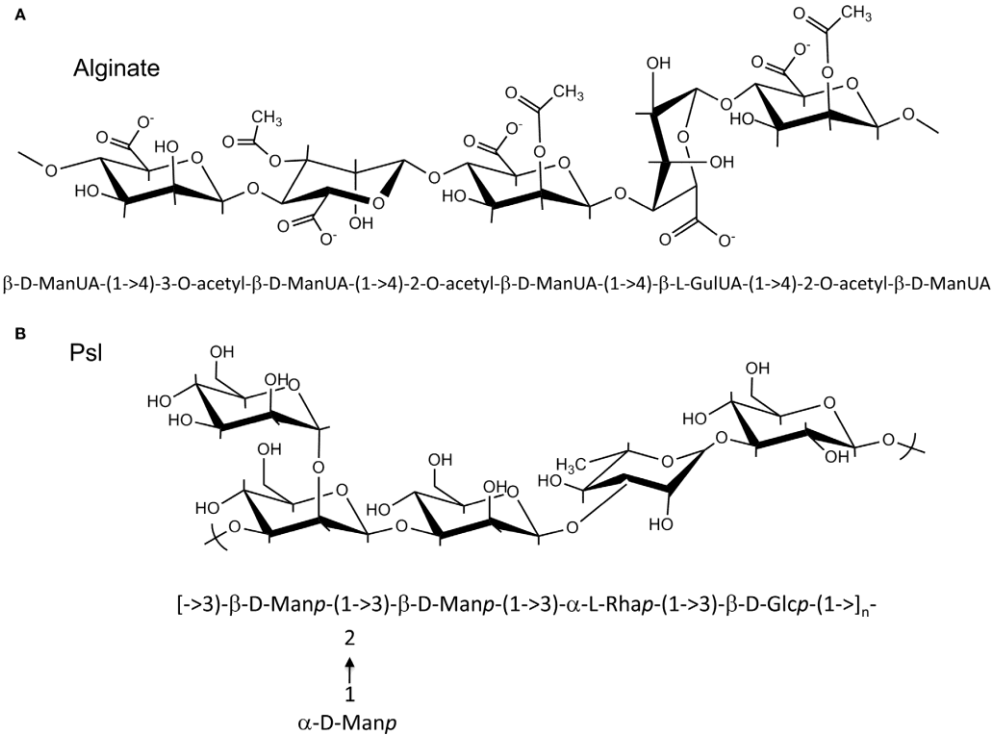

Figure 10. Chemical structures of alginate (A) and Psl (B) (adapted from [114]).

Proteins

Proteins abundantly secreted by the secretion system (T1SS-T6SS) act as significant virulence factors, playing crucial roles in nutrition acquisition, immune system invasion (e.g., biofilm formation), and cytotoxicity. Table 1 provides a summary of these virulence factors, encompassing proteases (Alkaline protease, Elastase A, Elastase B, and PrpL), phospholipases (PlcH and PlcN), lipases (Lipases),

metalloproteases (HasAP), exoenzymes (ExoS, ExoT, ExoY, and ExoU) and Exotoxin (Exotoxin A).

Table 1: Protein-like virulence factors secreted by the secretion system

Virulence factors	functions
Alkaline protease	evasion of immune detection through the degradation of free flagellin monomers; inhibition of chemotaxis of neutrophils to block phagocytosis; degradation of host proteins, including interleukins (e.g., IL-6), and complement proteins [115, 116]
HasAP	Binding heme from haemoglobin; promotion of proliferation [104, 107]
Elastase B	Cleavage of various proteins (e.g., elastin) [117]; contribution to inflammation and facilitation of host immune escape by diminishing phagocytosis [118].
Elastase A	Cleavage the glycyl-glycine and glycyl-alanine links in the pentaglycine bonds within the peptidoglycan of *S. aureus*, inducing its lysis [119, 120]; Cleavage of elastin, albeit less potent than LasB, and modification of elastin to increase its susceptibility to other elastases [117, 118].
Phospholipase C (PlcH, PlcN)	Preferential hydrolysis of sphingomyelin and phosphatidylcholine, along with hydrolysis activity, can lead to tissue damage, inflammation, and interference with the oxidative burst of immune cells [121].

PrpL protease	Inhibiting the migration and survival of fibroblasts, keratinocytes, and endothelial cells; inducing persistent inflammation and a prolonged inflammatory state [122].
Lipases	Motility, biofilm regulation, and rhamnolipid synthesis [123].
Exotoxin A	Inhibition of protein synthesis leading to cell death and depressing host response to infection [102, 124].
ExoS, ExoT, ExoY and ExoU	Toxin-mediated cytotoxicity involves altering host cell membrane integrity, which leads to cell death, as well as disrupting the actin cytoskeleton, impeding cell-cell adhesion, and triggering apoptosis in host cells [125].

Organic small molecules

The QS system generates diverse secondary metabolites (small molecules) functioning as weaponry in competition with other species and capable of impacting host cells. These compounds demonstrate a positive correlation with lung exacerbation in CF patients [126]. A summary of these organic small molecules is presented in Table 2.

Table 2: Organic small molecules produced by QS system.

Virulence factors	functions
pyocyanin	Generation of reactive oxygen species [102]; biofilm formation [127]; cytotoxicity to host cells or other species [128].
Siderophores (pyoverdine and pyochelin)	Chelation of iron, promotion of biofilm formation [129]; Pyoverdine translocates into host cells, binds to and extracts

	iron, causing damage to host mitochondria, disrupting their function, and initiating mitochondrial dysfunction [130].
rhamnolipids	Facilitation of biofilm dispersion to aid in bacterial recolonization [131]; exhibiting antimicrobial activity against other bacterial species, hemolytic activity towards host cells, modification of cell surface hydrophobicity, elevation of PQS signal solubility, and promotion of swarming motility [132-134].
HQNO	Inhibition of other species growth; biofilm formation [135].
2-heptyl-3-hydroxy-4-quinolone (PQS)	Activation of oxidative stress response, regulating the release of virulence and host-modifying factors, and serving as a stress warning signal, prompting the larger population to actively avoid cell stress included by antibiotics and phage exposure [136].
Hydrogen cyanide	Disruption cellular respiration [137, 138].

These virulence factors exhibit varying expression levels at different infection stages in CF patients. During the acute infection stage (early infection), *P. aeruginosa* pathogenicity in the lungs of CF patients is primarily associated with increased expression of virulence factors such as flagella, type II secretion, rhamnolipids, lipases, proteases, and pyoverdine [139]. However, during chronic infection, virulence factors often show a decreasing trend [140]. As described for *S. aureus*, *P. aeruginosa* pathogenicity in CF is not solely attributable to individual virulence factors but is instead influenced by multiple complex factors including virulence

factors expression, biofilm formation, small colony variants (SCVs). It is worth noting that increased expression of certain virulence factors, such as HCN, pyocyanin, ExoS, and alginate, often lead to severe clinical outcomes [141].

I.2.b-3. Quorum Sensing

Toxins, exoenzymes, and components of the biofilm are regulated by the Quorum Sensing (QS) system [142-144]. *P. aeruginosa* utilizes four QS pathways: Las, Rhl, Pqs, and Iqs systems. The corresponding autoinducers for these pathways are N-(3-oxododecanoyl)-L-homoserine lactone (OdDHL), N-butanoyl-L-homoserine lactone (BHL), 2-heptyl-3-hydroxy-4-quinolone (PQS), and 2-(2-hydroxyphenyl) -thiazole-4-carbaldehyde (IQS), respectively [145] (Figure 11).

These systems intricately intertwine, establishing a hierarchical relationship, with the Las system positioned at the apex of the signalling hierarchy. The OdHL produced by the LasI synthase binds to the LasR receptor, forming the lasR-OdHL complex. This complex stimulates *lasI* gene expression that controls the production of autoinducer, creating a positive feedback loop [146]. Concurrently, it activates the other three systems and regulates virulence factors such as LasA protease and LasB elastase [145]. The second Rhl system, besides its intrinsic positive feedback and activation through Las, is also upregulated by the Pqs and Iqs systems. Moreover, the third Pqs is also positively regulated by Iqs system [147].

In addition to its role in internal regulation, the QS system also governs the expression of secretion systems and other virulence factors, including the flagellum [148]. The Type I Secretion System (T1SS) is positively regulated by QS, exemplified by the dependence of the alkaline protease AprA on QS for secretion. The Xcp (extracellular protein) Type II Secretion System (T2SS) secretes QS-regulated virulence factors such as elastase A and B (LasA and LasB), as well as the

exotoxin A (ExoA). Moreover, the Xcp T2SS itself is positively regulated by QS. However, among the QS systems, the Rhl system exerts a negative regulatory influence on the expression of the Type III Secretion System (T3SS) [149].

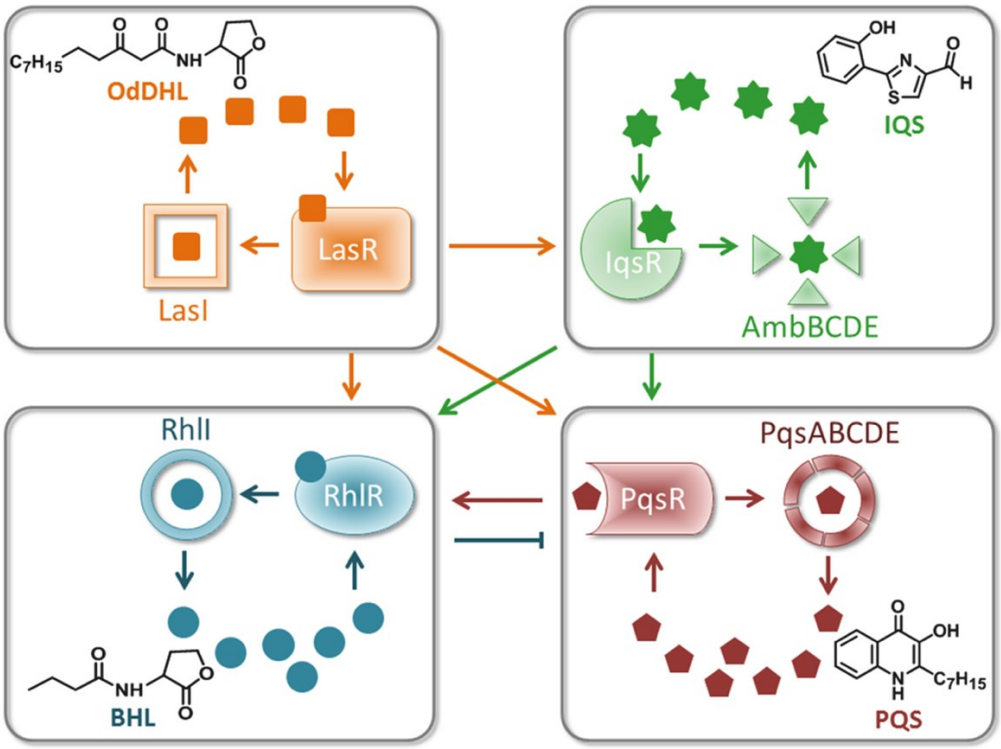

Figure 11: Schematic representation of the four QS systems in *P. aeruginosa*: Las (top left), Rhl (bottom left), Iqs (top right), and Pqs (bottom right). Each system produces specific autoinducer molecules: OdDHL for Las, BHL for Rhl, PQS for Pqs, and IQS for Iqs. Upon reaching a threshold concentration, these autoinducers bind to their corresponding receptors, forming receptor-autoinducer complexes (LasR-OdDHL, RhlR-BHL, PqsR-PQS, and IqsR-IQS), which activate genetic pathways for autoinducer synthesis, establishing positive feedback loops within each QS system. The figure also illustrates the hierarchical arrangement of the QS systems, with Las positioned at the top. Regulatory interactions

between systems are indicated by arrows (stimulatory effects) and perpendicular lines (inhibitory effects) (image adapted from [150]).

I.2.b-4. Adaptation to cystic fibrosis lung

Confronted with the thick and viscous mucus, where oxygen is restricted, along with the presence of other species, immune responses, and antibiotic stress, *P. aeruginosa* undergoes adaptations to thrive in the challenging environment of the airways in CF patients. These adaptations involve significant changes in both phenotypes, marked by the emergence of mucoid and small colony variant (SCV) phenotypes, or the loss of flagella and pili, and genotype, such as the occurrence of *lasR* mutations [151].

The excessive production of alginate in *P. aeruginosa* triggers a phenotype switch from nonmucoid to mucoid, potentially accompanied by the disappearance of pigment in certain strains [151]. The mucoid phenotype, characterized by abundant alginate, forms a physical barrier that shields the bacterium from immune cells, including neutrophils and alveolar macrophages. This barrier also hinders the penetration of antibiotics and immune molecules such as complement and immunoglobulins. Moreover, alginate will interact with positively charged antibiotics (such as aminoglycosides), contributing to an increased tolerance to these antimicrobial agents [152].

Another category of lung-adapted *P. aeruginosa* strains comprises Small Colony Variants (SCVs) – compact, self-aggregating isolates demonstrating heightened biofilm formation, robust surface attachment, and increased exopolysaccharide production [153]. The evolution of SCVs in the cystic fibrosis (CF) lung is linked to the overproduction of the ubiquitous bacterial signaling molecule cyclic-di-GMP, with increased levels of cyclic-di-GMP identified as responsible for the SCV phenotype in numerous CF lung isolates. This correlation is associated with

heightened resistance to antibiotics, compromised lung function, and prolonged persistence of infection.

Additionally, a significant proportion of *P. aeruginosa* isolates display reduced motility due to the loss or defect of flagella and pili. This reduction in motility contributes to *P. aeruginosa* adhesion, colonization, and biofilm formation. Furthermore, isolates from CF patients often lack the O-antigen polysaccharide of lipopolysaccharide, allowing them to evade recolonization by immune cells.

Unveiling a spectrum of adapted phenotypes, *P. aeruginosa* isolates from the lungs of CF patients showcase diverse genetic adaptations. In addition to mutations in genes associated with the aforementioned phenotypes, the most frequently mutated gene is *mexZ*—a negative regulator of *mexX* and *mexY*, components of the MexXY-OprM multidrug-efflux pump [154].

Mutations in the master regulator LasR result in the loss of function of exoproteases alkaline protease (AprA) and elastase B (LasB), which cleave C5a—a 74-amino acid residue polypeptide involved in recruiting neutrophils to the site of infection. However, an excessive amount of C5a impedes the generation of reactive oxygen species and the phagocytosis of bacteria by neutrophils [155]. The phenotypic and genotypic adaptations of *P. aeruginosa* to the lungs in CF patients contribute to recurrent and persistent infections, amplifying the challenges in treating lung infections in CF patients.

I.3. Biofilm

I.3-a. Definition and Formation of Biofilms

Biofilm is a predominant lifestyle of bacteria, where bacteria attach to biotic or abiotic surfaces or aggregate with each other. Simultaneously, they secrete extracellular polymeric substances (EPS), encase bacterial cells, and form a community of aggregates. In brief, a biofilm consists of bacterial aggregates embedded in self-produced matrix of EPS [156]. Matrix consists of proteins, DNA, polysaccharides, lipids, RNA, and other components. Among them, proteins, DNA, and polysaccharides are the most important [157].

Various bacterial species produce distinct matrix compositions. For example, PNAG is the primary polysaccharide component in *S. aureus* [158], while alginate, pel, or pls prevail in *P. aeruginosa* [159]. These matrix compositions play important role in biofilm formation.

Biofilm formation involve three key events (Figure 12):

Aggregation and Attachment

Bacterial cells attach to biotic surfaces (e.g., host tissues) or abiotic surfaces (such as medical devices). Attachment can occur through various mechanisms, including initial physical forces like Van der Waals interactions, electrostatic forces, or hydrophobic forces [160]. Additionally, chemotaxis guides bacterial cells to specific locations [161]. The surface structures of bacteria, such as pili and fimbriae found in *P. aeruginosa*, contribute to this attachment process [162, 163]. Furthermore, bacteria secrete adhesion-like proteins, such as MSCRAMMs (Microbial Surface

Components Recognizing Adhesive Matrix Molecules), which play a crucial role in attaching to surfaces or facilitating auto-aggregation [164].

Growth and Accumulation

During this stage, bacteria undergo multiplication, leading to the synthesis of an extensive matrix composed of various substances. The increased density of bacteria, coupled with the accumulation of matrix components, reinforces the attachment of microorganisms to the surface and promotes aggregation among them. Matrix polysaccharides play a crucial role in providing structural support. Additionally, extracellular DNA (eDNA) participates in horizontal gene transfer, contributing to both genetic diversity and the stability of the biofilm structure [165]. Proteins within the biofilm have diverse functions, including attachment, virulence, and metabolic activities [166]. Moreover, as bacterial density increases, the microenvironment within the biofilm becomes initially heterogeneous. For example, the deeper layers of the biofilm experience restricted oxygen availability and lower nutrient levels [167]. This heterogeneity further contributes to the complexity of the biofilm structure and the adaptation of bacteria to diverse conditions within the biofilm community.

Disaggregation and Detachment

Over time, biofilm structures can be influenced by various external and internal factors, resulting in the disaggregation and detachment of a portion of the biofilm.

External factors encompass physical elements like shear, and environmental signals (such as nutrient availability, oxygen levels, nitric oxide, pH changes, and exposure to certain chemical substances), leading to biofilm sloughing and erosion [168]. Internal factors involve enzymes and surfactant components produced by bacteria. The generation and accumulation of various enzymes within the biofilm degrade

matrix compositions, inducing changes in the biofilm structure, such as DNase degrading eDNA and alginate lyase breaking down alginate. Surfactant production further promotes the process, as surfactants facilitate the release of bacteria from the biofilm. Examples include rhamnolipids produced by *P. aeruginosa* [169] and amphipathic proteins (PSM) produced by *S. aureus* [170]. The process of disaggregation and detachment facilitates bacterial colonization of new sites and the formation of new biofilms.

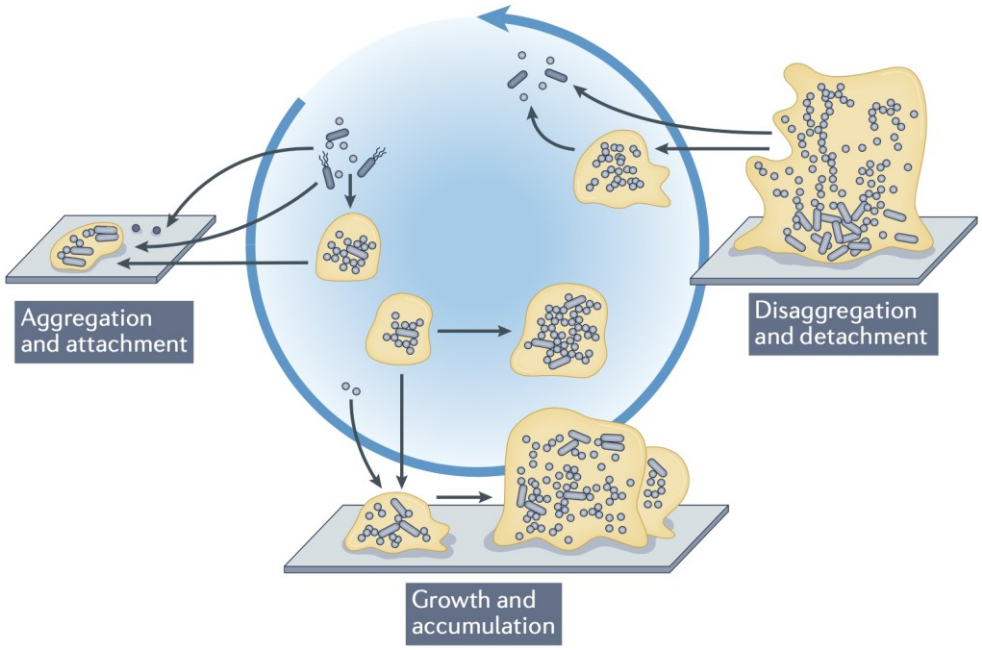

Figure 12: Biofilm formation generally involves three events. (1) Aggregation and attachment: During this event, bacteria aggregate with each other (inner ring) or attach to biotic and abiotic surfaces (outer ring). (2) Growth and accumulation: In this stage, aggregated and attached bacterial colonies expand through growth and the recruitment of surrounding cells. (3) Disaggregation and detachment: During this event, bacteria can exit the biofilm as aggregates and as single cells, depending on the mechanism [171].

I.3-b. Biofilm in CF patients

Chronic infection in CF patients is associated with biofilm formation. The earliest visualization of biofilm from CF patients was conducted by Joseph S. Lam and his colleagues in 1980 using an electron microscope. They examined postmortem excisions from a *P. aeruginosa*-infected CF patient's alveoli and found that *P. aeruginosa* appeared in aggregates surrounded by a "very thick fibrous mass of exopolysaccharides" (Figure 13) [172].

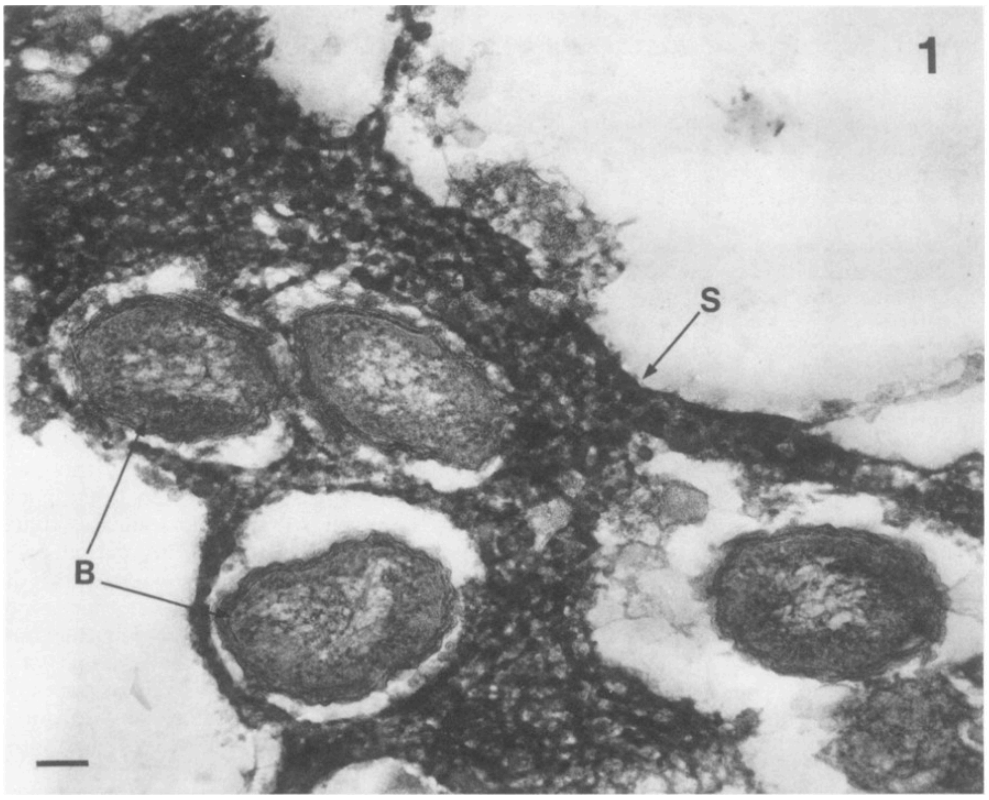

Figure 13: Electron micrograph of a thin section of ruthenium red-alveolar material obtained by postmortem excision from a *P. aeruginosa*-infected CF patients. *P. aeruginosa* aggregates (B) encased by "fibrous mass of bacterial exopolysaccharide" (S). The bar indicates 0.1 µm [172].

In vivo *P. aeruginosa* biofilms were more clearly visualized using peptide nucleic acid-fluorescence in situ hybridization (PNA-FISH), revealing growth within mucus rather than attachment to epithelial cells (Figure 14) [173]. Furthermore, the *S. aureus* biofilm was also localized within the mucus rather than on epithelial cells (Figure 15)[174].

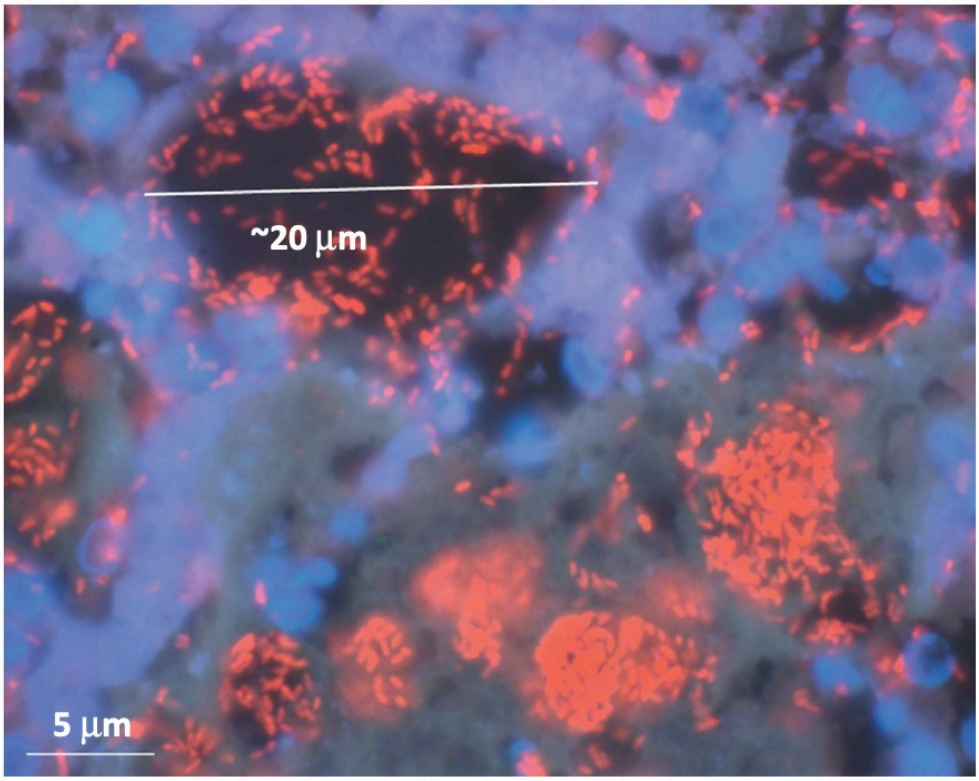

Figure 14: Intraluminal *P. aeruginosa* biofilm (highlighted in red) surrounded by polymorphonuclear leukocytes (shown in blue), visualized using PNA-FISH and DAPI staining [173, 175].

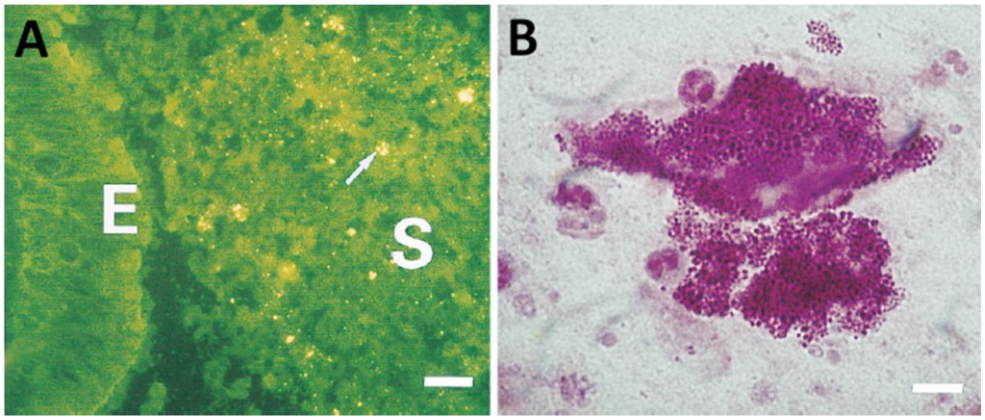

Figure 15: In vivo visualization of *S. aureus* biofilms. (A) Intraluminal *S. aureus* embedded in sputum (S) visualized by indirect immunofluorescence against protein A or teichoic acid, with no adhesion of *S. aureus* to the epithelium (E). Magnification: (A) x400; scale bar: 25 µm. (B) Gram stain of sputum isolated from the bronchus of a patient with CF showing *S. aureus* aggregates. Magnification: x1,000; scale bar: 10 mm [174, 176]

The aforementioned *in vivo* biofilm is visualized based on CF patients infected by single species either *P. aeruginosa* or *S. aureus*. Rudkjøbing et al. in 2014 examined multiple-species biofilms in CF patients, yet it appeared that these species aggregated separately (see Figure 16) [177]. Notably, their approach did not involve the simultaneous use of PNA probes specific to both *P. aeruginosa* and *S. aureus*, potentially limiting the visualization of dual-species aggregates. Up to date, there has been no examination of sputum or explanted lungs from patients with CF who are coinfected with both *S. aureus* and *P. aeruginosa*.

However, some in vitro studies have initiated investigations into dual-species biofilms, prompted by the frequent co-isolation of both species from CF patients. The majority of these dual-species biofilms are grown in conventional media, revealing disparities in gene expression and antibiotic susceptibility between dual-species and single-species biofilms [178]. A limited numbers of dual-species biofilm of *S. aureus* and *P. aeruginosa* were cultured using ASM, with these biofilms being

incubated for only 24 hours [179]. Currently, only one dual-species biofilm model, cultivated in ASM for a longer duration, has been reported by Rosana Monteiro and colleagues [180].

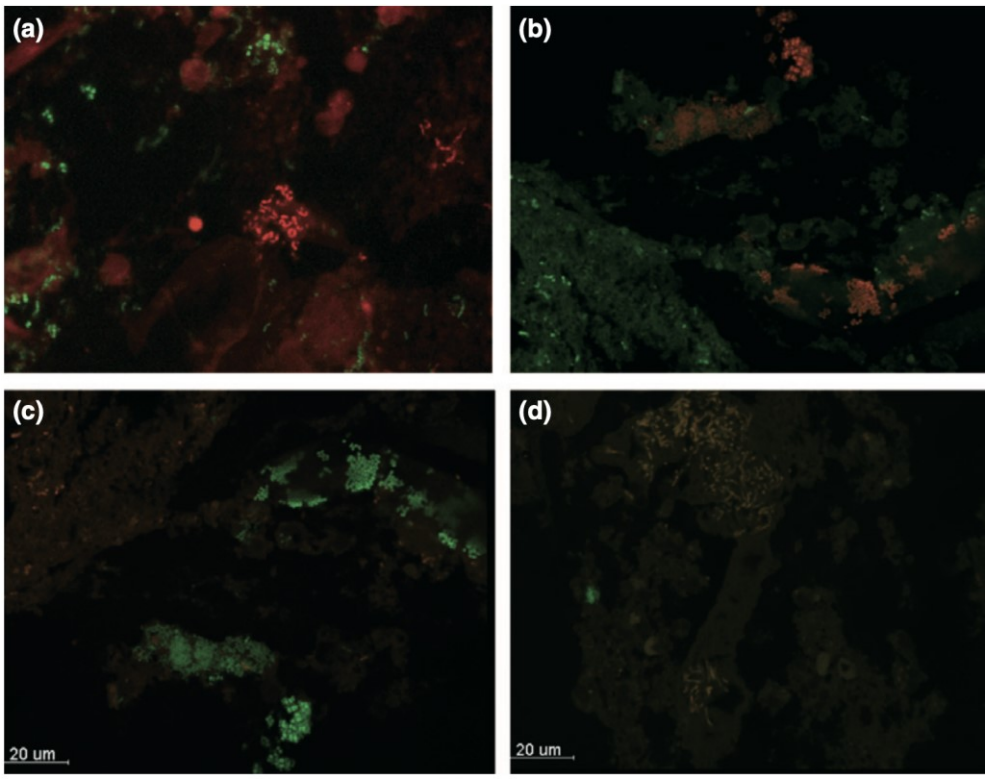

Figure 16: PNA FISH visualization of bacterial aggregates in expectorated sputum of CF patients. In panels (a), (c), and (d), *P. aeruginosa* clusters (red) and other bacterial species aggregates (green) are shown; in panel (b), *S. aureus* cluster (red) and other species aggregates (green) are shown [177].

I.3-c. Consequences of biofilm formation

The formation of biofilm is frequently linked to chronic infections and exerts a considerable impact on the evolution and treatment of such infections. The biofilm

serves as both a physical barrier to protect cells and employs chemical or genetic strategies to reduce susceptibility to antimicrobial agents.

The physically protective function of biofilms includes resistance to external mechanical stress, such as shear stress from surface and fluid flow during biofilm formation, and protection against mechanical clearance forces. Simultaneously, this function prevents the penetration of antibiotics and immune signal molecules while impeding phagocytosis from host cells. The resistance to external mechanical stress is attributed to the inherent viscoelastic properties of biofilms, combining viscous (similar to a fluid's resistance to flow) and elastic (similar to a solid's resistance to deformation) behaviors [181]. The viscoelastic properties are associated with matrix composition and the cross-linking of matrix components [182]. Increased viscoelasticity impedes the diffusion of antibiotics and immune signal molecules within the biofilm. Matrix absorption also restricts antibiotic penetration [183]. The interaction between antibiotics and the matrix, such as eDNA or alginate that can bind to positive charges, can further limits their efficacy, as observed for aminoglycosides [184]. In addition, the biofilm large size obstructs phagocytosis [185], which hinders the immune system's ability to effectively remove bacteria.

In addition to the restricted penetration of antibiotics and immune signal molecules caused by the EPS matrix, the transport of oxygen and nutrients within the biofilm, as well as the diffusion of metabolic by-products, is also hindered [184, 186]. Consequently, a concentration gradient of these molecules is observed within a biofilm. It is important to note that this gradient is not solely a result of restricted diffusion. For example, oxygen is primarily consumed in the upper layers of the biofilm by bacterial cells, creating more anaerobic niches in the deepest parts of the biofilm [167, 187]. Moreover, the accumulation of metabolic by-products in the inner biofilm contributes to a localized acidic environment, leading to a lower pH in the interior [188]. The limited or absent oxygen, the accumulation of toxic

metabolites, and the localized acidic conditions compels bacteria to adopt a dormant lifestyle with lower metabolic activity to withstand harsh conditions. This dormancy diminishes antibiotic susceptibility, given that most antibiotics target actively dividing cells. Persisters represent a subpopulation of dormant cells, constituting less than 1% of the total bacterial population in a biofilm. They can survive exposure to high concentrations of antibiotics by temporarily halting growth and resume normal division once antibiotics are removed [189].

The EPS matrix of biofilms also functions as a reservoir for enzymes capable of degrading antibiotics. These enzymes are predominantly situated in the outer layers of the biofilm, hindering antibiotics from reaching their cellular targets within the biofilm [190]. For instance, beta-lactamases produced by *K. pneumoniae* in biofilms have been shown to efficiently degrade ampicillin, preventing its penetration into biofilm cells [191]. Moreover, mature *P. aeruginosa* biofilms exhibit greater resistance to ceftazidime and meropenem compared to younger biofilms, likely attributed to an elevated presence of β-lactamases in the matrix [192].

Bacteria in biofilms also display differences in gene expression and gene transfer compared to planktonic cells and exhibit a greater mutation frequency [193-195]. This discrepancy in gene expression includes the overexpression of specific resistant genes in biofilms, such as those encoding efflux pumps, leading to reduced susceptibility to antimicrobials [196, 197]. Moreover, horizontal gene transfer is more prevalent in biofilms of both Gram-negative and Gram-positive species [198], promoting biofilm formation [199] and resulting in the acquisition of new resistance genes. These genes may undergo further selection due to exposure to sub-inhibitory antibiotic concentrations favored by the biofilm environment [200, 201].

Interactions between *S. aureus* and *P. aeruginosa* within a biofilm

Additional noteworthy factors contributing to increased tolerance to antibiotics and host immunity include bacterial interactions. These interactions are highly intricated and often depend on the bacterial habitat and specific strains involved [202]. In terms to *S. aureus* and *P. aeruginosa*, earlier studies suggested an antagonistic relationship between them, with *P. aeruginosa* often demonstrating a competitive advantage over *S. aureus*, sometimes even eradicating it. Notably, the prevalence of *S. aureus* is higher in younger patients with CF, while *P. aeruginosa* becomes dominant with increasing age. This pattern appears to support the idea of competition between *S. aureus* and *P. aeruginosa*, despite many cystic fibrosis patients are coinfected by both species. However, later studies have demonstrated successful in vitro coculturing of the two species. Their coexistence influences the secretion and transcription of certain virulence factors, leading to a more severe infection. Moreover, more recent evidence has identified that one bacterial strain often confers resistance or tolerance to another strain against the activity of antibiotics, increasing the difficulty of therapy.

Various small molecules and exoenzymes produced by *P. aeruginosa* are not only toxic to human tissue cells but also impact co-residing *S. aureus*. Here, we present a few well-studied virulence factors against *S. aureus*. The LasA protease degrades pentaglycine in the cell wall of *S. aureus*, leading to *S. aureus* cell lysis and the release of iron ions [119, 203]. Simultaneously, *P. aeruginosa* captures these ions through secreted siderophores (pyoverdine and pyochelin) when iron is limited [204]. Another molecule, PQS, has been reported to also bind to iron, aiding *P. aeruginosa* in taking in iron from the environment [205]. Additionally, QS molecules inhibit *S. aureus* growth. Representative compounds such as HQNO, hydrogen cyanide, and pyocyanin inhibit *S. aureus* growth by interfering with its oxidative respiration and disrupting electron transfer [206]. Moreover, this disruption shifts *S. aureus* towards

a fermentative pathway, presenting a phenotype of small colony variants (SCVs) [207].

Conversely, certain virulence factors produced by *S. aureus* also influence *P. aeruginosa*. The autoinducer-2, a small diffusible quorum-sensing signal molecule produced by *S. aureus*, induces the upregulation of virulence genes in *P. aeruginosa*. These include extracellular protease (*lasB*), rhamnosyltransferase involved in rhamnolipid synthesis (*rhlA*), exotoxins (*exoT*, *exoS*, *exoY*), and phenazines (*phzA1* and *pha2*) [208]. Additionally, N-Acetyl glucosamine enhances the virulence of *P. aeruginosa* by promoting the production of PQS [209]. SpA, a cell-wall-associated extracellular adhesive protein of *S. aureus*, selectively binds to psl, thereby inhibiting the adhesion of *P. aeruginosa*. In the absence of psl, it binds to type IV and impedes the formation of *P. aeruginosa* biofilm [208]. A cocktail of small organic acid molecules produced by *S. aureus*, grown in the presence of a high concentration of glucose, can inhibit the growth of *P. aeruginosa* when exposed to the supernatant of *S. aureus* [210].

Both species strengthen cooperation when facing a hostile environment despite their inherent antagonism. For example, there is HAQ-mediated protection of *S. aureus* from the killing effect of tobramycin [211] and 2-heptyl-4-hydroxyquinoline N-oxide (HQNO) induces multidrug tolerance in *S. aureus* through respiratory inhibition and a reduction in cellular ATP [212, 213]. In dual-species biofilms, polysaccharides like alginate produced by *P. aeruginosa* help *S. aureus* protect itself from antibiotic therapy [214, 215]. But some metabolite compounds produced by *P. aeruginosa* also increase the activity of antibiotics against *S. aureus*. For instance, rhamnolipids and LasA also enhance the killing of *S. aureus* by vancomycin and tobramycin, by promoting lysis and facilitating proton-motive force-independent tobramycin uptake, respectively [216, 217]. It's worth noting that *S. aureus* cells and

their supernatant can also induce the SCVs phenotype and antibiotic tolerance in CF-adapted strains of *P. aeruginosa* [218].

Taken together, the interactions between *S. aureus* and *P. aeruginosa* also contribute to the tolerance of antimicrobial agents, facilitating recurrent, persistent, and chronically severe infections.

I.3-d. Therapy of Biofilm-associated infection

Biofilm is 100 to 1000 times more tolerant to antibiotics than planktonic cells. The treatment of biofilm is challenging due to multiple factors, as mentioned above, such as matrix EPS protection, a heterogeneous microenvironment within the biofilm, lower dividing cells, and interactions between different species. Among adjuvant strategies, enzymes or phages represent an ongoing, promising, and actively researched area. In addition to enzymes and phages, other therapies include mechanically removing biofilm, nanoparticle-metal treatment, photodynamic treatment, quorum sensing inhibitors, and nano-based antibiotic delivery.

Enzyme therapy

Polysaccharides, proteins, and eDNA are the focus as they constitute the primary matrix composition. Accordingly, proteases, glycoside hydrolase enzymes, and deoxyribonucleases are frequently utilized to degrade these three macromolecules, disrupting biofilm structure, and augmenting antibiotic efficacy against biofilm infections. Enzymes, with their specificity and minimized stress production for bacteria, contribute to lower resistance development.

Glycoside hydrolase enzymes

The main polysaccharide produced by *S. aureus,* PNAG, can undergo hydrolysis by Dispersin B (DspB) and PgaB. DspB, a member of glycoside hydrolase family 20 first isolated from *Aggregatibacter actinomycetemcomitans*, exhibits both endo- and exo-glycoside hydrolase activity, leading to the hydrolysis of PNAG in biofilm. When combined with rifampicin or vancomycin, DspB significantly reduces biomass and cell viability embedded in biofilm formed by *S. aureus* using tryptone soya broth medium [219]. Another glycoside hydrolase, PgaB, is a two-domain periplasmic protein featuring an N-terminal deacetylase domain and a C-terminal PNAG binding domain. Encoded by the *pgaABCD* operon in *Escherichia coli* and *Bordetella species*, PgaB can hydrolyze deacetylated PNAG (dPNAG) from *S. aureus*. It also disrupts PNAG-dependent biofilms formed by *Bordetella pertussis*, *Staphylococcus carnosus*, *Staphylococcus epidermidis*, and *E. coli*, enhancing bacterial killing by gentamicin [220]. However, there are currently no directly experimental studies against *S. aureus* biofilm.

For the three polysaccharides (alginate, psl, and pel) produced by *P. aeruginosa*, the degradation requires three glycoside hydrolases: alginate lyase, Psl glycoside hydrolase (PslG), and pel glycoside hydrolase (PelA). Alginate lyase, responsible for degrading alginate, has been isolated from various organisms with different substrate specificities, including algae, marine mollusks, marine and terrestrial bacteria, viruses, and fungi. A purified marine alginate lyase enzyme (AlyP1400) can degrade *P. aeruginosa* biofilm, enhance the bactericidal activity of tobramycin, and modulate the expression of efflux antibiotic resistance-related genes (*bdlA, mexF, mexY, and ndvB*). PslG is a periplasmic glycoside hydrolase encoded by the Psl exopolysaccharide biosynthetic operon, belonging to glycoside hydrolase family 39. After removing the N-terminal transmembrane domain, PslG can hydrolyze Psl polysaccharide produced by *P. aeruginosa*, enhancing the antibacterial effect of

colistin. Moreover, PslG is noncytotoxic and supports immune defense [221]. The last glycoside hydrolase, PelA, is also a periplasmic glycoside hydrolase encoded in the pel exopolysaccharide biosynthetic operons. After removing the N-terminal domain of PelA, the resulting $PelA_h$ was identified, resulting in significant biofilm dispersal within 24 hours. $PelA_h$ also increased the antibiotic efficacy of colistin and neutrophil killing [221].

Proteases

A range of proteases can be applied to disperse biofilm and enhance the effectiveness of antibiotics when used in combination. Here, we focus on several well-established and extensively studied proteases, such as proteinase K, trypsin, pepsin, Peptidase M16, and other proteases secreted by *S. aureus* (including Aureolysin, V8 serine protease, Staphopain A and Staphopain B).

Proteinase K is a broad-spectrum serine protease known for its remarkable pH tolerance and thermostability [222]. It specifically cleaves peptide bonds in proximity to carboxylic groups of aliphatic and aromatic amino acids. This enzyme has the ability to inhibit the formation of new biofilms and disperse preformed biofilms in various bacterial strains. Additionally, when combined with antibiotics, proteinase K demonstrates a synergistic effect in treating mature biofilms. For example, combining proteinase K with daptomycin or vancomycin for treating MASR biofilm showed a significant synergy effect [223].

Trypsin, a serine protease derived from the pancreas, displays specificity in cleaving peptide bonds on the carboxyl side of lysine and arginine residues. Its successful application has been observed in dispersing biofilms formed on teeth and wounds [224, 225]. Bovine trypsin has proven effective in degrading mature biofilms of various Gram-positive and Gram-negative bacterial species. Additionally, when combined with pepsin and carvacrol (a natural phenolic compound), trypsin

demonstrates enhanced efficacy in dispersing mature biofilms of *P. aeruginosa* [226].

Pepsin is a promiscuous endopeptidase characterized by a catalytic aspartate in its active site, facilitating preferential cleavage of Phe (phenylalanine) and Leu (leucine) residues [226]. The preformed *P. aeruginosa* can be effectively eradicated through co-administration of trypsin with pepsin [227].

Peptidase M16 is a metalloprotease secreted by *Microbacterium* sp. SKS10, displaying optimal activity at 60˚C and pH 12 [228]. Additionally, it exhibits remarkable stability, retaining its activity in the presence of various salts and organic solvents. Peptidase M16 effectively disperses mature *S. aureus* biofilms at concentrations lower than trypsin. Furthermore, it can be co-administered with kanamycin to augment antimicrobial efficacy [228].

Another set of proteases secreted by *S. aureus* includes Aureolysin (Aur), V8 serine protease (V8 or SspA), Staphopain A (ScpA) and Staphopain B (SspB). Aur, functioning as an extracellular metalloprotease [229], can effectively inhibit biofilm formation and disperse established biofilms in various *S. aureus* strains when purified [230]. SspA, an extracellular protease, plays a role in preventing the formation of *S. epidermidis* biofilms by degrading Bap, a surface-anchored protein [226]. Both ScpA and SspB are cysteine proteases, with purified ScpA demonstrating the ability to hinder *S. aureus* biofilm formation and disperse established biofilms [231].

Deoxyribonucleases

Enzymes currently involved in the degradation of eDNA comprise DNase I, Nuclease Xds (Xds), Nuclease Dns (Dns), streptodornase (Varidase), and NucB. DNase I, a widely used pancreatic endonuclease, can break down both single- and

double-stranded DNA into oligonucleotides with 5′ monophosphate and 3′ hydroxyl DNA ends [226]. The clinical application of recombinant human DNase I (rhDNase) has proven effective in CF patients, reducing the viscosity of purulent sputum [232]. It's worth noting that since the introduction of elexacaftor/tezacaftor/ivacaftor (ETI) therapy, it has been found that discontinuing rhDNase therapy does not result in a significant difference in lung function compared to continuing DNase I therapy for patients receiving ETI [233]. Additionally, a significant improvement in lung mucociliary clearance was observed after discontinuing DNase I use in patients undergoing ETI treatment [234]. Nucleases Xds and Dns, both produced by V. cholerae, demonstrate the ability to degrade circular and linearized DNA within biofilms, with the deletion of their genes resulting in increased biofilm formation [235]. Streptodornase, a mixture of four DNase enzymes from *P. aeruginosa*, actively disrupts preformed biofilms of *P. aeruginosa* and is employed against focal infections [226]. The metal-dependent nuclease NucB, derived from marine *B. licheniformis*, is notable for effectively degrading preformed biofilms of bacterial strains isolated from chronic rhinosinusitis infections [236, 237]. Investigation of the in vivo application of these enzymes, apart from DNase I, is currently limited.

Phage therapy

Phages are viruses that infect bacteria and possess typical viral characteristics, including relatively small genomes, replication occurring solely within host cells, extensive utilization of host machinery for their replication, and a high degree of specificity for host cells.

Infection initiates with the attachment of the phage particle to its host cell through the specific recognition of a receptor on the host surface, followed by the delivery of phage nucleic acids into the infected cell. Once inside the bacterium, the phage assumes control of the bacterial cell, commandeering its cellular components, and

deactivating its defense mechanisms. Phage genes are expressed, and the phage genome undergoes replication, eventually being packed into self-assembled phage particles. The lytic infection cycle concludes with progeny phage particles emerging from the cell, typically involving cell lysis facilitated by phage proteins (Figure 17A) [238]. Phages display diversity in both morphology and genomes. Over 95% of the phages isolated to date possess linear, double-stranded DNA (dsDNA) genomes packed into a tailed proteinaceous capsid [238]. Other groups of phages may feature non-tailed capsids with dsDNA genomes or non-tailed capsids with single-stranded DNA (ssDNA) or RNA genomes (Figure 17B) [238].

Phages were extensively used to treat bacterial infections in humans and animals in the 1930s, well before penicillin became commercially available. However, phages fell out of favor in the West when penicillin was introduced to the market in the early 1940s due to its broad-spectrum activity against bacteria compared to phages. The post-war hostility between the United States and the Soviet Union not only fuelled distrust of scientific advancements from the former Soviet Bloc but also perpetuated suspicions regarding the therapeutic use of phages for decades [239, 240]. Nevertheless, with the rise of antibiotic-resistant bacteria and a decline in the discovery of new antibiotics, phages have experienced a revival. An increasing number of successful phage therapies have been reported, marking a renewed interest in their potential medical applications.

The antimicrobial mechanism of phages involves two main enzymes: depolymerases and lysins. Depolymerases, often displayed at the phage's tip as tail fibers, degrade capsular polysaccharides. Lysins, encoded either inside or on the virion's tail, cleave the peptidoglycan cell wall from the inside and outside, respectively [241]. Lysin-induced host cell lysis prevents biofilm formation, while depolymerase's degradation of matrix EPS destroys biofilm structure. Additionally, phages can penetrate existing

biofilm, aiding in its destruction. Notably, phages can kill dormant cells within biofilm [242].

Biofilm therapeutic approaches using phages are classified into five groups (Figure 17B): Bacteriophage therapy, including single phage and phage cocktail, endolysin or depolymerase combination therapy with other antimicrobial agents, and genetic medication. Phage cocktails have an advantage over single-phage treatments as bacteria easily develop resistance to phages. Currently, the most common therapy involves a phage cocktail in combination with other antimicrobial agents such as antibiotics. Phages have been applied to various in vitro studies of biofilm-related infections, including CF infection, urinary tract infection, orthopedic infection, and oral infection [243, 244].

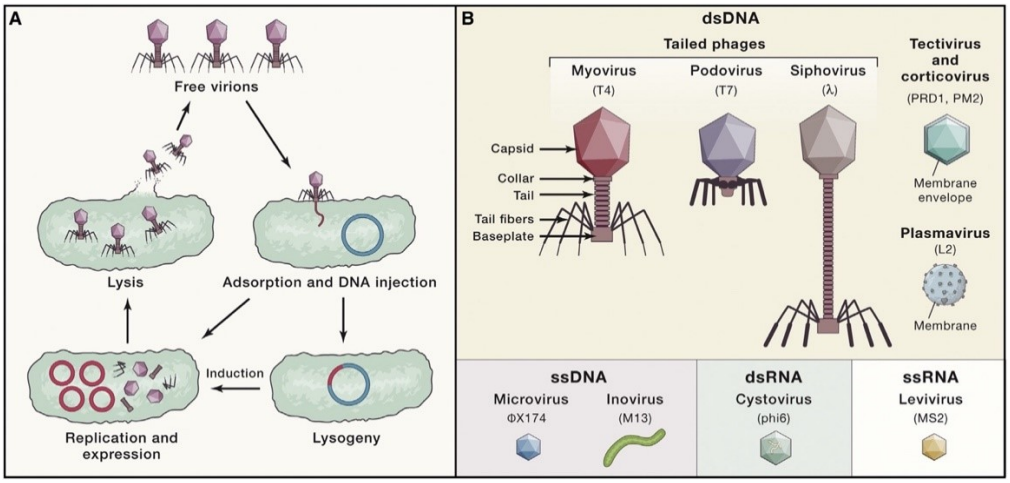

Figure 17: Phage Life Cycle and Morphologies. (A) Overview of the phage life cycle; (B) Phage taxonomy categorized by morphology and genome composition, with a representative phage indicated in parentheses for each taxonomical group [238].

Other therapy strategies

Other strategies for combating biofilms include mechanical removal, nanoparticle-metal therapy, photodynamic treatment, quorum sensing inhibitors, and antibiotics used with a Nano-Based Delivery approach.

Mechanically removing

Biofilm formed on biotic surfaces such as teeth, implanted devices, and industrial pipettes can be effectively treated through mechanical removal processes. This involves physically disrupting and eliminating the biofilm, commonly achieved through actions like scraping, brushing, or utilizing specialized tools tailored for this purpose.

Nanoparticle-metal

Metal oxygen nanoparticles can effectively penetrate biofilms, inhibiting bacterial growth through three well-established mechanisms. These include (1) inducing mechanical cell wall damage through electrostatic interaction, (2) generating reactive oxygen species (ROS) to induce oxidative stress, and (3) causing metal cation leakage, disrupting protein functioning and cell structure. Among metal oxide nanoparticles (NPs), Cuo and Zno nanoparticles have demonstrated robust antibacterial qualities and the most potent antibiofilm properties when compared to other nanoparticle-metals such as MgO and TiO2. However, a significant challenge in the therapeutic use of nanoparticles remains concerns related to systemic safety and potential long-term impacts on the body [245].

Photodynamic treatment

Photodynamic treatment relies primarily on light, a photosensitizer, and oxygen. A photosensitizer can generate reactive oxygen species (ROS) when exposed to visible

or infrared light in the presence of oxygen. The produced ROS has the ability to oxidize cellular macromolecules such as lipids and proteins involved in membrane function, ultimately leading to bacterial death [246].

Quorum Sensing Inhibitor

Quorum Sensing (QS) system regulates biofilm development in most of strains. For example, in *Pseudomonas aeruginosa*, QS products such as pyocyanin and HQNO actively contribute to promoting biofilm formation. Additionally, *P. aeruginosa*-produced rhamnolipids, along with *Staphylococcus aureus*-produced PSM, act as surfactants, assisting in the facilitation of biofilm spread. Consequently, inhibiting the QS system emerges as a promising strategy to reduce biofilm formation. This involves mechanisms such as inhibiting signal molecule synthesis, enzymatic degradation of signal molecules, competing with signal molecule-receptor analogs, and obstructing autoinducer (AI)-receptor complex formation (e.g., by blocking AI-receptor complex assembly). Various QS inhibitors (QSIs) are employed for this purpose, encompassing natural molecules (e.g., flavonoids, phenols, phenolic acids, saponins, coumarins, tannins, terpenoids, alkaloids, and polyacetylenes) [247]. Additionally, chemical synthesis of molecules, such as Norspermidine, which inhibits QS gene expression in *P. aeruginosa (lasI, lasR, rhlI, rhlI, rhlR,* and *mvfR* genes), is explored [248]. Inflammation agents like Aspirin, meloxicam, and piroxicam have shown efficacy in inhibiting *P. aeruginosa* QS signaling molecules and biofilm growth [248].

Nano-Based Antibiotic Delivery

Nano-Based Antibiotic Delivery overcomes antibiotic inactivity and interactions with extracellular polymeric substances (EPS), enabling antibiotics to reach deeper layers of biofilm. Nanoparticles possess the capability to penetrate biofilms, addressing this challenge [245]. This approach offers several advantages, including

improved stability, targeted delivery, controlled antibiotic release, and enhanced bioavailability. As an illustration, erythromycin, clindamycin, amoxicillin, and vancomycin demonstrated increased efficacy against *E. coli* and *S. aureus* when combined with Silver Nanoparticles (AgNPs) [249].

The treatment of biofilm infections needs to be tailored, as different infection sites require different therapeutic strategies. For instance, while biofilms on implanted devices can often be mechanically removed, this is not the case in CF lung infections. Specifically targeting biofilms in the context of patients with CF, these strategies incorporate the use of enzymes, phages, QS inhibitors as adjuvants to antibiotics, and enhanced antibiotic delivery. Additionally, compounds that reduce intracellular cyclic-di-GMP (c-di-GMP) levels and disrupt iron metabolism show promise in combating biofilms. C-di-GMP is involved in regulating genes expressed in the biofilm lifestyle, and lower levels result in reduced biofilm formation [250]. Nitric Oxide (NO) has been shown to reduce the level of c-di-GMP and increase susceptibility to antibiotics [251]. A clinical trial of high-dose (160 ppb) inhaled NO in CF patients is currently underway in the USA [252].

Furthermore, clinical trials of anti-pseudomonal bacteriophages in CF patients with chronic infections are ongoing in phase 1a/2b [252]. It's worth noting that currently, the most common strategies for treating biofilms in CF patients remain antibiotics or dual antibiotic combinations (such as colistin/tobramycin), despite their demonstrated lower efficacy.

Chapter II. Objectives

The overall aim of this thesis was to establish an in vitro dual-species biofilm model of *S. aureus* and *P. aeruginosa* relevant to lung infections in CF patients and to use it to evaluate the potential therapeutic efficacy of antibiotics when combined with an adjuvant.

Pathogens primarily exist as biofilms in the mucus of the airways of individuals with CF. The formation of biofilms in these airways leads to persistent, chronic, and recurrent lung infections in individuals with CF, contributing to severe respiratory disease. Despite advancements in treatment, respiratory disease resulting from bacterial infections continues to be the primary cause of morbidity and mortality in individuals with CF. This underscores the importance of seeking and optimizing anti-infective strategies to combat biofilm-infected airways in CF patients. To screen and select potential innovative strategies, the establishment of a versatile in vitro dual-species biofilm model, is of utmost importance and is considered a prerequisite.

Antibiotic therapy is constrained due to the protective effect of the matrix, the accumulation of resistance-associated enzymes that deactivate antibiotics within the matrix, and the tolerance of bacterial cells to antibiotics due to altered metabolic activity. Additionally, stagnant mucus in vivo amplifies tolerance to antibiotics. Combining antibiotics with agents capable of destructuring the matrix is therefore an appealing strategy, as it could contribute to improve the access of antibiotics as well as of nutrients to bacterial cells, possibly improving antibiotic activity and reversing tolerance.

In this context, three specific aims were pursued in this thesis (Figure 1):

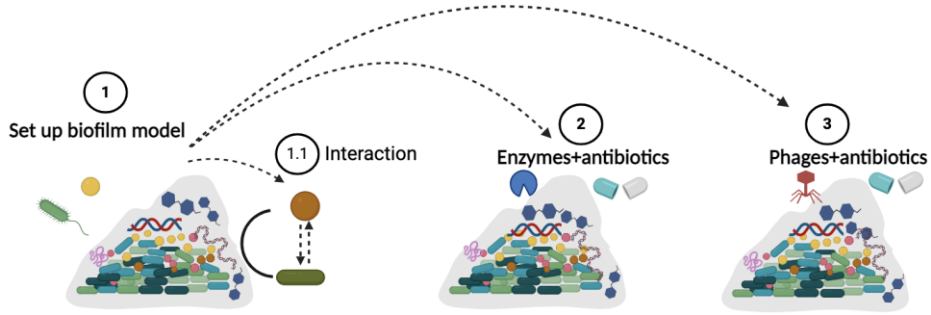

Figure 1. Schematic representation of the objectives of this thesis

Design and Development of Dual-Species Biofilm Model (Chapter III, Paper 1):

The first aim is to set up an in-vitro dual-species biofilm model using two dominant pathogens relevant to lung infection of CF patients, namely *S. aureus* and *P. aeruginosa*. Artificial Sputum Medium (ASM+) was employed for biofilm cultivation to closely replicate the habitat environment where bacteria grow and aggregate in vivo. This choice was based on ASM+'s similarity in constituents and viscoelastic properties to the sputum found in CF patients. Moreover, the colonization sequences of both species in individuals with CF were replicated by inoculating *S. aureus* before *P. aeruginosa*. Following the establishment of the biofilm model, the interaction between *S. aureus* and *P. aeruginosa* was investigated, particularly with coisolates pairs from the same patients, and the mechanisms involved in their interaction were explored. The interplay between these two species not only is associated with stability of the biofilm model but also contributes to the bacteria's tolerance to antibiotics.

Potentiation of Antibiotic Activity with Enzymes (Chapter III, Paper 2):

The second objective is to enhance the activity of antibiotics by combining them with enzymes that degrade the EPS matrix. Our focus is on degrading eDNA and alginate polysaccharides, as both are dominant components of the matrix and are associated with the higher-viscoelastic properties of mucus in the airways of CF patients. Additionally, common isolates of *P. aeruginosa* from CF patients exhibit a mucoid phenotype and overproduce alginate. To address this, Deoxyribonuclease I (DNase I or dornase-α) and alginate lyase, specifically targeting eDNA and alginate, were selected as adjuvants to antibiotics to improve their activity. It's worth noting that DNase I has been used to clear mucus in the airways of CF patients. Although alginate lyase has not yet been used for patients, in-vitro studies have identified its potential to decrease the viscoelasticity of mucus.

Potentiation of Antibiotic Activity with Phages (Chapter III, paper 3):

The last aim is to enhance antibiotic activity by combining them with phages. As previously discussed in the introduction, phages possess the ability to lyse host cells through the production of endolysins and digest matrix polysaccharides via the production of depolymerases. Additionally, they can target dormant cells within biofilms. Therefore, two phages, specifically targeting *S. aureus* (phage ISP) and *P. aeruginos*a (phage PSP3), were combined with one broad-spectrum antibiotic (ciprofloxacin, ceftazidime, meropenem, or tobramycin) to augment the effectiveness in treating dual-species biofilm.

The main novelties of our work are thus

1. the use of ASM+ to mimic the viscoelastic properties of the sputum of CF patients to develop a dual species biofilm model with co-isolates of *S. aureus*

and *P. aeruginosa* from the same patients. This approach allows to better mimic in vivo conditions than the previously published models.

2. The evaluation of enzymes and phages in this more relevant model, and, for enzymes, the evaluation of the clinical relevance of the active concentrations.
3. The evaluation of a combination of phages targeting respectively each of the two species, and the evaluation of a prescreening test of their activity on planktonic culture as a way to predict their activity on biofilms.

Chapter III. Results

III.1. Dual-Species Biofilm Model and Bacterial Interactions

Adapted from paper:

Reciprocal adaptation of *Staphylococcus aureus* and *Pseudomonas aeruginosa* co-isolated from same patients with Cystic Fibrosis in a new model of dual species biofilm grown in artificial sputum medium

Zhifen Wang,[1] Emily Giedraitis,[2] Christiane Knoop,[3] Daniel J. Breiner,[2] Vanessa V. Phelan,[2] Françoise Van Bambeke. [1,*]

[1] Pharmacologie cellulaire et moléculaire, Louvain Drug Research Institute, Université catholique de Louvain, Brussels, Belgium

[2] Department of Pharmaceutical Sciences, Skaggs School of Pharmacy and Pharmaceutical Sciences, University of Colorado Anschutz Medical Campus, Aurora, Colorado, USA

[3] Erasme Hospital, Université libre de Bruxelles, Brussels, Belgium

Submitted for publication in February 2024.

III.1.a. Abstract

Co-infections by *Staphylococcus aureus* and *Pseudomonas aeruginosa* are frequent in patients with cystic fibrosis. They represent a therapeutic challenge, notably due to the formation of mixed-species biofilms with heightened antibiotic tolerance. *In vitro* models have been developed to study interspecies interactions in biofilms, but few none culture clinical isolates showing characteristic phenotypes, including mucoid, pigmented, or SCV character in a culture medium representative of the sticky mucus found in the patients' airways. Here, we established a dual species biofilm model grown in artificial sputum medium, where *S. aureus* was inoculated before *P. aeruginosa* to facilitate the maintenance of both species over time. It was successfully applied to ten pairs of clinical isolates exhibiting different phenotypes. Cross-cultures involving strains from different pairs or a combination of one clinical isolate and a reference strain were less favourable than co-cultures of co-isolates from a single patient, suggesting that cross-adaptation takes place *in vivo*. Mechanistic investigations suggested that this cross-adaptation is unrelated to the quantities of exoproducts produced by *P. aeruginosa,* but rather is associated to a reduced motility in *P. aeruginosa* clinical isolates, and, on the *S. aureus* side, to an increased motility in the presence of *P. aeruginosa* rhamnolipids, an overexpression of the *crtN* gene involved in the synthesis of the anti-oxidant pigment staphyloxantin, or a downregulation of *spa* gene encoding protein A, which inhibits biofilm formation in *P. aeruginosa*. This clinically-relevant model provides a useful tool for exploring interspecies interactions in the context of cystic fibrosis.

Keywords: cystic fibrosis, dual species biofilm, *Staphylococcus aureus, Pseudomonas aeruginosa,* artificial sputum medium, motilit

Highlights

- *S. aureus* and *P. aeruginosa* are often co-isolated in sputum from patients with CF.
- A dual-species biofilm model in artificial sputum medium was set up.
- Better survival was observed for co-cultures of co-isolates than for reference strains.
- *P. aeruginosa* adaptation involves downregulation of QS genes and reduced motility.
- *S. aureus* adaptation includes downregulation of *spa*, overexpression of *crtN* and spreading motility in the presence of rhamnolipids.

III.1.b. Introduction

Cystic Fibrosis (CF) is an autosomal genetic disease caused by mutations in the cystic fibrosis transmembrane conductance regulator (CFTR) gene encoding the epithelial ion channel that normally transports chloride and bicarbonate [253]. Mutations in CFTR lead to the accumulation of thick mucus in airways of patients with CF [254], which is a beneficial niche for colonization by multiple bacteria. Among them, *Staphylococcus aureus* and *Pseudomonas aeruginosa* are the most prevalent [33]. *S. aureus* is predominant in children and adolescents (present in 80% of the patients) while *P. aeruginosa* is more prevalent in adults (present in 70% of the patients). It has therefore been suggested for a long time that *P. aeruginosa* can replace *S. aureus* during the course of the infection. This hypothesis was based on *in vitro* works having demonstrated competitive interactions between the two species [255-257]. Yet, both species are also isolated concomitantly in the sputum of 20-30% of the patients with CF [33]. A longitudinal study of 134 CF patients confirmed that both species can remain stable over years in sputum cultures, with even an increase

in the proportion of patients being co-infected over the 10 years period of the survey (from 30 to 50%) [258].

In spite of this increasingly recognized importance of coinfections in multispecies biofilms, many studies still focus on single species biofilms of either *S. aureus* or *P. aeruginosa* (see for recent examples [259-262]). However, it is well established that these two species commonly exist as aggregates embedded in a self-produced matrix, known as biofilms [263]. When polymicrobial, these infections are more virulent [264], associated with higher morbidity and mortality [265, 266], and complicate the antibiotic treatment [267]. Although a variety of in vitro models of dual species biofilms have been developed, they typically result in *P. aeruginosa* overgrowing *S. aureus* [268, 269], use reference strains rather than clinical isolates [255, 270, 271] and/or grow biofilms in conventional broth media [215, 255, 268]. Therefore, these conditions do not mimic the nutrient conditions or microbial genetic diversity prevailing in the lung of the patients with CF, both of which are well described to influence bacteria behavior [272-274].

In this context, the aim of this study was to develop a dual species biofilm model including *S. aureus* and *P. aeruginosa* grown in an artificial sputum medium previously shown to mimic the viscoelastic properties of the mucus of patients with CF [275]. We compared the growth, biofilm formation, aggregation, and chemical interactions of reference strains with clinical isolates collected in pairs from patients with CF. In brief, we show that biofilms were more stable when formed by co-isolated pairs than by reference strains and we identify some of the factors that could contribute to this cross adaptation.

III.1.c. Materials and methods

Laboratory strains and clinical isolates

Laboratory strains *P. aeruginosa* PAO1 and *S. aureus* ATCC25923 were selected as reference strains to establish dual species biofilm. Ten pairs of *S. aureus* and *P. aeruginosa* were collected as routine samples and isolated concomitantly from bronchopulmonary-sputum of seven CF patients (Table 1).

Artificial sputum medium

Artificial sputum medium (ASM+) was prepared as reported by Diaz Iglesias *et al.* [275], with the following modifications: agar was bought from Sigma-Aldrich (St Louis, MO) rather than from Becton Dickinson (Franklin Lakes, NJ), and pH was adjusted to a range of 7.1-7.4 with 0.2 N of NaOH. The prepared ASM+ were stored at 4°C for a fortnight and thoroughly homogenized by agitation before use. It was used in a period of 2 months.

Development of dual species biofilms

S. aureus or *P. aeruginosa* were suspended in cation-adjusted Mueller Hinton Broth (MHB-Ca; Sigma-Aldrich) from overnight cultures on Trypticase soy agar (TSA; VWR) and adjusted to OD_{620nm} of 0.5 (or 2.6 McFarland units). Subsequently, *S. aureus* was diluted 10-fold in MHB-Ca (final inoculum: approx. 2.1 x 10^7 CFU/mL), and *P. aeruginosa,* 20- (1.35 x 10^7 CFU/mL), 200- (1.35 x 10^6 CFU/mL), or 1000-fold (2.7 x 10^5 CFU/mL) in MHB-Ca. For protocol #1 [276], *S. aureus* at 2.1 x 10^7 CFU/mL and *P. aeruginosa* at each overmentioned dilution were mixed separately at an equal volume ratio, then 200 µL were inoculated in the wells of 96-well polystyrene plates (VWR) and incubated for 2 h to favor attachment, after which MHB-Ca was replaced by ASM+, and biofilms were further incubated for 24, 48, or

72h (Fig. 1E). In protocol #2 [255], *S. aureus* (approx. 2.1 x 10^7 CFU/mL) was inoculated as described for protocol #1 (200 µL per well) and incubated for 24 h. After which, 20 µL of *P. aeruginosa* at 1.35 x 10^7 or 2.7x10^6 CFU/mL was added to the pre-established *S. aureus* biofilm, and 180 µL of ASM+ was also added to reach a volume of 200 µL per well (Fig. 1E). ASM+ was renewed every 24 h up to 120 h (5 days), with parts of the wells harvested every 24 h.

Quantification of biofilms

Biofilms were quantified using bacterial counts and total biomass. For CFU counting, biofilms were washed once with sterile phosphate buffer saline (PBS) and mechanically disrupted using the tip of a disposable bacterial inoculation loop, then re-suspended in 200 µL PBS and sonicated for 30 s at 60% amplitude using a Q700 sonicator (QSonica). Resuspended bacteria were diluted 10 to 10^6 times in PBS, and 50 µL were plated on Mannitol Salt Agar (MSA) for *S. aureus* or Pseudomonas Isolation Agar (PIA) for *P. aeruginosa*. CFU were counted after 24 h for PAO1 or at least 48 h for all *S. aureus* and *P. aeruginosa* clinical isolates, depending on sufficient growth for accurate counting

For estimation of the total biomass, washed biofilms were dried at 60˚C for at least 24 h, and 0.5% (V/V) crystal violet (100%, Sigma-Aldrich) in water was added to 96-well plates (200 µL/well)[275]. The plates were incubated for 10 min at room temperature, non-bound crystal violet was discarded by inversion of plates and the stained biofilm was rinsed with running water, after which bound crystal violet was re-solubilized in 200 µL of 66% (V/V) acetic acid and incubated 1 h in the dark. Biofilm biomass was quantified by measuring crystal violet absorbance at 570 nm in a SpectraMax M3 plate reader (Molecular Devices LLC). Wells containing ASM only were used as blanks, and the absorbance measured in these wells removed from all values.

Confocal laser scanning microscopy of spatial organization for *S. aureus* and *P. aeruginosa* within biofilms after DNA-FISH labelling

Dual species biofilms were grown as described above on 12 mm coverslips placed in 24-well polystyrene plates for 72 h. After 72 h, biofilms were washed once in PBS and fixed with 4% formaldehyde in PBS for 1 h at room temperature. The fixed biofilms were incubated in pre-heated permeabilization reagent (1000 µL per well) (Tris-HCl 20 mM, EDTA 5 mM, lysozyme 1 mg/mL (Sigma-Aldrich), lysostaphin 0.1 mg/mL (Sigma-Aldrich), pH 7.7) for 10 min at 37°C, after which hybridization buffer (Tris-HCl 20 mM, NaCl 900 mM, SDS 0.1 mg/L, formamide 20% V/V, pH 7.7) without DNA-probe was added and incubated for 15 min at 46°C [277]. Then, the biofilm was hybridized with *S. aureus*-specific DNA-FISH probe (5'-Cy5-TCC TCC ATA TCT CTG CGC-3' [278]) and *P. aeruginosa*-specific DNA-FISH probe (5'-Atto 488-GGT AAC CGT CCC CCT TGC-3' [279]) for 3 h at 47°C in darkness. Non-bound probes were removed by incubation in washing buffer (Tris-HCl 20 mM, EDTA 5 mM, SDS 0.1 mg/L, NaCl 450 mM, pH 7.7) for 15 min at 46˚C. Then, coverslips were mounted by inversion on a 100 mm glass coverslip with DAKA mounting oil. The stained dual species biofilms were observed in an inverted cell observation spinning disk microscope (Carl Zeiss) with an oil immersion 40x objective. *P. aeruginosa* targeted by PA-Atto 488 was detected in the green channel (excitation/emission, 488/533 nm), and *S. aureus* targeted by Sa-cy5, in the red channel (excitation/emission, 633/678 nm), and biofilms were analyzed using Z-stacks scanning model. 3D- images of biofilms were obtained using the ZEN 2.6 (blue edition) software.

Quantitative reverse Transcription PCR analysis

The relative expression of *sigB, icaA, clfA, and spa* genes of *S. aureus* VBB496*, crtM, crtN, krtA and agrA* of *S. aureus* UEQ310, and *lasI, pvdS, pqsL* and *pqzH,*

acoR and PA4148 of *P. aeruginosa* VBB496 was analyzed in different biofilms (see primers in Table S1). Mature biofilms were washed once in PBS after 72 h of incubation and recovered by vigorous pipetting. The recovered biofilms in the different wells were pooled in 2 mL of tubes and centrifuged at 10,000 g for 15 min at 4°C, after which the pellet was suspended in an appropriate volume of PBS, then transferred to a new tube and centrifuged at 10,000 g for 10 min. The pellet was treated with 300 µL of 3 mg/mL lysozyme in TE buffer (Tris-HCl 10 mM, EDTA 1 mM (Thermofisher Scientific) at pH 8.0) for 30 min at room temperature. When *S. aureus* was present in the sample, a final concentration of 100 µg/mL lysostaphin (Sigma Aldrich) was added. Total RNA was extracted from dual species biofilms using the Invitrap Spin Cell RNA mini kit (Invitek Molecular) according to the manufacturer's instructions, followed by DNase (TURBO DNA-free kit, Thermofisher Scientific) treatment 30 min. cDNA synthesis was performed using the First Strand cDNA Synthesis kit (Roche, Basel, Switzerland) following the manufacturer's instructions.

The relative quantification of cDNA was performed by real-time PCR with detection by SYBR Green Supermix (Bio-Rad). Data were expressed as the relative fold change in gene expression determined via 2−ΔΔCT method [280] using *gmk* and *16s-RNA* as a housekeeping gene for *S. aureus* and *P. aeruginosa*, respectively.

Metabolomics analysis of *P. aeruginosa* exoproducts

Mono-culture and co-culture biofilms were cultured following the procedures outlined in protocol 2#, for 24 h, 48 h, and 72 h after *P. aeruginosa* inoculation. At each time point, biofilms were mechanically disrupted and homogenized by pipetting up and down with tips. The resulting suspensions were then transferred into 96-well polypropylene plates (100 µL per well), supplemented with 10 µM nalidixic acid as an internal stand, and chemically disrupted using an equal volume of 1:1

ethyl acetate (EtOAc, VWR HiperSolv Chromanorm) and methanol (MeOH, Fisher Scientific Optima-grade), followed by 10 min of sonication in a water bath sonicator. All samples were dried overnight in a chemical hood and stored at -20°C until use. Samples were resuspended in resuspended in 100% MeOH containing 1 μM glycocholic acid (Calbiochem; 100.1% pure). Mass spectrometry data acquisition was performed using a Bruker Daltonics Maxis II HD quadrupole time of flight (qTOF) mass spectrometer equipped with a standard electrospray ionization (ESI) source as previously described [281]. Briefly, the mass spectrometer was tuned by infusion of tuning mix ESI-TOF (Agilent Technologies) at a 3-ml/min flow rate. For accurate mass measurements, a wick saturated with hexakis (1H,1H,2H-difluoroethoxy) phosphazene ions (Apollo Scientific, m/z 622.1978) located within the source was used as a lock mass internal calibrant. Samples were introduced by an Agilent 1290 ultraperformance liquid chromatography (UPLC) system. Optima-grade (Fisher Scientific) acetonitrile (ACN), formic acid (FA), and water were used for UPLC separation. Extracts were separated using a Phenomenex Kinetex 2.6-mm C18 column (2.1 mm by 50 mm) using a 9 min, linear water-ACN gradient (from 98:2 to 2:98% water/ACN) containing 0.1% FA at a flow rate of 0.5 ml/min. The mass spectrometer was operated in data-dependent positive ion mode, automatically switching between full-scan MS and MS/MS acquisitions. Full-scan MS spectra *(m/z* 50 to 1,500) were acquired in the TOF-MS, and the top five most intense ions in a particular scan were fragmented via collision-induced dissociation (CID) using the stepping function in the collision cell. Data for PA mix, a set of *P. aeruginosa* secondary metabolite external standards, were acquired under identical conditions. Bruker Daltonics CompassXport was used to apply lock mass calibration and convert the data from proprietary format to open-source format. MZmine (version 2.53) [282] was used to perform feature finding and the resulting feature table was normalized to the abundance of the internal standard (nalidixic acid). Identification of features in the molecular network as metabolites [283] was accomplished by comparing the

experimental data (exact mass, MS/MS fragmentation, and retention time) to (i) the data acquired for the PA Mix standards (level 1 annotation) or (ii) reported structural data [284, 285] for features with MS/MS spectral matches to the GNPS libraries [286] (level 2 annotation) using GNPS Dashboard [287]. Principal components analysis was performed using MetaboAnalyst 5.0 [288]. Comparison of relative abundance of select *P. aeruginosa* secondary metabolites between samples was performed using GraphPad Prism (version 9.3.1).

Preparation of cell-free supernatants of biofilm cultures

Single or dual species biofilms were cultivated following the conditions described in protocol #2 and incubated up to 72 h, after which supernatants were collected, mixed by vigorous pipetting and centrifuged at 12,000 g for 20 min at 4 °C. The collected supernatants were then filtered (0.22 µm-pore-size filter (Merck Millipore)) and stored at -20°C until use.

Effect of biofilm supernatants on *S. aureus* viability

The effect of *P. aeruginosa* biofilm supernatant on *S. aureus* growth was assayed on agar plates. Twenty milliliters of Trypticase soy agar (TSA) were poured in a 90 mm deep Petri dishes (Sarstedt) and dried for 15 min. During this time, *S. aureus* suspension at 10^8 CFU/mL was prepared in MHB-Ca and diluted 10-fold in fresh liquid TSA below 60 °C. Five mL of this suspension was added and evenly spread on top of the dried TSA, followed by another 15-minute drying period. Paper discs pre-soaked in the *P. aeruginosa* biofilm supernatant were placed on the TSA plates, which were then incubated for 24 h at 37 °C. Growth inhibition circles were observed and photographed after 24 h.

Effect of exoproducts of *P. aeruginosa* on *S. aureus* viability and biofilm formation

S. aureus at a concentration of approximately 10^7 CFU/mL was incubated for 2 h in MHB-Ca. Following incubation, the medium was removed and replaced with fresh ASM containing 50 µg/mL of pyocyanin or rhamnolipids (Sigma-Aldrich). Plates were incubated for 24 h, after which CFU and biomass were quantified.

Impact of biofilm supernatants or of exoproducts on motility of *P. aeruginosa* or *S. aureus*

P. aeruginosa swarming, swimming, and twitching motilities were assessed as previously described with slight modifications [289, 290]. When applicable, 250 µL of supernatant from *S. aureus* biofilm were transferred into Petri dishes and mixed with 24.75 mL of media (w/v: 0.8% nutrient broth N.2, 0.5% glucose and 0.5% agar for swarming; 0.1% tryptone, 0.05% yeast extract [Becton Dickinson], 0.5% NaCl, 0.3% agar for swimming; 1.5% agar, lysogeny broth [Alfa Aesar] for twitching). Two microliters of an overnight culture of *P. aeruginosa* adjusted to an OD_{620nm} of 0.1 were then either spotted on swarming plates or stabbed onto swimming and twitching plates and incubated overnight. Motility was evaluated by measuring the diameter of growth after overnight incubation.

Motility agar plates for *S. aureus* were prepared as described previously [291]. In brief, 15 g of Tryptone Soy Broth (VWR) and 1.7 g of agar (Becton Dickinson) were dissolved in 460 mL of distilled water and autoclaved. Fourty milliliters of D-Glucose solution at 112.5 mg/mL sterilized by filtration was then added, after which 24.75 mL of media were transferred into 90 mm deep Petri dish with 0.25 mL of supernatant of *P. aeruginosa* biofilm or 1 µg/mL exogenous products of *P. aeruginosa* (pyocyanin, pyoverdine and rhamnolipids), and dried for 30 min. Next, 2 µL of an overnight culture of *S. aureus* in MHB-Ca (diluted to an $OD_{620\ nm}$ of 0.1)

was spotted on the plates center and motility was evaluated by measuring the diameter of growth after overnight incubation.

III.1.d. Results

Development of dual species biofilm model with reference strains

We first used reference strains to establish a dual species biofilm model. In a first protocol (#1; Fig. 1E), *S. aureus* ATCC25923 (diluted 10 times from an OD_{620nm} 0.5 culture) and *P. aeruginosa* PAO1 at different inocula (Fig.1 A-D) were co-incubated. When diluted 20 or 200 times (Fig. 1A-B), PAO1 CFU remained stable over time (8.4-8.8 log_{10} CFU/mL). At a dilution of 1000 times (Fig. 1C), CFU counts were lower at 24 h (7.2 log_{10} CFU/mL) but bacteria grew over time, reaching an abundance close to that measured under the other conditions at 72 h (9.2 log_{10} CFU/mL). *S. aureus* counts at 24 h were slightly higher when PAO1 was more diluted (5.7, 6.2, 6.6 log_{10} CFU/mL, respectively). Notably, *S. aureus* CFU decreased over time and this effect was more rapid when PAO1 inoculum was higher (Fig. 1 B-C). Biofilm biomass remained similar at 48 and 72 h in all conditions (Fig. 1D).

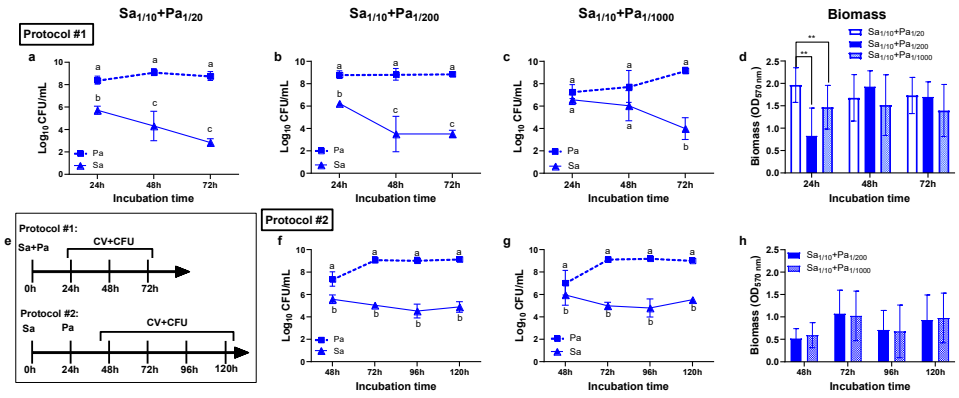

Figure 1. Evolution over time of dual species biofilm growth according to protocol #1 (top) or protocol #2 (bottom). For protocol #1, *S. aureus* ATCC259723 and *P. aeruginosa* PAO1 (OD_{620nm} 0.5) were inoculated simultaneously at a dilution ratio of 10:20, 10:200 or 10:1000 in 96 wells plates, respectively and incubated together during 72h. For protocol #2, *P. aeruginosa* was added after 24 h, after which both strains were incubated together for an additional 96 h period. a-c and f-g: CFU counts per mL of PBS in log scale; d and h: Biomass evaluated by $OD_{570\ nm}$ of crystal violet; e: timeline of the protocols. Values are means ± SEM from 3 or 4 independent experiments performed in triplicates. Statistical analysis (two-way ANOVA with Tukey's multiple comparisons test): for CFUs: comparison over time for two strains: values with different letters are different from one another ($p<0.05$). For biomass, comparison of different inoculum ratios of *S. aureus* and *P. aeruginosa* over time: **, $p< 0.01$ using two-way ANOVA followed by Tukey's multiple comparisons test.

To enhance the survival of *S. aureus* ATCC25923 in the presence of PAO1, *S. aureus* was inoculated first and cultured for 24 h before the addition of PAO1 diluted 200 or 1000 times (protocol #2; Fig. 1E). In these conditions, *S. aureus* ATCC25923 was not outcompeted by PAO1 and remained stable over time, while PAO1 gained 1 $\log_{10}$ CFU during the first 24 h and remained stable thereafter. No remarkable differences were observed for biomass when comparing the two PAO1 inocula or the evolution over time, but variability was noticed among replicate samples. However, biomass was lower than in protocol #1. Lastly, when selectively collecting biofilm formed at the air-surface interface or at the bottom of the plate, we noticed that it was more abundant at the air-surface interface (Fig. S1). On these bases, protocol #2 with *P. aeruginosa* diluted 200 times was selected for further studies.

Application of this model in clinical isolates

Ten pairs of clinical co-isolated *S. aureus* and *P. aeruginosa* from patients with CF (Table 1) were examined for their capacity to form dual-species biofilms over time (Fig. 2).

Table 1. Identification of clinical isolates and phenotype of *P. aeruginosa*.

Isolate ID	Date of isolation	Specific isolates[a]	Name of the corresponding pair
857JBJ	08.04.2021	Sa 857JBJ Pa 857JBJ (pigmented non-mucoid)	857JBJ
UEQ307	25.03.2021	Sa UEQ307 Pa UEQ307-3 (pigmented non-mucoid)	UEQ307-3
		Pa UEQ307-4 (pigmented non-mucoid)	UEQ307-4
		Pa UEQ307-5 (pigmented non-mucoid)	UEQ307-5
UEQ310	29.03.2021	Sa UEQ310 Pa UEQ310 (pigmented mucoid)	UEQ310
VBB496	12.04.2021	Sa VBB496 Pa VBB496 (non-pigmented mucoid)	VBB496
492IVJ	29.03.2021	Sa 492IVJ Pa 492IVJ (non-pigmented mucoid)	492IVJ
UEQ301	15.03.2021	Sa UEQ301 Pa UEQ301 (non-pigmented mucoid)	UEQ301
UEQ306	25.03.2021	Sa UEQ306 Pa UEQ306-2 (SCV)	UEQ306-2
		Pa UEQ306-3 (SCV)	UEQ306-3

[a] Sa: *S. aureus*; Pa : *P. aeruginosa*

P. aeruginosa CFU counts were stable over time (8.5-9 $\log_{10}$ CFU/mL) except for the mucoid non-pigmented strains VBB496 and 492IVJ, which gained respectively approx. 2 and 3.5 $\log_{10}$ CFU/mL between time 48 and 72 h (Fig. 2F and H). *S. aureus* 857JBJ CFU decreased over time (Fig. 2A), but not to the extent observed for ATCC25923. All the other *S. aureus* remained stable over time. *S. aureus* CFU counts (8-8.5 $\log_{10}$ CFU/mL) were close from those of *P. aeruginosa,* except for UEQ307, UEQ310 and UEQ301, which were slightly less abundant during at least part of the incubation (Fig. 2B, E and G). Non-mucoid pigmented 857JBJ and pigmented mucoid UEQ310 produced more abundant biomass compared to other pairs. Biomass was stable over time for all biofilms except for UEQ310, which produced more biomass at 72-120 h (Fig. 2K). These data suggest that this biofilm model can be applied to clinical isolates from CF patients with different phenotypes of *P. aeruginosa.*

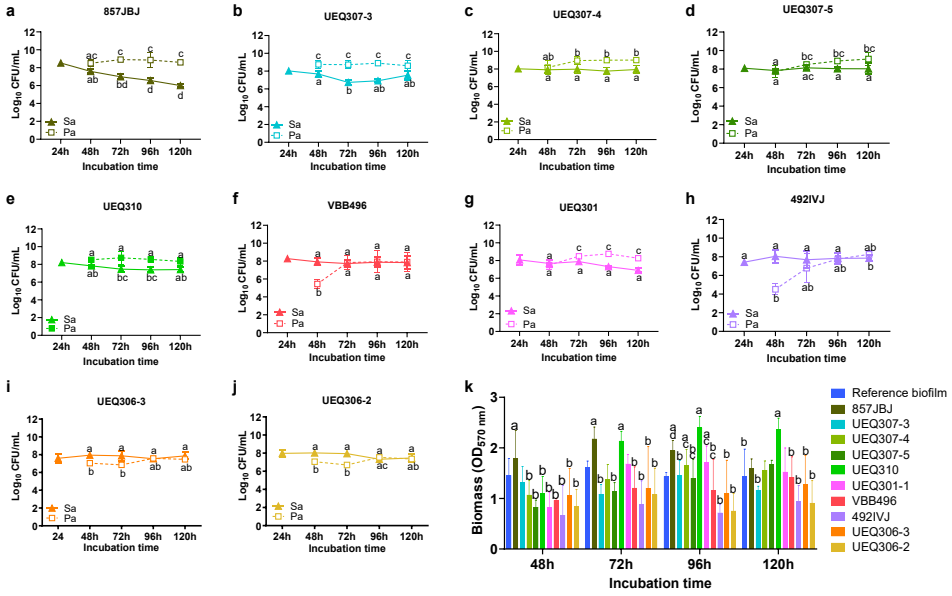

Figure 2. Evolution over time of dual species biofilm growth for clinical co-isolates pairs cultivated according to protocol #2 (panels a-j: CFU/mL) and biomass (panel k: $OD_{570\ nm}$ of crystal violet for the all biofilms compared to reference biofilms (PAO1-ATCC25923)). Phenotype of *P. aeruginosa*: a-d: pigmented non-mucoid; e: pigmented mucoid; f-h: non-pigmented mucoid; i-j: SCVs. Values are means ± SEM from 3 or 4 independent experiments performed in more than triplicates. Statistical analysis for CFU and biomass over time (two-way ANOVA with Tukey's multiple comparisons test): values with different letters are significantly different from each other ($p<0.05$).

Visualization of *S. aureus* and *P. aeruginosa* in dual species biofilm using DNA FISH

We measured the spatial organization of *S. aureus* and *P. aeruginosa* in reference biofilm and biofilms formed by representative non-mucoid or mucoid co-isolated pairs using DNA-FISH (Fig. 3). As clinical pairs, we aimed at selecting one pair with *P. aeruginosa* slightly more abundant than *S. aureus*, and one pair with both species

equally represented, in order to evaluate if this difference could be ascribed to different distribution within the biofilm. The mucoid UEQ310, with pigmented, mucoid *P. aeruginosa*, used in most of the next experiments, could not be included in this specific experiment, as the abundance of the biofilm it forms prevented adequate labeling. We therefore rather used here the non-mucoid UEQ307-3, which shows a similar growth pattern as UEQ310, with *P. aeruginosa* slightly more abundant than *S. aureus* all over the incubation period (see Fig. 2 B vs E). The mucoid VBB496 pair was used as a representative pair for which both species were equally abundant.

The reference strain *S. aureus* ATCC25923 and PAO1 auto-aggregated separately. This phenotype was replicated with the UEQ307-3 co-isolate pair. In contrast, both species co-aggregated together throughout the deepness of the biofilm formed by the VBB496 co-isolates, suggesting a better cross-adaptation in this pair.

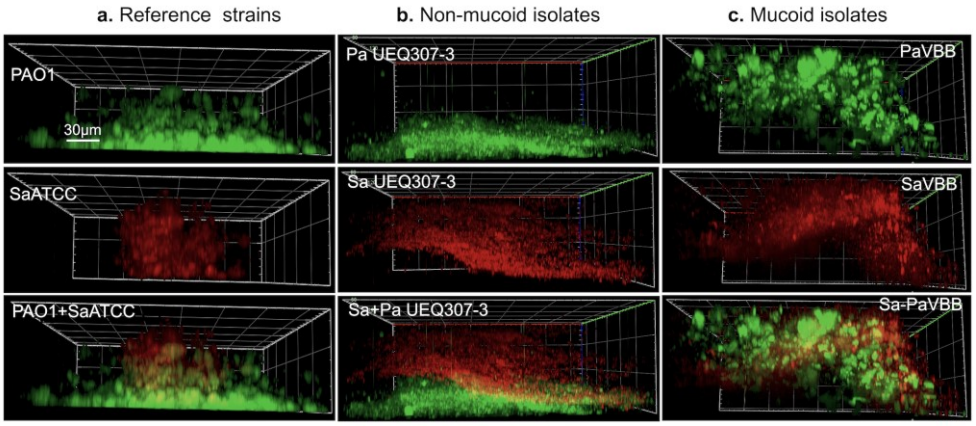

Figure 3. Fluorescence confocal microscopy of dual species biofilm after DNA FISH using *P. aeruginosa*-specific (green signal) and the *S. aureus*-specific probes (red signal). Scale bar (shown in top left panel): 30 µm. (a) reference strains; (b) co-isolates of *S. aureus* and non-mucoid *P. aeruginosa* UEQ307-3; (c) co-isolates of *S. aureus* and non-pigmented mucoid *P. aeruginosa* VBB496. First row: *P. aeruginosa*; Second row*: S. aureus;* Third row: overlay

Cross-strains cocultures

To investigate the reciprocal adaptation of *S. aureus* and *P. aeruginosa* in dual species biofilms, we performed cross-strains cultures, i.e. co-culture of one reference strain with one clinical isolate from the other species or of clinical isolates of *S. aureus* and *P. aeruginosa* from different pairs. Based on the assumption that *P. aeruginosa* pigments are reported as toxic for *S. aureus*, UEQ310 and VBB496 were selected as representative co-isolate pairs with mucoid- pigmented, and mucoid, non-pigmented *P. aeruginosa,* respectively [215, 292].

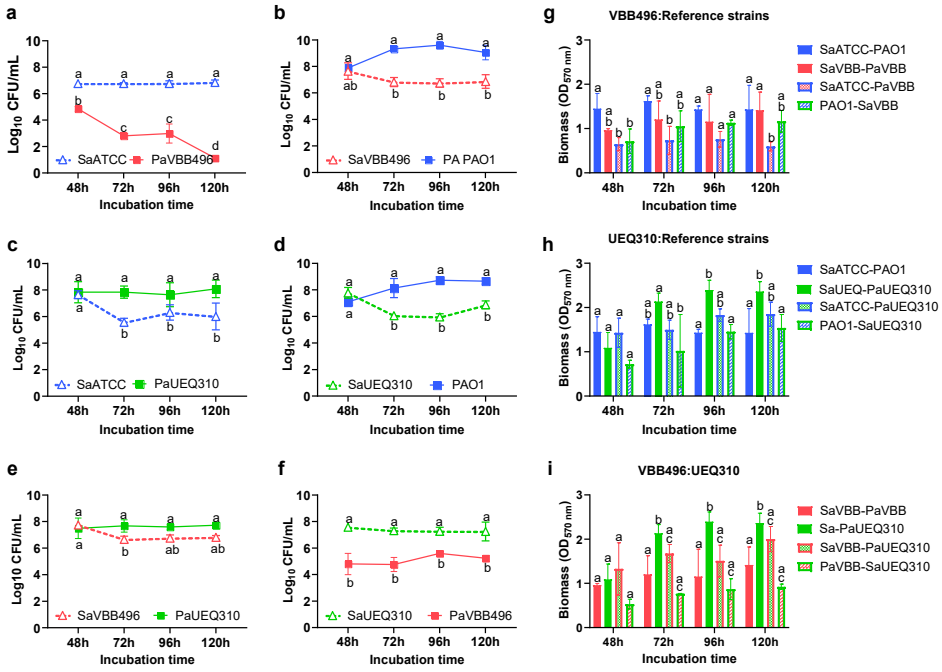

Figure 4. Application of the biofilm model to cross strains cultures, e.g., one clinical isolate cocultured with one reference strain from other species (SaVBB496 + PAO1; PaVBB496 + SaATCC25923; SaUEQ310+PAO1 and PaUEQ310+SaATCC), or co-culture of clinical isolates of *S. aureus* and *P. aeruginosa* from different patients (SaVBB496 + PaUEQ310;

PaVBB496 + SaUEQ310). a-f: Evolution over time of CFU in cross strains cultures; g-i: comparisons of biomass for different dual species biofilms formed by cross strains, reference strains or co-isolated pairs. Statistical analysis (Two-way ANOVA followed by Tukey's multiple comparisons test): Comparison between different culture at a given time point: data with different letters are significantly different from each other ($p<0.05$).

Recovery of *S. aureus* remained steady over time in dual species biofilms across all combinations of cross-strains after 48h of co-culture (i.e. time 72 h) (Fig. 4A-F). *P. aeruginosa* also remained stable and slightly more abundant than *S. aureus* over time, except for VBB496: in co-culture with *S. aureus* ATCC25923, *P. aeruginosa* VBB496 decreased to the point of nearly disappearing at the end of the incubation period (Fig. 4A). Furthermore, *P. aeruginosa* VBB496 showed lower abundance in co-culture with *S. aureus* UEQ310 (Fig. 4F) than in co-culture with the co-isolated *S. aureus* VBB496 (Fig. 2F).

Biomass (Fig. 4G-I) was more abundant in all biofilms formed by *P. aeruginosa* UEQ310, particularly when co-cultured with *S. aureus* UEQ310. Conversely, biomass was the lowest in biofilms formed by *P. aeruginosa* VBB496 co-cultivated with *S. aureus* ATCC25923, likely due to the low viability of *P. aeruginosa* VBB496 in these conditions (Fig. 4A).

Fig. S2 illustrates the same dataset but comparing the abundance of each strain in the different co-cultures and in single species biofilms. It emphasizes that *S. aureus* CFU counts for ATCC25923 and UEQ310 were lower in the presence of PAO1 compared to other conditions. Conversely, *S. aureus* VBB496 survived equally well in both monoculture and in co-culture with any *P. aeruginosa.* This suggests that the laboratory strain PAO1 is more competitive against *S. aureus* than clinical isolates of *P. aeruginosa*, while *S. aureus* VBB496 shows higher tolerance to *P. aeruginosa* toxicity than the other *S. aureus.* Conversely, *P. aeruginosa* VBB496 could only survive and proliferate when co-cultured with the co-isolated *S. aureus,* while the

other *P. aeruginosa* strains were unaffected by the presence of any *S. aureus*. Overall, these results suggest a cross-adaptation between co-isolates clinical strains.

Relative expression of genes in clinical isolates VBB496 vs reference strains

Since clinical isolates of *P. aeruginosa* demonstrated reduced virulence against *S. aureus* compared to PAO1, and clinical isolates of *S. aureus* exhibited enhanced tolerance to *P. aeruginosa* in comparison to the laboratory strain *S. aureus* ATCC25923, we investigated whether this bidirectional adaptation could be linked to changes in the expression of specific genes in *P. aeruginosa,* namely QS genes (*lasI, pvdS, phzH* and *pqsL*) and genes involved in the catabolism of acetoin (*acoR* and *PA4148*), a toxic metabolite produced by *S. aureus* [210] (Fig. 5A). In parallel, we examined genes in *S. aureus* encoding proteins involved in inhibition of *P. aeruginosa* biofilm formation (*spa*), and biofilm development of *S. aureus* (*icaA, clfA, sarA*) (Fig. 5B). All data were acquired using biofilm samples at 72 h. We focused on reference strains and on the clinical pair VBB496, based on the strong phenotype of *P. aeruginosa* VBB496 in cross-culture experiments.

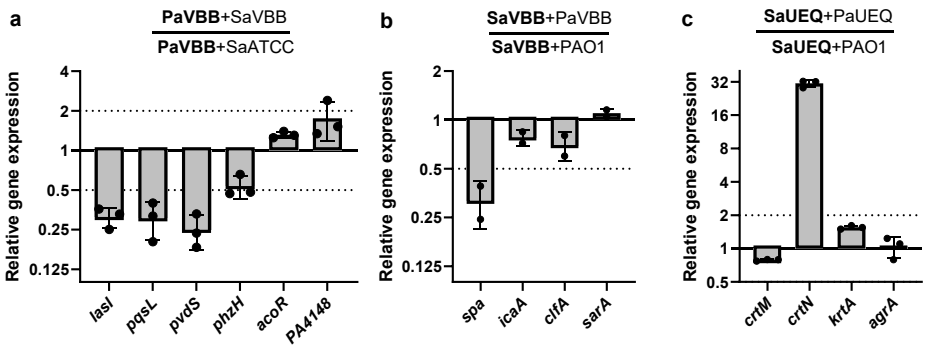

Figure 5. Relative expression of genes of *P. aeruginosa* (a) or *S. aureus* (b-c) in biofilms at 72h. Data are expressed as the ratio between the level of expression in (a) co-culture of *P.*

aeruginosa + *S. aureus* VBB496 and cross-culture of *P. aeruginosa* VBB496 + *S. aureus* ATCC25923; (b) co-culture of *S. aureus* + *P. aeruginosa* VBB496 and cross-culture of *S. aureus* VBB496 + *P. aeruginosa* PAO1 (c) co-culture of *S. aureus* + *P. aeruginosa* UEQ310 and cross-culture of *S. aureus* UEQ310 + *P. aeruginosa* PAO1. Negative and positive values therefore highlight a downregulation or overexpression of the gene in co-culture vs. cross-cultures, respectively. Data are mean ± SEM of up to 3 experiments in three replicates. A relative change of more than twofold in the expression level (limit highlighted by the dotted line) was considered significant.

P. aeruginosa VBB496 QS genes were significantly downregulated when co-cultured with co-isolated *S. aureus* VBB496 compared to reference ATCC25923. In *S. aureus* VBB496, *spa* was downregulated in co-culture with the co-isolated *P. aeruginosa vs*. PAO1. The expression of the other *S. aureus* genes was not significantly different in co-culture with PAVBB496 or PAO1. Thus, the reduced expression of QS-related genes in *P. aeruginosa* and of *spa* in *S. aureus* from the VBB496 pair suggests that the downregulation of metabolic processes unfavorable to the other species could be one of the reasons for the mutual adaptation of *S. aureus* and *P. aeruginosa* in co-culture.

Metabolomic analysis of *P. aeruginosa* exoproducts

To substantiate this hypothesis, we performed secondary metabolite profiling of the *P. aeruginosa* PAO1, UEQ310, and VBB496 mono-cultures as well as paired and cross strain co-cultures. Principal component analysis (PCA) revealed that the metabolomics of the mono- and co-cultures were highly similar at 24 h, but diverged at 48 h and 72 h by *P. aeruginosa* strain (Fig. 6A-C). Further evaluation of the data revealed that the secondary metabolites of *P. aeruginosa* dominated the metabolomics profile, driving the chemical similarity between the co-cultures to the mono-cultures. The abundance of select functionally characterized *P. aeruginosa* secondary metabolites, including pyocyanin (PYO), phenazine-1-carboxylic acid

(PCA), 2-heptyl-4-quinolone (HHQ) and its C9 congener 2-nonyl-4-quinolone (NHQ), 2-heptyl-4-hydroxyquinoline N-oxide (HQNO) and its C9 congener 2-nonyl-4-hydroxyquinoline N-oxide (NQNO), mono-RL (RC10C10), di-RL (RRC10C10), and pyochelin (PCH), were compared between samples (Fig. 6D, Fig. S3). The homoserine lactones (HSLs), 1-hydroxyphenazine (1-HP), phenazine-1-carboxamide (PCN), Pseudomonas quinolone signal (PQS), and pyoverdine (PVD) were below the limit of detection of this analysis.

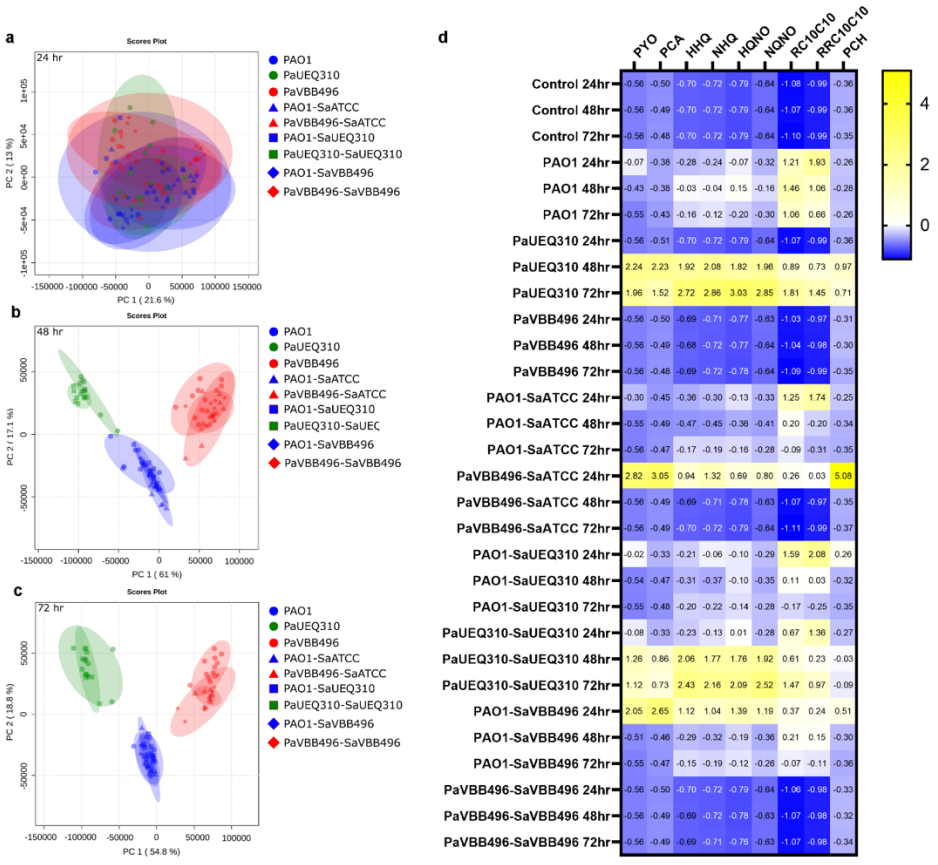

Figure 6: analysis of the metabolome of *P. aeruginosa* in different biofilms. (a-c): Principal-component analysis of untargeted metabolomics data of *P. aeruginosa* in single species biofilms or in the indicated dual species biofilms and collected 24 (a), 48 (b), or 72 (c) hours

after the addition of *P. aeruginosa* to growing *S. aureus* cultures. Individual samples are colored by *P. aeruginosa* strain – PAO1, blue; PaUEQ310, green; PaVBB496, red. Shapes indicate *P. aeruginosa* mono-cultures (circles) or co-culture with SaATCC25923 (triangle), SaUEQ310 (square), or SaVBB496 (diamond) and drawn with 95% confidence ellipses. Data points represent 9-12 replicates per sample. (d) heatmap representation of normalized Z-scores for averages of select *P. aeruginosa* secondary metabolites across sample groups. PYO, pyocyanin; PCA, phenazine-1-carboxamide; HHQ, 2-heptyl-4-quinolone; NHQ, 2-nonyl-4-quinolone; HQNO, 2-heptyl-4-hydroxyquinoline *N*-oxide; NQNO, 2-nonyl-4-hydroxyquinoline *N*-oxide; RC10C10, mono-rhamnolipid; RRC10C10, di-rhamnolipid; PCH, pyochelin.

In PAO1 monocultures, secondary metabolites were produced within 24 h of inoculation with relatively steady concentration through 72 h, except for a significant decrease in the levels of pyocyanin. UEQ310 monocultures produced secondary metabolites within 48 h of inoculation, maintaining similar levels through 72 h. No metabolites were detected from VBB496 mono-cultures. At 48 h, UEQ310 monocultures produced higher concentrations of all secondary metabolites compared to PAO1, except for the RL molecular family. The most conspicuous difference in the *P. aeruginosa* secondary metabolite profiles were observed at 24 h in co-cultures with *S. aureus* VBB496, where both PAO1 and *P. aeruginosa* VBB496 produced higher concentrations of secondary metabolites at 24 h, with a marked decrease at 48 h approaching mono-culture levels. No marked changes in the metabolome of *P. aeruginosa* UEQ310 was observed in co-culture with the co-isolated *S. aureus*.

Relative expression of genes in *S. aureus* UEQ310

Based on the observation that *P. aeruginosa* UEQ310 produced more metabolites than the other strains but does not impair the survival of *S. aureus* UEQ310, we wondered whether the co-isolated *S. aureus* showed some specific adaptation to these toxic products. We examined the expression of *S. aureus* genes involved in the synthesis of the anti-oxidant staphyloxantin (*crtM, crtN),* the oxidative stress

response *(krtA)*, or biofilm formation (*agrA*) [293]. Only *ctrN* was markedly overexpressed at 72 h when *S. aureus* was co-cultured with *P. aeruginosa* UEQ310 *vs.* PAO1 (Fig. 5C).

Susceptibility of *S. aureus* to *P. aeruginosa* metabolites

A common explanation for the eradication of *S. aureus* by *P. aeruginosa in vitro* study is the lethality of the QS product of *P. aeruginosa* against *S. aureus*, more specifically of pyocyanin, pyoverdine, rhamnolipids and HQNO [215, 292, 294-296].

As the metabolite profiles of *P. aeruginosa* strains in monoculture or in co-culture overlapped in the PCA, we hypothesized that clinical isolates of *S. aureus* could be better adapted to *P. aeruginosa* exoproducts than the reference ATCC25923 strain. We first tested the inhibition of *S. aureus* growth by supernatants from PAO1 or *P. aeruginosa* UEQ310 (Fig. 7A). Clinical *S. aureus* isolates VBB496 and UEQ310 were resistant to the supernatants of PAO1, which was not the case of *S. aureus* ATCC25923. The supernatant of *P. aeruginosa* UEQ310 prevented to growth of all three *S. aureus,* in accordance with the fact it produces more exoproducts than PAO1. No difference was seen if using supernatants from monoculture or from dual-species biofilms. We also determined the MIC of *P. aeruginosa* exoproducts on *S. aureus* (Fig. 7B). Pyocyanin was the only toxic molecule among those tested (pyocyanin, pyoverdine, rhamnolipids, HQNO), and its MIC was higher against *S. aureus* clinical isolates than ATCC25923.

As differences in *S. aureus* survival were observed in dual-species biofilms, we then tested the effect of pyocyanin or rhamnolipids (known to disperse *S. aureus* biofilm [169]) on biofilm formation by the three *S. aureus* strains (Fig. 7C). Pyocyanin inhibited biofilm growth for ATCC25923 but not for clinical isolates, confirming that pyocyanin resistance is contributing to adaptation of clinical *S. aureus* to *P. aeruginosa.*

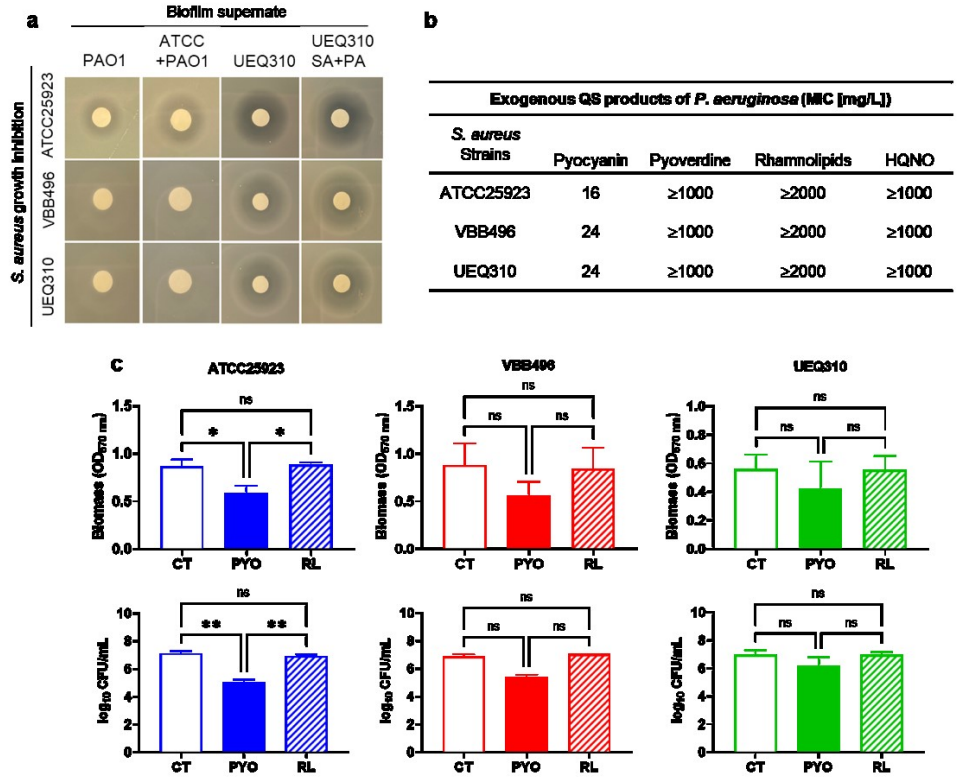

Figure 7. Effect of exoproducts of *P. aeruginosa* on *S. aureus.* a: inhibition of growth in agar plates of *S. aureus* in the presence of supernatants of biofilms (from PAO1 single species (PAO1) or dual species with ATCC25923 (PAO1+ATCC), *P. aeruginosa* UEQ310 single species (UEQ310) or with co-isolated *S. aureus* (UEQ SA+PA)), spotted on paper disks. b: MICs of *P. aeruginosa* exoproducts against *S. aureus* strains. c: influence of pyocyanin (PYO) or rhamnolipids (RL, both added at 50 µg/mL) on biofilm formation by *S. aureus.* Biomass and CFU counts were analysed after 24 h of incubation. Data are mean ± SEM of two independent experiments with at least 3 replicates for biomass, and the mean ± SD one experiment in two replicates for CFU. Statistical analysis: ns, not significant; **, $p<0.01$, using one-way ANOVA followed by Tukey's multiple comparisons test.

Bacterial motility

Bacterial motility is important at the stage of biofilm formation but may also affect interspecies cross-adaptation. *P. aeruginosa* strains with low motility tend to be less virulent for *S. aureus* [95, 96], but their impact on *S. aureus* motility is ill characterized. We first evaluated the swarming, swimming, and twitching in PAO1 and clinical isolates of *P. aeruginosa* (Fig. 8A and C). Clinical isolates showed reduced swimming and swarming capacity in comparison with PAO1 but similar twitching motility. In the presence of supernatant of *S. aureus* biofilm culture, swarming and swimming were increased for PAO1 (Fig. 8C). We then studied *S. aureus* motility (Fig. 8B and D). In control conditions, none of the strains was motile (Fig. 8B) but all of them gained some degree of spreading motility [297] in the presence of supernatants of *P. aeruginosa* PAO1 or UEQ310 (Fig. 8D), probably related to the presence of rhamnolipids (Fig. 8B).

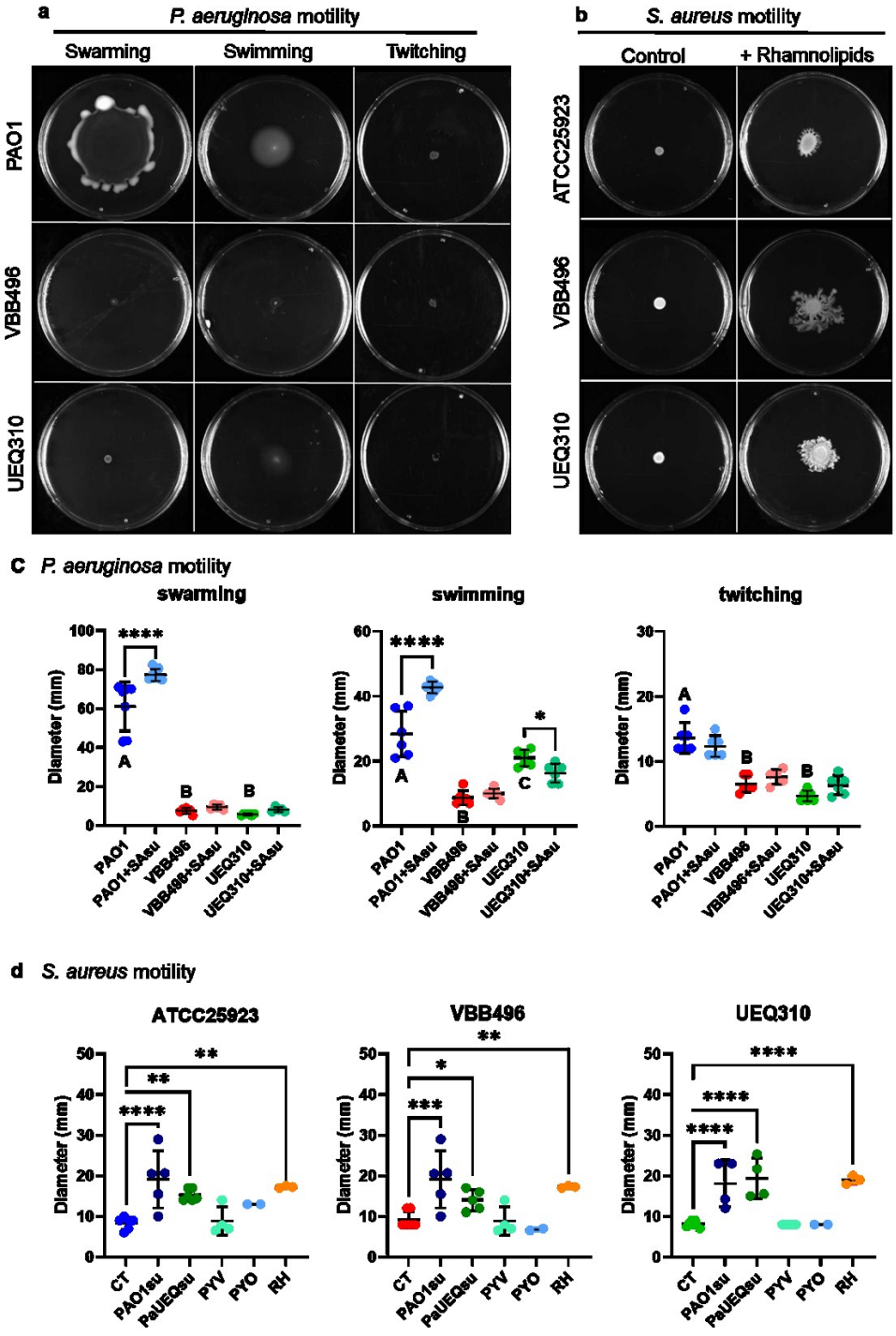
a
P. aeruginosa motility
Swarming
Swimming
Twitching
PAO1
VBB496
UEQ310
b
S. aureus motility
Control
+ Rhamnolipids
ATCC25923
VBB496
UEQ310
c
P. aeruginosa motility
swarming
swimming
twitching
Diameter (mm)
PAO1
PAO1+SAsu
VBB496
VBB496+SAsu
UEQ310
UEQ310+SAsu
d
S. aureus motility
ATCC25923
VBB496
UEQ310
CT
PAO1su
PaUEQsu
PYV
PYO
RH

Figure 8. Motility of *P. aeruginosa* and *S. aureus*. For *P. aeruginosa,* swarming, swimming and twitching motilities are shown in control conditions (a), and diameters were measured in control conditions or in the presence of *S. aureus* ATCC25923 biofilm supernatant (Sasu) (c). For *S. aureus*, motility is shown in control conditions and in the presence of 1 µg/mL rhamnolipids (b), and diameters were measured in control conditions (CT) or in the presence of supernatant of PAO1 or *P. aeruginosa* UEQ310 (PAO1su or PAUEQsu), 1 µg/mL pyoverdine (PYV), 1 µg/mL pyocyanin (PYO), or 1 µg/mL rhamnolipids (RH). Experiments were performed in three replicates in 3 independent experiments. A representative image was shown in panels (a) and (b). Statistical analyses (c-d): One-way ANOVA followed by Tukey's multiple comparisons test (*, $p < 0.05$; **, $p < 0.01$; ***, $p < 0.001$; ****, $p < 0.0001$).

III.1.e. Discussion

To the best of our knowledge, this study is the first one to examine the cross-adaptation of *S. aureus* and *P. aeruginosa* in biofilms grown in an artificial sputum medium mimicking the viscoelastic properties of the mucus found in patients with CF, and to compare in this setting reference strains with clinical isolates.

As already reported in conventional culture media [256, 298-300] or in another CF-relevant medium (synthetic cystic fibrosis sputum medium 2; SCFM2 [301]), we observed that *P. aeruginosa* outcompetes *S. aureus* when both species are inoculated at the same time in ASM+. This has been attributed to several factors, including the production of molecules toxic for *S. aureus* by *P. aeruginosa* [215, 255, 292, 294-296] or the low concentrations of oxygen or glucose within the biofilm [301]. Conversely, both species can be maintained together over time if inoculating *S. aureus* first, as already reported in conventional media [178, 255, 269]. This observation aligns with the fact that *S. aureus* predominates in early biofilms [276] and that *in vivo*, *S. aureus* precedes *P. aeruginosa* in the colonization of the lungs [33].

Remarkably, this model proved applicable to various clinical isolates, irrespective of the *P. aeruginosa* phenotype (whether mucoid or not, pigmented or not, SCV). Notably, it performed even better than with reference strains: in most cases, the abundance of *S. aureus* surpassed that observed for ATCC25923. This strongly supports the notion that a form of cross-adaptation between both species may occur *in vivo* [272]. Cross-cultures experiments further substantiate this reciprocal adaptation and reveal important differences among the three pairs of strains we examined in detail, shedding light on some mechanisms of adaptation.

Among the three *P. aeruginosa* strains included in cross-cultures, PAO1 is the most virulent, as it overgrows the three *S. aureus.* This toxicity is probably not associated with a high production of secondary metabolites, as *P. aeruginosa* UEQ310 produces larger amounts. In addition, the presence of *S. aureus* did not change the metabolomic profile of *P. aeruginosa* after 48 h of biofilm formation, suggesting that after adapting to each other, physical interactions may be more important than chemical interplay. We indeed rather noticed that PAO1 shows the highest motility among *P. aeruginosa* strains, which is not impaired by the supernatant of *S. aureus* culture. Motility of *P. aeruginosa* could be associated with toxicity for *S. aureus* by different mechanisms. First, motility can help *P. aeruginosa* to cover the available space rapidly and compete with other species for available nutrients, particularly at the early stages of culture [302]. More subtly, in the presence of *S. aureus, P. aeruginosa* can transition from collective to single-cell motility through the action of type IV pili, and dismantle *S. aureus* colonies [303]. This mechanism likely does not apply here, since twitching is not increased in the presence of supernatant of *S. aureus* culture. However, more globally, motility can drive *P. aeruginosa* in the vicinity of *S. aureus*, exposing the cocci to high local concentrations of toxic metabolites, like rhamnolipids or pyocyanin, can disrupt staphylococcal biofilms [169, 304].

Conversely, *P. aeruginosa* VBB496 is almost unable to form biofilms, unless in coculture with its co-isolated *S. aureus*. Actually, most of the secondary metabolites known to be involved in biofilm growth (pyocyanin, rhamnolipids, QS molecules) or in toxicity towards *S. aureus* (pyocyanin, PCA) were undetectable for this strain, including in dual species biofilms with the co-isolated *S. aureus*. Genes involved in QS or pigment synthesis (*lasI, pvdS, phzH, pqsL*) are all downregulated, indicating that this isolate has a low tendency to form biofilm: biofilms are only formed in coculture with *S. aureus* VBB496, as this isolate markedly downregulates the expression of SpA. This protein inhibits biofilm formation and motility of *P. aeruginosa* by binding to exopolysaccharides or type IV pili [305]. Importantly also, confocal microscopy images show that both species are intimately intermixed in the VBB496 biofilm contrarily to the other strains, further confirming that they better survive when in close proximity.

Lastly, *P. aeruginosa* UEQ310 produces the highest amounts of secondary metabolites, and as a consequence, the most abundant biofilm biomass. In spite of this, the co-isolated *S. aureus* survives well in its presence, possibly thanks to the overexpression of the diapophytoene desaturase (*CrtN*), an enzyme essential for carotenoid pigment synthesis. Staphyloxanthin is involved in the resistance of *S. aureus* to oxidative stress, which can be generated by the large amounts of pyocyanin produced by *P. aeruginosa* UEQ310. Indeed, pyocyanin interferes with the electron transfer chain in *S. aureus* and diverts them to produce reactive oxygen species can induce death [206].

This brings us to consider the other mechanisms by which clinical isolates of *S. aureus* better survive in the presence of *P. aeruginosa* than the reference strain. Both *S. aureus* VBB496 and UEQ310 are more resistant to pyocyanin than *S. aureus* ATCC25923 as witnessed by the larger MIC of this compound against these isolates. Although generally considered as non-motile, *S. aureus* can spread on soft agar when

the *agr* quorum sensing (QS) is activated, triggering the production of phenol soluble modulins that act as surfactants [297]. Here we show that *S. aureus* also react to other surfactants like *P. aeruginosa* rhamnolipids. This rhamnolipid-triggered motility of *S. aureus* may thus represent an alternative mechanism to the previously described hitchhiking on swimming *P. aeruginosa* [306] and help *S. aureus* to join *P. aeruginosa* to form a robust at the air-liquid interface, rather than on the bottom of the plates. This location mimics the site where *S. aureus* and *P. aeruginosa* grow *in vivo*, since *S. aureus* and *P. aeruginosa* inhabit the airway lumen in CF patients filled with sputum, rather than on epithelial surface [174, 307].

Remarkably also, the *S. aureus* that does not survive well in our collection is co-isolated with a non-mucoid *P. aeruginosa* (857JBJ). Alginate, abundantly produced by mucoid isolates, has been shown to protect *S. aureus* from *P. aeruginosa* toxicity by downregulating *pvdA,* a gene required for the production of the iron-scavenging siderophore pyoverdine [215].

Our study has some limitations. First, we did not explore the full transcriptome of the isolates in coculture. This analysis has been recently completed for dual species biofilms of reference strains grown in conventional broth, revealing essential metabolic changes [178]. Confirmation of these findings in a more relevant model as the one we propose here, has yet to be completed. Yet, this confirmation would constitute a separate and substantial undertaking. Rather, we based our study on a phenotypic approach to the interaction between species in this model, guided by the influence of culture supernatant of one species on the other, which suggested a role for soluble compounds. These phenotypic results directed us towards an analysis of the metabolites produced by *P. aeruginosa,* which could be extended to those produced by *S. aureus* in the future. Of note, the exact composition of the ASM medium has been shown to modulate metabolite productions or inter-species interaction, confirming the difficulty of this task [281, 308]. Second, the number of

clinical isolates studied remained limited, as our first primary aim was to access the applicability of the novel model we established to isolates with diverse, representative phenotypes. Of note, *in vitro* studies based on agar competition assays suggest, in larger collections, that two thirds of co-isolates show coexistence interactions, while the remaining one third rather exhibit a competition phenotype, confirming the predominance of cross-adaptation in patients [266].

While the present work serves as an initial milestone, showcasing the viability of cultivating dual-species biofilms in a clinically relevant in vitro medium, it opens the door to a more in-depth analysis of the molecular interactions that govern the coexistence of these two species within the lungs of patients with cystic fibrosis. Conducting longitudinal studies in this model would also be highly instructive, as *P. aeruginosa* collected after several years of infection tend to lose their capacity to overgrow *S. aureus* [299], suggesting evolution from competition to coexistence over chronicity of the infection [263].

III.1.f. Acknowledgments and Conflicts of interest

Acknowledgments

Z.W. was recipient of a Chinese Scholarship Council (CSC) PhD grant and a grant from the King Baudouin Foundation (Fonds Forton) and the Belgian Mucovereniging/Association Muco. F.V.B. is research director from the Belgian Fonds de la Recherche Scientifique (FNRS-FRS). This work was supported by grants from the Belgian FNRS (grants J.0162.19 and J.0177.23) and the King Baudouin Foundation (Fonds Forton) and the Belgian Mucovereniging/Association Muco to F.V.B., and by National Institutes of Health grant R35 GM128690 and the

L.S. Skaggs Professorship from ALSAM Foundation to V.V.P. The authors thank V. Mohymont, M. Scopa, and R. Tricot for dedicated technical assistance.

Conflicts of interest

The authors have no conflict of interest to declare.

III.1.h. Supplementary material

Table S1: Primers used in this study

Genes	Forward	Reverse	Hybridization temperature (˚C) [a]	reference
rpoD	GGGCGAAGAAGGAAATGGTC	CAGGTGGCGTAGGTGGAGAA	58	[309]
lasI	ATCGTACAAATTGGTCGGCG	CTTTGCGCTCCTTGAACACT	58	This study
pvdS	CCAGGCATTCGTCGATAACC	ATCCTGGACCACATCTTCGG	58	This study
phzH	CCTACACCGACCATGAGCTG	CTTGAGCAGCCACTTCTCCT	61	This study
pqsL	AGCTGGAGGTCTATCACGAC	GCAGGGCATGAGGATGAAAT	61	This study
acoR	GCGAGGATCTCTACTTCCGC	CTCACCGAGTTCGATGCGTA	56.5	[310]
PA4148	GCGGATCGTCAACCTGTCAT	CGATCACGGCAAACTTCGAG	58	[310]

gmK	TCAGGACCATCTGGA GTAGGTAAA	TTCACGCATTTGACGT GTTG	58	[277]
sigB	CTGATCGCGAACGAG AAATCA	GCCGTTCTTTGAAGTC TGGA	58	[277]
icaA	CGAGAAAAAGAATAT GGCTG	ACCATGTTGCGTAACC ACCT	58	[277]
clfA	ACGAGTGACACAGGA TCAGA	GTGAATTAGGCGGCA CTACA	58	[277]
spA	AGACGATCCTTCAGT GAG CAA	TGTTGTCTTCCTCTTTT GGTG C	56	This study
sarA	CAG CGA AAA CAA AGA GAA AG	TCG TTG TTT GCT TCA GTG AT	61	[255]
crtM	GGTGTTGCTGGTACA GTAGGTGAAG	GCAACGATTCACCAA GTCTTCTTGCG	58	[293]
crtN	CAGTGATTGGTGCAG GTGTC	CATACGCCCGCCTACA TTAT	58	[293]
katA	TAGACCAGTCCCAATT GCACCACC	TCGCTTTACAGTACTA AATAGTTATTG	58	[311]
agrA	TGATAATCCTTATGA GGTGCTT	CACTGTGACTCGTAA CGAAAA	58	[293]

[a] PCR program: denaturation: 95°C for 3 min; 39 cycles (95°C for 10 sec, 30 sec at the hybridization temperature); melt curve (from 65 to 95°C by increment of 0.5°C for sec)

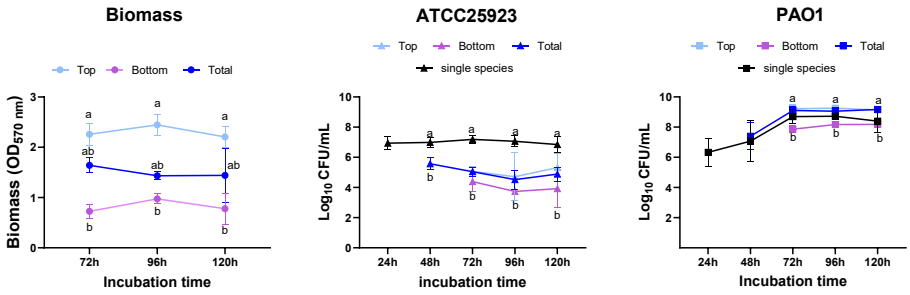

Fig. S1. Biofilm quantification at different locations for reference strains: top, surface air-liquid (collected using inoculation loop); bottom, plate surface (collected after discarding ASM+ by inversion of the plate); total (collected after removing ASM+ by pipetting). CFU are also compared to single species biofilms. Values are means ± SEM from three independent experiments performed in more than triplicates. Statistical analysis: data points with different letters are significantly different from each other ($p<0.05$) when comparing different location at the same time point (two-way analysis of variance (ANOVA) followed by Tukey's multiple comparisons test).

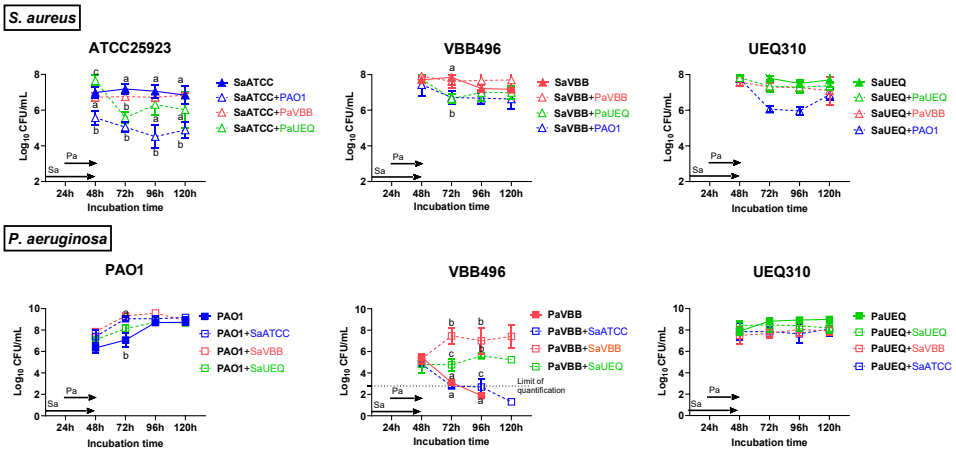

Fig. S2. Comparison of the viability of single strain in different dual species biofilms or in mono species biofilm. Values are recorded at times points ranging between 48 h and 120 h, i.e. 48 after inoculation of *S. aureus* and 24 h after inoculation of *P. aeruginosa* in dual species biofilms. Data for single species biofilms are aligned on the same time line. Values are means ± SEM from independent experiments performed in more than triplicates. Statistical analysis: data with different letters are significantly different from each other ($p<0.05$) when comparing 2 different biofilms at the same time point (Two-way ANOVA followed by Tukey's multiple comparisons test).

P. aeruginosa secondary metabolites quantified from single species biofilms at 24-48-72 h

24 h

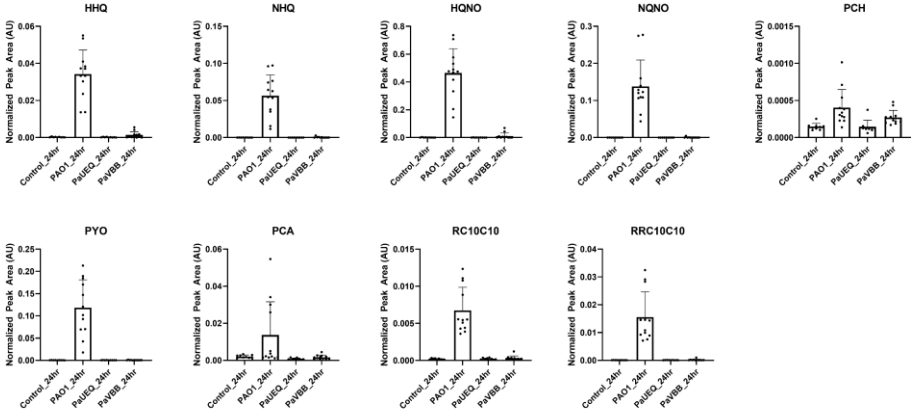

48 h

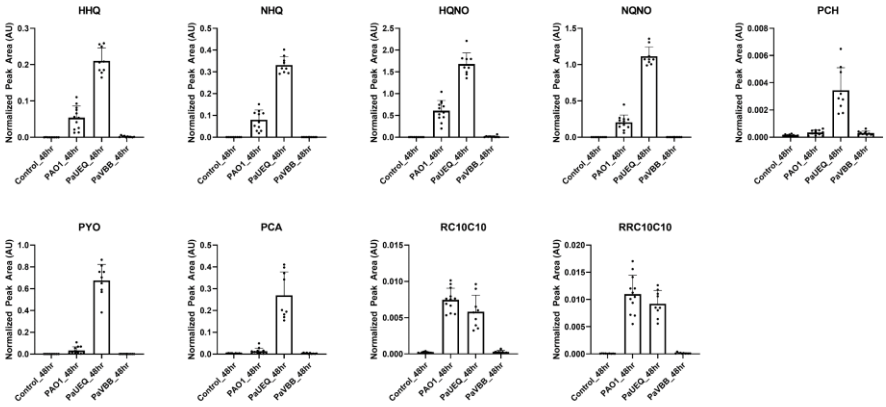

72 h

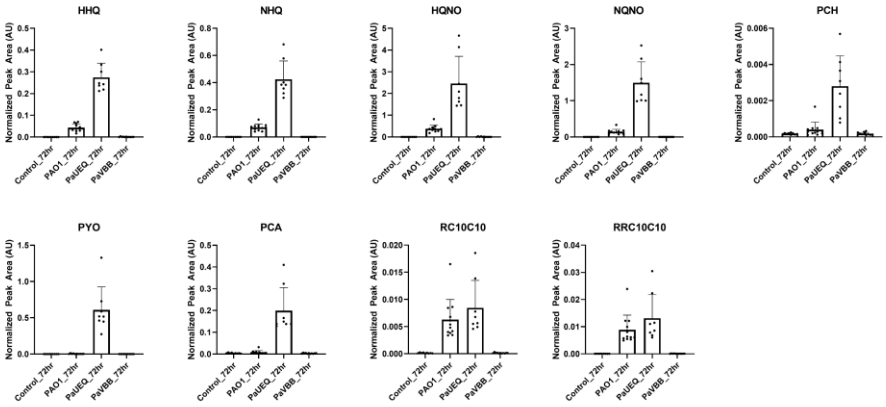
HHQ
NHQ
HQNO
NQNO
PCH
PYO
PCA
RC10C10
RRC10C10
Normalized Peak Area (AU)
Control_72hr
PAO1_72hr
PaUEQ_72hr
PaVBB_72hr

B. *P. aeruginosa* secondary metabolites quantified from *P. aeruginosa* VBB496 monocultures and cocultures with *S. aureus* VBB496 or ATCC25923 at 24, 48, 72 h

24 h

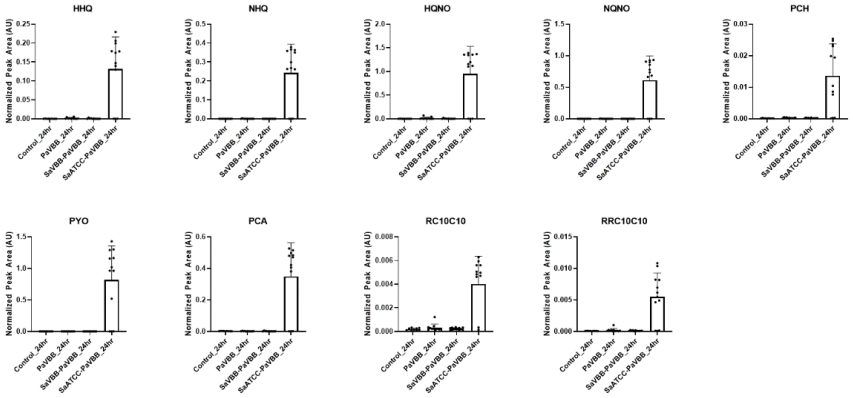

48 h

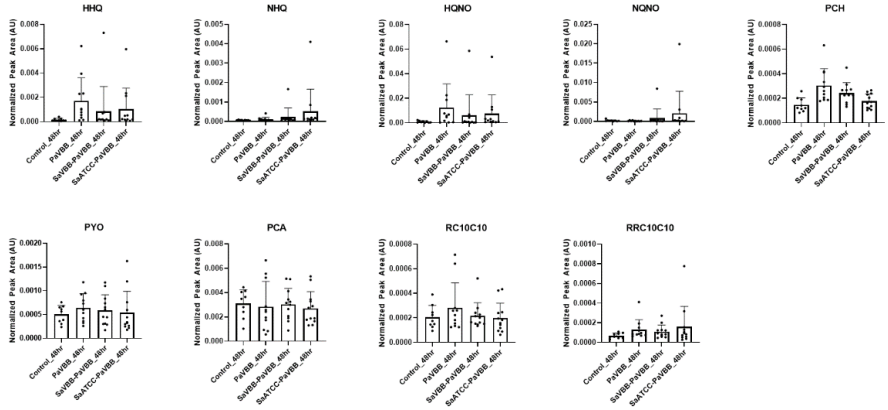

72 h

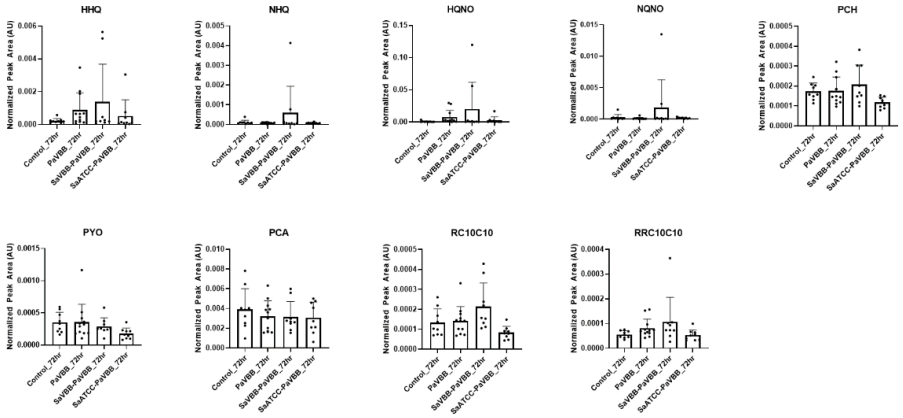
HHQ
NHQ
HQNO
NQNO
PCH
PYO
PCA
RC10C10
RRC10C10
Normalized Peak Area (AU)
Control_72hr
PaVBB_72hr
SaVBB-PaVBB_72hr
SaATCC-PaVBB_72hr

C. *P. aeruginosa* secondary metabolites quantified from P. aeruginosa PAO1 or UEQ310 alone or cocultured with *S. aureus* UEQ310 at 24, 48, 72 h

24 h

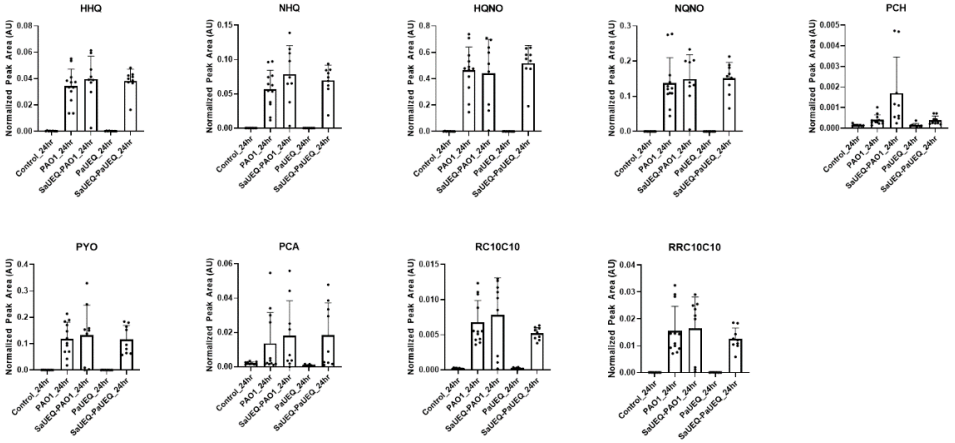

48 h

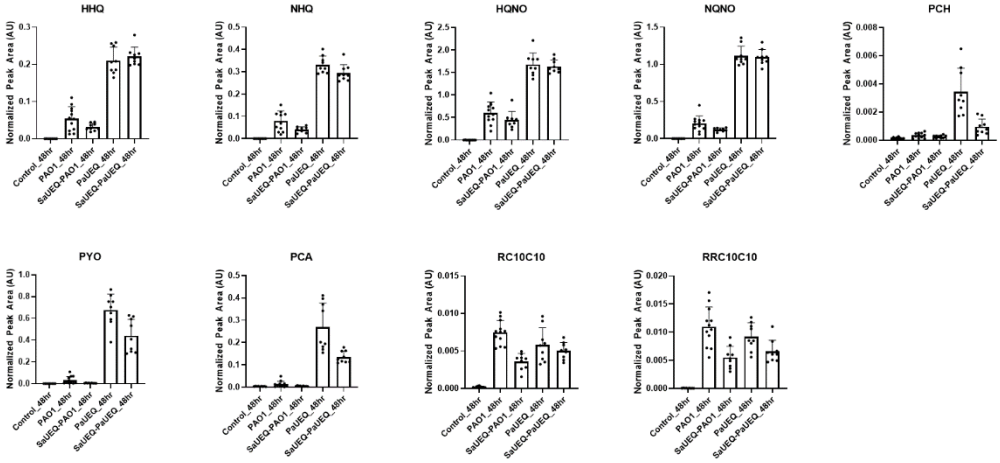

72 h

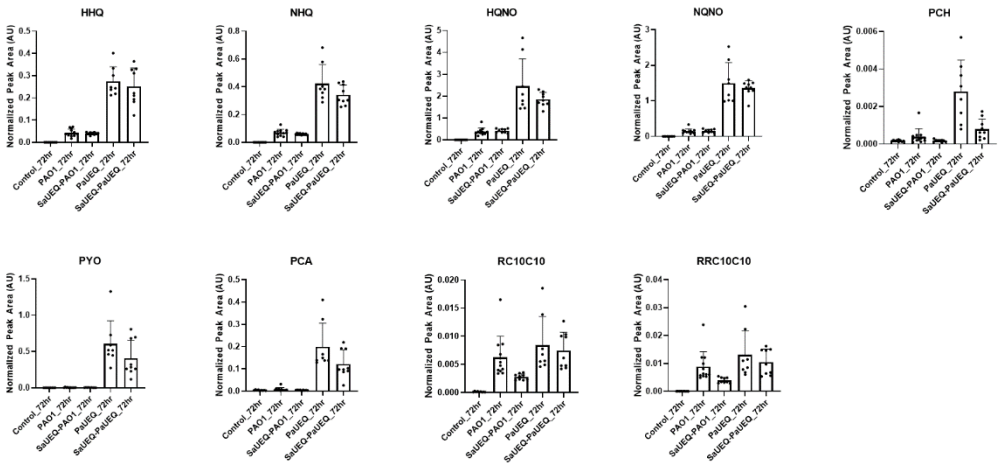

Fig. S3. Normalized relative abundance of *P. aeruginosa* secondary metabolites in (A) PAO1, UEQ310, and VBB496 monocultures at (1) 24, (2) 48, and (3) 72 h post-inoculation; (B) *P. aeruginosa* VBB496 monocultures and cocultures with *S. aureus* VBB496 or ATCC25923 at (1) 24, (2) 48, (3) 72 h post-inoculation of *P. aeruginosa;* (C) *P. aeruginosa* PAO1 or UEQ310 alone or cocultured with *S. aureus* UEQ310 at (1) 24, (2) 48, (3) 72 h post-inoculation of *P. aeruginosa.* Data points represent 9-12 replicates per sample with error bars representing SD. PYO, pyocyanin; PCA, phenazine-1-carboxamide; HHQ, 2-heptyl-4-quinolone; NHQ, 2-nonyl-4-quinolone; HQNO, 2-heptyl-4-hydroxyquinoline *N*-oxide; NQNO, 2-nonyl-4-hydroxyquinoline *N*-oxide; RC10C10, mono-rhamnolipid; RRC10C10, di-rhamnolipid; PCH, pyochelin.

III.2. Enzyme-antibiotics combination therapy

Adapted from:

Repurposing DNase I and alginate lyase to degrade the biofilm matrix of dual-species biofilms of *Staphylococcus aureus* and *Pseudomonas aeruginosa* grown in artificial sputum medium: in-vitro assessment of their activity in combination with broad-spectrum antibiotics

Zhifen Wang,[1] Rita Vanbever,[2] Joseph H. Lorent,[1] Jessica Solis, [1] Christiane Knoop,[3] Françoise Van Bambeke[1,*]

[1] Pharmacologie cellulaire et moléculaire, Louvain Drug Research Institute, Université catholique de Louvain, Brussels, Belgium

[2] Advanced Drug Delivery and Biomaterials, Louvain Drug Research Institute, Université catholique de Louvain, Brussels, Belgium

[3] Erasme Hospital, Université libre de Bruxelles, Brussels, Belgium

Published in **Journal of Cystic Fibrosis**, February 2024, S1569-1993(24)00027-4. Advance online publication

DOI: https://doi.org/10.1016/j.jcf.2024.02.012.

III.2.a. Abstract:

Background

Biofilm-associated pulmonary infections pose therapeutic challenges in cystic fibrosis patients, especially when involving multiple bacterial species. Enzymatic degradation of the biofilm matrix may offer a potential solution to enhance antibiotic efficacy. This study investigated the repurposing of DNase I, commonly used for its mucolytic activity in cystic fibrosis, to target extracellular DNA within biofilms, as well as potential synergies with alginate lyase and broad-spectrum antibiotics in dual-species biofilms of *Pseudomonas aeruginosa* and *Staphylococcus aureus.*

Keywords: dual-species biofilm, *Pseudomonas aeruginosa, Staphylococcus aureus,* DNase I, alginate lyase, meropenem, tobramycin, artificial sputum medium, cystic fibrosis

Methods

Dual-species biofilms were grown in artificial sputum medium using *S. aureus* and *P. aeruginosa* isolated by pairs from the same patients and exposed to various combinations of enzymes, meropenem, or tobramycin. Activity was assessed by measuring biofilm biomass and viable counts. Matrix degradation and decrease in bacterial load were visualized using confocal microscopy. Biofilm viscoelasticity was estimated by rheology.

Results

Nearly complete destruction of the biofilms was achieved only if combining the enzymatic cocktail with the two antibiotics, and if using supratherapeutic levels of DNase I and high concentrations of alginate lyase. Biofilms containing non-

pigmented mucoid *P. aeruginosa* required higher antibiotic concentrations, despite low viscoelasticity. In contrast, for biofilms with pigmented mucoid *P. aeruginosa,* a correlation was observed between the efficacy of different treatments and the reduction they caused in elasticity and viscosity of the biofilm.

Conclusions

In this complex, highly drug-tolerant biofilm model, enzymes prove useful adjuvants to enhance antibiotic activity. However, the necessity for high enzyme concentrations emphasizes the need for thorough concentration-response evaluations and safety assessments before considering clinical applications.

Highlights

- Mixed-species biofilms pose a therapeutic challenge in cystic fibrosis.
- Antibiotics alone fail to eradicate *S. aureus*/*P. aeruginosa* mixed biofilms in ASM.
- Cocktail of alginate lyase, DNase I, meropenem, tobramycin is effective.
- Yet, high (alginate lyase), supratherapeutic (DNase I) concentrations are required.
- Further concentration-response and safety studies are needed.

III.2.b. Introduction

Lung infections are a leading cause of morbidity and mortality in patients with cystic fibrosis (CF). The sticky mucus that accumulates in their airways provides a favorable environment for microorganisms to form biofilms that lead to chronic infections [312]. Biofilms are bacterial aggregates encased in self-produced matrix mainly composed of extracellular DNA (eDNA), polysaccharides and proteins [186, 313].

In these structures, antibiotic efficacy is reduced not only by the facilitated spread of resistance mechanisms, but also by the increased tolerance of bacteria to these drugs [314]. Tolerance is due in part to the physical or chemical barrier opposed by the biofilms matrix to antibiotics [314]. For instance, the negatively-charged eDNA can bind cationic antibiotics like aminoglycosides and the acidic local environment can impair their uptake in bacteria by attenuating inner-membrane proton motive force [315, 316]. Alginate-rich biofilms are also more tolerant to cationic drugs due to charge interactions [314]. In addition, the limited access to oxygen and nutrients in biofilms slows down bacterial metabolism, making antibiotics acting on growing bacteria less effective [314].

Among the bacterial species found in these niches, *Staphylococcus aureus* and *Pseudomonas aeruginosa* are the most frequent and are often co-isolated in the same patients [258]. The interactions between these two species in biofilms may contribute to a better survival as well as to increased tolerance to antibiotics. For example, the alginate produced by *P. aeruginosa* favors strong biofilm formation and protects *S. aureus* from *P. aeruginosa* toxicity [215]. Conversely, *S. aureus* protein A binds to Psl polysaccharides secreted by *P. aeruginosa,* facilitating aggregates formation and tolerance to tobramycin [317].

In this context, adjuvant strategies to break down the biofilm matrix may help antibiotics to recover activity [318]. Enzymes are particularly appealing in the context of CF. eDNA and, to a lower extent, alginate increase the viscoelasticity of the sputum [319, 320], preventing antibiotics from reaching bacterial cells [321]. Deoxyribonuclease I (DNase I or dornase-α) and alginate lyase have been shown to decrease the viscoelasticity of the respiratory mucus of patients with CF in-vitro [320, 322] and inhalation of DNase I has been a gold-standard mucolytic therapy in the management of the respiratory disease in CF for almost three decades. The newly-introduced CFTR modulators prove successful to restore respiratory function in patients with class II or III mutations [56]. However, we do not know their effect on biofilms, especially in older patients with bronchiectasis. Moreover, not all patients can benefit from them because the treatment is too expensive, ineffective on their mutations, or because they experience adverse drug reactions, leaving thus room for the use of enzymes.

The aim of this study was therefore to establish whether DNase I or alginate lyase could also prove useful to digest the biofilm matrix, since it is rich in eDNA and alginate, and therefore be possibly repurposed for this indication. To this effect, we used an in-vitro dual-species biofilm model with pairs of *S. aureus* and *P. aeruginosa* co-isolated from the same patients with CF, grown in an artificial sputum medium mimicking the viscoelastic properties of the mucus of these patients. Biofilms were exposed to these enzymes individually or mixed, and combined or not with two broad-spectrum antibiotics, namely meropenem and tobramycin, also used alone or in mixture. These antibiotics were selected because they are part of the arsenal used in patients with CF and are also considered as active against biofilms [314]. Additionally, the selection of antibiotics was based on the susceptibility of each pair of coisolates, as indicated by clinical records. Consequently, only a few antibiotics

have the capability to target both *S. aureus* and *P. aeruginosa* simultaneously, with meropenem and tobramycin being among them.

To the best of our knowledge, this study is the first to test these enzymes in combination against dual-species biofilms formed by clinical isolates. In brief, we show a strong synergy between antibiotics and enzymes to destroy the biofilms and kill the bacteria, if high enough concentrations of both enzymes and antibiotics are used.

III.2.c. Materials and Methods

Materials

Two pairs of *S. aureus* and *P. aeruginosa* co-isolated from the same patients were used. *P. aeruginosa* showed a pigmented mucoid phenotype in the UEQ310 pair, and a non-pigmented mucoid phenotype in the VBB496 pair. Tryptic soy agar (TSA; VWR) and Mueller-Hinton broth (MHB-ca; Sigma-Aldrich) were used for routine cultures. Artificial sputum medium (ASM+; see [289] for detailed composition [agar originating now from Sigma-Aldrich rather than Becton-Dickinson]) was used for biofilm cultures. Mannitol Salt Agar (peptone 5 g/L, NaCl 75 g/L, D-mannitol 10 g/L, agar 15 g/L) and *Pseudomonas* Isolation Agar (Sigma-Aldrich) were used for selective growth of *S. aureus* and *P. aeruginosa,* respectively. Meropenem (potency, 92%) and tobramycin (potency, 100%) were obtained from Hospira Benelux and Galephar. Alginate lyase and bovine pancreatic DNase I were purchased from Sigma-Aldrich.

Antibiotics susceptibility testing

Minimal inhibitory concentrations (MIC) were determined by microdilution in MHB-ca following CLSI guidelines.

Biofilm culture

Dual-species biofilms were grown using a protocol adapted from [255]. Briefly, an overnight culture of *S. aureus* was adjusted to approximately $2.1x10^7$ CFU/mL in MHB-ca, inoculated at 200 µL per well into 96-wells plates and incubated at 37°C for 2 h to allow bacteria attachment, after which MHB-ca was replaced with ASM+ and plates were incubated for an additional 24 h. Medium was then removed and 20 µL of *P. aeruginosa* (approximately 1.35×10^7 CFU/mL) in MHB-Ca were added to the 24-h *S. aureus* biofilm and diluted with 180 µL of ASM+ to achieve a concentration of around 1.35×10^6 CFU/mL. Incubation was continued during 72 h to obtain mature and stable biofilms (Fig. S1). The mucoid character of *P. aeruginosa* was checked at the end of the experiments and systematically maintained for VBB496 and for the vast majority of the colonies for UEQ310.

Biofilm treatments

Mature dual-species biofilms were incubated at 37°C with antibiotics, enzymes or combinations thereof in fresh ASM+ during 24 h, after which the medium was removed by pipetting. Biofilms were washed once in phosphate-buffered saline (PBS), destroyed by scratching with disposable inoculation loops and resuspended in 200 µL of PBS for each well. The resulting suspension was sonicated (Q700 sonicator, Qsonica) at an amplitude of 60% for 30 s to release culturable bacteria, serially diluted, and 50 µL aliquots were spread on selective media for *S. aureus* and *P. aeruginosa*. Other wells where biofilms were not disrupted were dried at 60°C for 1 day, then stained with 0.5% crystal violet (Sigma-Aldrich) for 10 min [289]. The excess of dye was eliminated by running water and the dye bound to biofilms resolubilized in 66% of acetic acid (Sigma-Aldrich) and incubated at room temperature for 1 h in the dark. Absorbance was measured at 570 nm using a SpectraMax M3 spectrophotometer (Molecular Devices).

Biofilm imaging

Biofilms were cultured on glass coverslips placed in 24-well polystyrene plates and stained with 300 µL of a mixture of 10 µM SYTO-60 and 2 µM of TOTO-1 in PBS (membrane-permeant fluorophore targeting double-stranded DNA used to detect cells, and membrane-impermeant probe fluorescent when bound to eDNA, respectively [323]; Thermo Fisher Scientific) in darkness. After 20 minutes, the liquid was removed, and the biofilms further stained with 300 µL of calcofluor white (1 g/L calcofluor White M2R and 0.5 g/L Evans Blue at a 1:1 ratio in a 10% KOH solution), successfully used to stain alginate [324]. After 1 min incubation in darkness, the liquid was removed, and biofilms washed twice in PBS. Coverslips were mounted by inversion on 100 mm glass coverslips and visualized on a cell observation spinning disk microscope (Carl-Zeiss) with an oil immersion 40-fold objective. SYTO-60, TOTO-1, and calcofluor white were detected in the red, green, and blue channels (excitation/emission: 633/678, 488/533 nm, 405/433 nm, respectively). The 3D images were obtained using ZEN 2.6 software with Z-stacks scanning mode. The method used for quantitative analysis is described in Supplementary Method S1.

Rheology

The viscoelastic properties of biofilms were determined using a rheometer MCR102 (Anton-Paar) and a 50 mm stain cone plate with a 1° angle (CP50-1°) [325]. Eight hundred microliters of biofilm at 37°C were loaded on the rheometer and submitted to shear strains limited to the 0.01 to 1% range for which no destruction of the samples was observed (Fig. S2). Values were recorded with RheoCompass™ software (Anton-Paar).

Statistical analysis

Statistical analyses were performed with GrahPad Software (version 9.1.1).

III.2.d. Results

Antibiotic susceptibility

MIC of antibiotics are shown in Table 1, with tobramycin MIC above the susceptibility breakpoint for *P. aeruginosa* VBB496. In the next experiments, their concentrations were adjusted to multiples of the MIC of the less susceptible isolate from each pair.

Table 1: MIC of antibiotics in MHB-ca (mg/L)

Antibiotics [a]	Co-isolated pair of *S. aureus* and *P. aeruginosa*.			
	UEQ310		VBB496	
	S. aureus	*P. aeruginosa*	*S. aureus*	*P. aeruginosa*
Meropenem	0.03	0.06	0.06	0.03
Tobramycin	0.5	2	1	4

[a] EUCAST susceptibility breakpoints (S): ≤ 2 mg/L for meropenem against *P. aeruginosa* and tobramycin against both strains (no breakpoint set for meropenem against *S. aureus* but both strains are MSSA and therefore considered as susceptible).

Effect of individual antibiotics in combination with enzymes on dual-species biofilms

Individual antibiotics at 10-fold MIC of the less susceptible strain in each pair (UEQ310: 0.6 mg/L meropenem; 20 mg/L tobramycin; VBB496: 0.6 mg/L meropenem; 40 mg/L tobramycin) were combined with alginate lyase (250 mg/L) or DNase I (40 mg/L) or a mixture of them to treat dual-species biofilms. Preliminary

experiments showed that 10-fold lower concentrations of both enzymes did not reduce biomass or CFU in biofilms (Fig. S3).

For UEQ310 biofilm, DNase I alone or combined with alginate lyase significantly decreased biomass and markedly increased the effect of meropenem on biomass, but not that of tobramycin, which was already active alone (Fig. 1A). *S. aureus* and *P. aeruginosa* UEQ310 viability was not influenced by enzymes (Fig. 1B-C). Meropenem reduced *S. aureus* CFU of 2.1 $\log_{10}$ but was ineffective against *P. aeruginosa* while tobramycin reduced *S. aureus* and *P. aeruginosa* CFU counts of 3.8 and 3.5 $\log_{10}$, respectively. The enzymes did not systematically improve antibiotic effects on CFU.

For VBB496 biofilm, none of the treatments was capable of reducing biomass (Fig. 1D) while treatments including tobramycin reduced only *S. aureus* counts (Fig.1 E-F). Meropenem concentration was therefore increased to 100-fold MIC (6 mg/L) against VBB496, but no major improvement was noticed (Fig. S4).

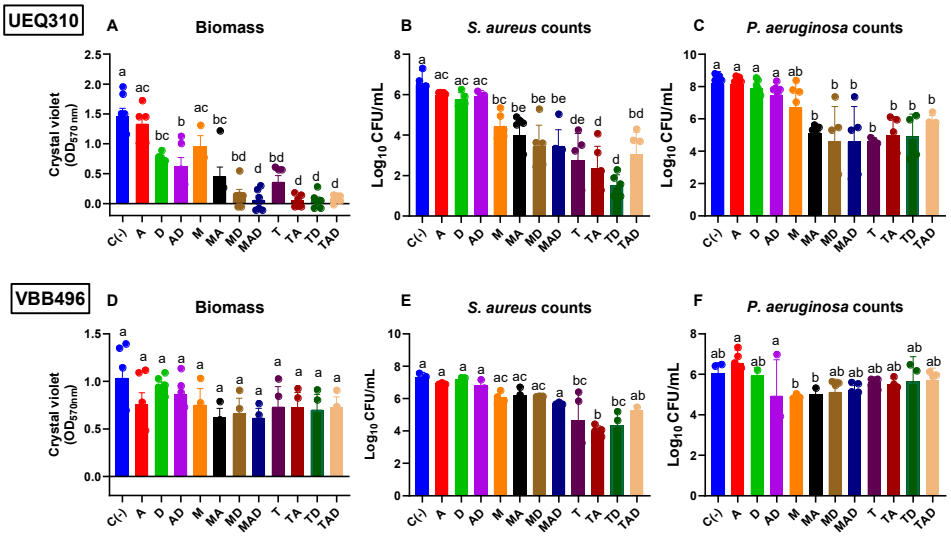

Figure 1. Activity of alginate lyase (250 mg/L), DNase I (40 mg/L), meropenem or tobramycin against dual species biofilm of co-isolated *S. aureus* and *P. aeruginosa* UEQ310 (A-C) or VBB496 (D-F). 72-h biofilms were exposed during 24 h to the different treatments. Antibiotic concentrations were set at 10-fold the highest MIC (0.6 mg/L for meropenem and 20 mg/L for tobramycin against UEQ310 [A-C], and 0.6 mg/L for meropenem and 40 mg/L for tobramycin against VBB496 [D-F]). Abbreviations (from left to right): C(-): non-treated control; A: alginate lyase; D: DNase I; AD: alginate lyase and DNase I; M: meropenem; MA: meropenem and alginate lyase; MD: meropenem and DNase I; MAD: meropenem, alginate lyase and DNase I; T: tobramycin; TA: tobramycin and alginate lyase; TD: tobramycin and DNase I; TAD: tobramycin, alginate lyase and DNase I. Values are means ± SEM from at least 3 experiments performed in triplicates for biomass and means ± SD of at least three independent experiments for CFU counts. Statistical analyses: bars with different letters are statistically different from each other ($p < 0.05$; one-way ANOVA with Tukey post-hoc analysis).

Effect of combined antibiotics in combination with enzymes on dual-species biofilms

Individual antibiotics being not highly effective, they were combined in the next experiments. Tobramycin was first used at 5-fold the highest MIC, and meropenem, at 5-fold the highest MIC against UEQ310 but 25-fold MIC against VBB496; enzymes maintained at the concentrations used before (Fig. S5). Biomass was reduced by all treatments containing DNase I and/or antibiotics for the UEQ310 biofilm, and by antibiotics combined with any enzyme for the VBB496 biofilm. Bacterial counts of both species were significantly reduced by the antibiotic mixture for both dual-species biofilms, but combining them with enzymes did not bring further improvement. Noteworthy, *S. aureus* counts in the UEQ310 biofilm were below the quantification limit when exposed to antibiotics combined or not with enzymes.

Similar results were obtained when antibiotic concentrations were doubled (10-fold the highest MIC for tobramycin [both stains] and meropenem against UEQ310; 50-fold MIC for meropenem against VBB496), except that the biomass was even more decreased when the UEQ310 biofilm was exposed to the antibiotic mix, combined or not with enzymes (Fig. S6).

As VBB496 dual species biofilm was still not responsive to this treatment, antibiotic concentrations were further increased to 50-fold MIC against VBB496 (3 mg/L meropenem and 200 mg/L tobramycin) and to only 20-fold MIC against UEQ310 (1.2 mg/L meropenem and 40 mg/L tobramycin). At the same time, DNase I concentration was raised to 400 mg/L but alginate lyase was kept at 250 mg/L.

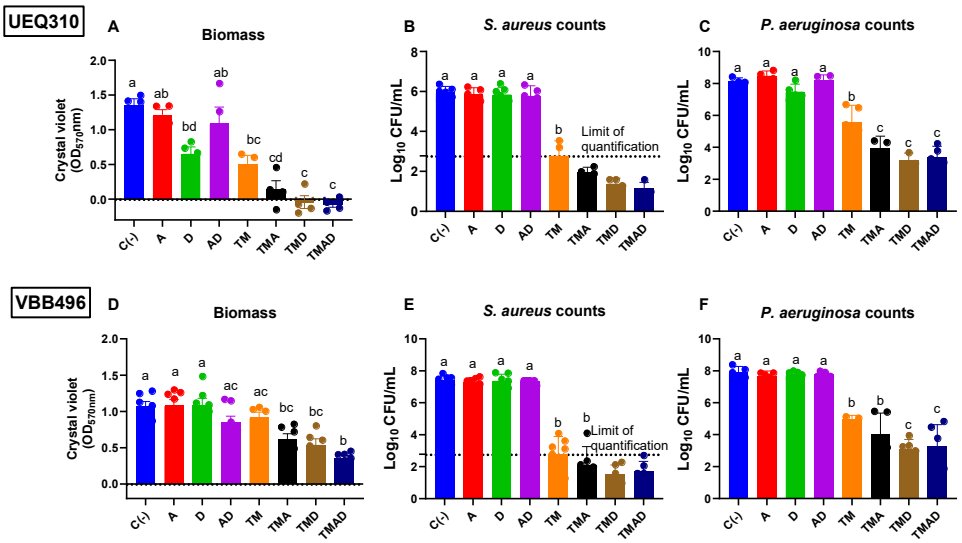

Figure 2. Activity of alginate lyase (250 mg/L), DNase I (400 mg/L), meropenem or tobramycin against dual species biofilm of co-isolated *S. aureus* and *P. aeruginosa* UEQ310 (A-C) or VBB496 (D-F). 72-h biofilms were exposed during 24 h to the different treatments. Antibiotic concentrations were set at 20-fold the highest MIC for UEQ310 (1.2 mg/L meropenem and 40 mg/L tobramycin [A-C]) and 50-fold the highest MIC for VBB496 (3 mg/L meropenem and 200 mg/L tobramycin [D-F]). Abbreviations (from left to right): C(-): non-treated control; A: Alginate lyase; D: DNase I; AD: alginate lyase and DNase I; TM: tobramycin and meropenem; TMA: tobramycin, meropenem, and alginate lyase; TMD: tobramycin, meropenem and DNase I; TMAD: tobramycin, meropenem, alginate lyase and DNase I. Values are means ± SEM from at least 3 experiments performed in triplicates for biomass and means ± SD of at least three independent experiments for CFU counts. Statistical analyses: bars with different letters are statistically different from each other ($p < 0.05$; one-way ANOVA with Tukey post-hoc analysis). The dotted line shows the limit of quantification.

For UEQ310 biofilm, the activity was similar to that observed with 10-fold MIC of antibiotics and 40 mg/L DNase I (Fig. 2A-C). For VBB496 biofilm, a significant synergistic effect was observed between antibiotics and enzymes, resulting in (i) a

substantial reduction in biomass when the antibiotic mix was combined with the two enzymes, (ii) a decrease in the CFUs of *P. aeruginosa* that was more important when antibiotic mix was combined with DNase I alone or mixed with alginate lyase, and (iii) *S. aureus* counts falling below the limit of quantification (Fig. 2D-F). For UEQ310, monospecies biofilms were subjected to the same treatments (Fig. S7). Reduction in *P. aeruginosa* biomass and counts were similar in monospecies and mixed species biofilms, while *S. aureus* biomass and counts were less affected in monospecies than in mixed species biofilm, illustrating that interspecies interactions modify their susceptibility to treatments. *P. aeruginosa* VBB496 did not grow alone, preventing us from studying single species biofilms for this pair.

Visualizing antibiotics-enzymes synergies using confocal laser microscopy

Fig. 3 shows confocal microscopy images of biofilms exposed to antibiotics and enzymes in the conditions described in Fig. 2, with staining of bacteria (red; SYTO-60), eDNA (green, TOTO-1) and polysaccharides (blue; calcofluor white).

A strong reduction in TOTO-1 and calcofluor white signals was observed in UEQ310 biofilm exposed to enzymes, suggesting a degradation of the matrix. SYTO-60 signal was markedly reduced by antibiotics, indicating bacterial elimination. All three signals vanished in biofilms exposed to the enzymes-antibiotics combination, demonstrating their combined and synergistic effects on the biofilm. Similar observations were made for VBB496, but the reduction in TOTO-1 and SYTO-60 signals were less important.

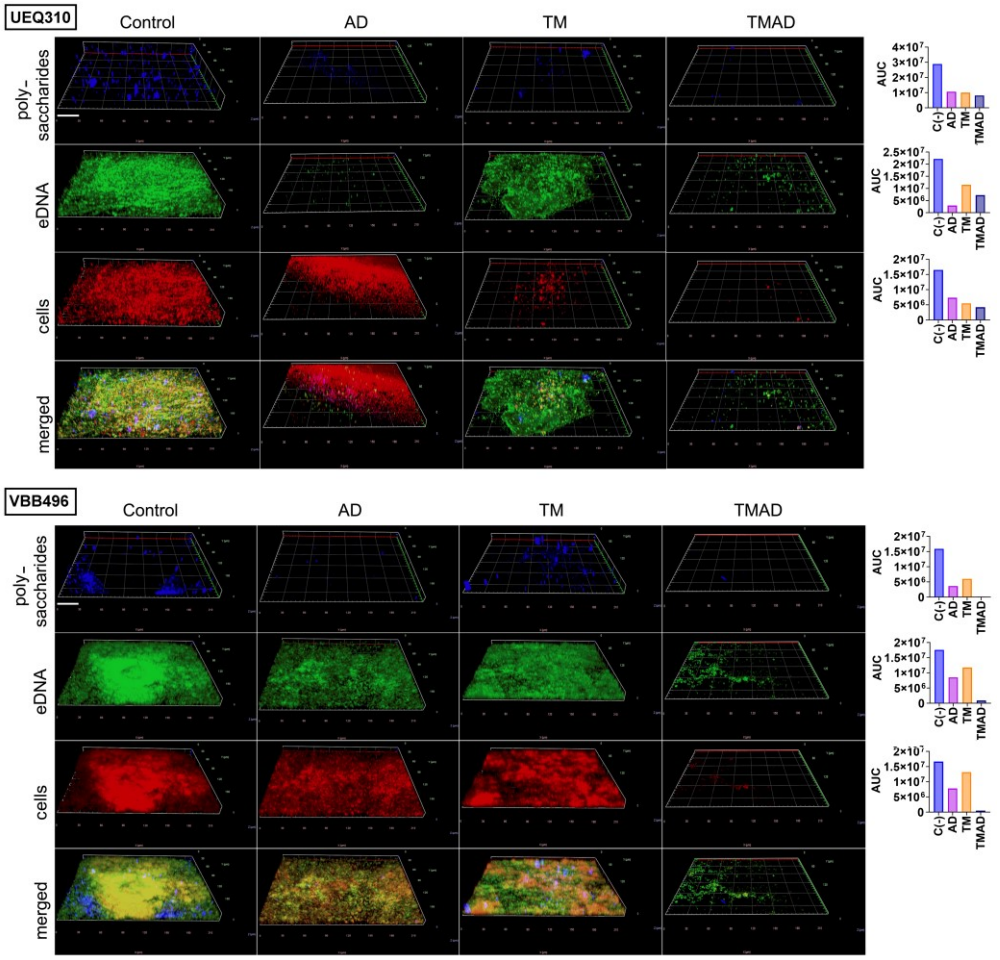

Figure 3: Confocal microscopy images of dual species biofilms of UEQ310 (a) or VBB496 (b) exposed to antibiotics, enzymes or their combination at the same concentrations as those described in Fig. 2 (A: Alginate lyase 250 mg/L; D: DNase I 400 mg/L; T: Tobramycin 40 mg/L (for UEQ310) or 200 mg/L (for VBB496); M: meropenem 1.2 mg/L (for UEQ310) or 3 mg/L (for VBB496). Polysaccharides were stained with calcofluor white (blue), eDNA with TOTO-1 (green), and cells with SYTO 60 (red). The right panel displays the total amount of significant fluorescence signal in the z-stack (calculus described in supplementary methods S1). Two independent experiments were performed, and different views within the

same biofilm were observed under a confocal microscope. Scale bar (on top left panel for each biofilm= 30 μm)

Viscoelasticity of biofilms in correlation with treatment efficacy

Biofilms are characterized by their elasticity (resistance to deformation) and viscosity (resistance to flow), which protect them against mechanical and chemical challenges during growth and maturation, contributing to the severity of infection [181]. Viscoelasticity was measured in biofilms treated as in Fig. 2. Elasticity and viscosity were higher in biofilms than in ASM+ (Fig. S2).

Fig. 4 shows the correlation between the reduction in elastic modulus of the biofilms and the effect of the treatments on biomass or CFU counts. For UEQ310 biofilm, a clear correlation was observed, with the antibiotic mix combined with one or two enzymes bringing the elastic modulus back to ASM+ values. For the much less elastic VBB496 biofilm, no correlation was seen, but all treatments containing DNase I caused a decrease in elasticity associated with a decrease in biomass and CFUs only when antibiotics were present. A similar analysis was performed *versus* viscous modulus and came to similar conclusions for UEQ310 (Fig. S8). The viscous modulus of VBB4 96 was so low (very close to the ASM+ value) that no conclusion could be drawn.

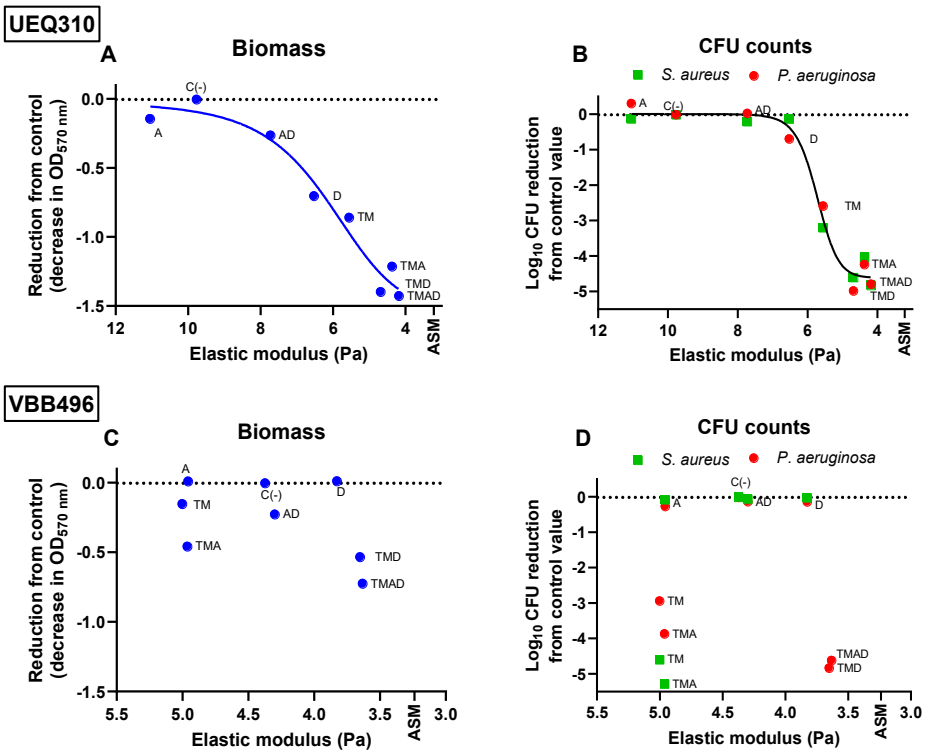

Figure. 4. Correlation between the elastic modulus of biofilms in control or treated conditions and the effect of the treatments on biofilm biomass or CFU counts. The different agents were added at the same concentrations as those described in Fig. 2 (A: Alginate lyase 250 mg/L; D: DNase I 400 mg/L; T: Tobramycin 40 mg/L for UEQ310 and 200 mg/L for VBB496; M: meropenem 1.2 mg/L for UEQ310 and 3 mg/L for VBB496).

III.2.e. Discussion

This work demonstrates the efficacy of a combined approach using two broad-spectrum antibiotics and a mixture of enzymes degrading eDNA and alginate, to disrupt biofilm matrix and kill embedded bacteria, in a complex, clinically-relevant, in-vitro model of dual-species *S. aureus-P. aeruginosa* biofilm growing in artificial sputum medium.

In this model, enzymes alone do not influence bacterial counts and do not consistently reduce biomass. Antibiotics alone prove ineffective in reducing biofilm biomass, and have modest effects on CFU counts, with tobramycin being more active than meropenem. Interestingly, the combination of enzymes and antibiotics cause a substantial reduction in biomass for the UEQ310 biofilm, but not for the VBB496 biofilm. Given that the biomass of the UEQ310 biofilm is more abundant than that of VBB496 biofilm, it may better respond to the applied enzymatic treatments than the VBB496 biofilm.

Remarkably, when the two antibiotics are combined with DNase I and/or alginate lyase, there is almost complete elimination of biofilm biomass, eradication of *S. aureus,* and a significant reduction in *P. aeruginosa* counts in both biofilms. Confocal microscopy supports these findings by demonstrating a substantial reduction in eDNA and polysaccharide content when the enzymatic cocktail is applied, a decrease in bacterial viability with the antibiotic cocktail for UEQ310, and a drastic reduction in both biomass constituents and viable cell counts when these treatments are combined.

The UEQ310 biofilm displays higher elasticity and viscosity than the VBB496 biofilm, probably because pyocyanin, produced in higher amounts by the pigmented UEQ310 *P. aeruginosa,* increases biofilm viscosity and surface hydrophobicity by binding to eDNA [326]. Interestingly, for this biofilm, a correlation is observed between the decrease in the biofilm viscoelasticity and the efficacy of the treatments applied. Among enzymes, only DNase I has an impact, in accordance to the fact that eDNA is the main contributor to the mucus viscoelasticity [321]. Intriguingly, the antibiotic cocktail also reduces biofilm viscoelasticity. This contrasts with a recent study showing that tobramycin, used at much higher concentrations than those utilized here, does not affect the viscoelasticity in a mono-species biofilm of *P. aeruginosa* grown in mucus [327]. Yet, clinical data indicate that the

rheological properties of mucopurulent mucus are altered due to infection and inflammation, and that the mucus elastic modulus is reduced when patients are treated by antibiotics, in relation with the resolution of their infection [328]. This supports our in-vitro observations, and suggests that the primary action of antibiotics, consisting in reducing bacterial counts, results in a subsequent reduction in the viscoelasticity of the biofilm. Conversely, the degradation of the matrix by the enzymes leads to a reduction in viscoelasticity, which helps antibiotics to exert their activity.

The VBB496 biofilm displays low viscoelasticity, implying that additional factors may hinder drug activity. Indeed, although DNase I still contributes to slightly reduce the elastic modulus of this biofilm, this reduction is not associated with a reduction in biomass or CFU counts in the absence of antibiotics.

Noteworthy, the impressive effects of the treatment combining two enzymes and two antibiotics are obtained with high concentrations. The highest concentrations of tobramycin and meropenem we used (200 mg/L and 3 mg/L, respectively) still fall in the range of concentrations measured in the sputum of patients receiving these drugs by inhalation (> 1000 mg/L [329] for tobramycin and 2.2 mg/L for a dose of 500 mg of meropenem [330], inferior to the unitary dose used nowadays (1-2 g)). Concerning enzymes, low concentrations of DNase I (4 mg/L, close to the concentration measured in sputum of treated patients [325]) or alginate lyase (25 mg/L) proved active on single species biofilms of *S. aureus* or *P. aeruginosa* [331, 332]. This was not the case in our dual-species biofilm model, indicating the need for further exploring the potential benefits of these enzymes at higher concentrations in-vivo in more complex situations.

Some limitations of this study need to be acknowledged. Firstly, the use of only two pairs of clinical isolates may not fully represent the diversity of clinical isolates, although they were deliberately selected for their different phenotypes to provide some coverage of this variability, as exemplified by the difference in biomass or in bacterial counts observed for both types between their biofilms. Secondly, a detailed analysis of the composition of the biofilm matrix was not performed. This type of analysis is currently not feasible in clinical practice. Therefore, if matrix-degrading enzymes were considered for clinical use, their selection would be empirical.

In conclusion, this study highlights that synergy between antibiotic combinations and matrix-degrading enzymes is a valuable approach for addressing challenging dual-species biofilm infections. The elevated enzyme concentrations required point towards the use of inhalation systems offering targeted drug deposition in predefined areas of the lung [333]. However, they may even though raise safety concerns that must be addressed before considering potential clinical applications.

III.2.f. Acknowledgments and Conflicts of interest

Acknowledgments

Z.W. is recipient of a Chinese Scholarship Council (CSC) PhD grant. R.V. and F.V.B. are research directors from the Belgian Fonds de la Recherche Scientifique (FNRS-FRS). This work was supported by the Belgian FNRS (grants J.0162.19 and J.0177.23) and by a grant from the King Baudouin Foundation (Fonds Forton) and the Belgian Mucovereniging/Association Muco. The authors thank V. Mohymont, M. Scopa, and R. Tricot for dedicated technical assistance.

Conflicts of interest

The authors have no conflict of interest to declare.

III.3. Bacteriophage-antibiotics combination therapy

Adopted from:

Bacteriophages as potential antibiotic potentiators in cystic fibrosis:

A new model to study the combination of antibiotics with a bacteriophage cocktail targeting dual species biofilms of *Staphylococcus aureus* and *Pseudomonas aeruginosa*

Zhifen Wang[1,$], Steven De Soir[1,2,$], Antoine Glorieux[1,2], Maia Merabishvili[2], C. Knoop[3], Daniel De Vos[2], Jean-Paul Pirnay[2], Françoise Van Bambeke[1,*]

[1] Pharmacologie cellulaire et moléculaire, Louvain Drug Research Institute, Université catholique de Louvain, Brussels, Belgium

[2] Laboratory for Molecular and Cellular Technology, Queen Astrid Military Hospital, Neder-over-Heembeek, Belgium

[3] Erasme Hospital, Université libre de Bruxelles, Brussels, Belgium

[$] equal contribution as first authors

Submitted for publication in February 2024; revision in progress.

III. 3.a. Abstract

Staphylococcus aureus and *Pseudomonas aeruginosa* co-infections in patients with cystic fibrosis (CF) are associated with disease severity. Their treatment is complicated by biofilm formation in the sticky mucus obstructing the airways. Using a dual species biofilm (*P. aeruginosa/S. aureus*) formed in artificial sputum medium, we investigated the activity of broad-spectrum antibiotics (meropenem, ceftazidime, ciprofloxacin, tobramycin) combined with a cocktail of two (bacterio)phages (PSP3 and ISP) proven active via spot tests and double agar on *P. aeruginosa* PAO1 and *S. aureus* ATCC25923. At the highest tested concentrations (100 x MIC), antibiotics alone caused a 20-50% reduction in biomass and reduced *S. aureus* and *P. aeruginosa* CFU of 2.3 to 2.8 and 2.1 to 3.6 $\log_{10}$, respectively. Phages alone reduced biofilm biomass by 23% and reduced *P. aeruginosa* CFU of 2.1 $\log_{10}$, but did not affect *S. aureus* viability. Phages enhanced antibiotic effects on biomass and exhibited additive effects with antibiotics against *P. aeruginosa*, but not against *S. aureus.* Following inhibition of bacterial respiration by phages in planktonic cultures rationalized these observations by demonstrating that PSP3 was effective at multiplicities of infection (MOI) as low as 10^{-4} plaque forming units (PFU)/CFU on *P. aeruginosa*, but ISP, at higher MOI (> 0.1 PFU/CFU) against *S. aureus*. Thus, prescreening inhibition of bacterial respiration by phages may assist in selecting those showing activity at sufficiently low titers to showcase anti-biofilm activity in this complex but clinically-relevant in vitro model of biofilm.

Keywords: phages, antibiotics, cystic fibrosis, dual-species biofilm, *Staphylococcus aureus, Pseudomonas aeruginosa*

Highlights

- Dual-species (*S. aureus-P. aeruginosa*) biofilms in CF are difficult to eradicate.
- A dual-species model in artificial sputum medium was set up.
- Combinations of broad-spectrum antibiotics and phages were tested.
- Synergy was observed between antibiotics and phages to reduce biofilm biomass.
- Synergy on CFU in biofilm was observed only for phages active at low PFU/CFU.

III. 3.b. Introduction

Cystic fibrosis (CF) affects over 150,000 people worldwide, mostly of Caucasian descent. It is caused by genetic mutations in the *CFTR* gene. Altered CFTR channel leads to disruption in salts and water balance in mucosal epithelia, causing the thickening of mucus in the lungs. This sticky mucus fosters persistent bacterial infections, which remain the main cause of morbidity and mortality in patients with CF [334].

Eradicating infections in cystic fibrosis is hindered by this protective mucus layer, shielding microbes from immunological and antibiotic pressures, and promoting biofilm formation [334]. Within these bacterial aggregates, cells become metabolically inactive and are protected by the self-produced extracellular matrix consisting of polysaccharides, extracellular DNA, and proteins, which results in antibiotic tolerance. The predominant pathogens, *Staphylococcus aureus* and *Pseudomonas aeruginosa*, co-infect more than 25% of the patients. *S. aureus,* highly prevalent in children and adolescents (50-80%) contributes to airway inflammation and reduced lung function, while *P. aeruginosa,* infecting 20-30% of children and

up to 80% of adults, is a major cause of respiratory failures and death [334]. Given the scarcity of effective antibiotics against biofilms, there is an urgent need for new treatment strategies.

In this context, bacteriophages have emerged as potential antibiotic potentiators and biofilm disruptors. As natural bacterial predators, bacteriophages have co-evolved with their hosts to coexist in various micro-environments. Over the last two decades bacteriophages garnered renewed interest and proven consistently safe. They have demonstrated lytic activity in the sputum from infected patients with CF [335], and synergetic interactions in combination with antibiotics, including in in-vitro models with CF isolates [243, 336, 337] or in a few patients with CF [338].

In this study, we aim to assess a combination of antibiotics with a bacteriophage cocktail consisting of two phages targeting respectively *S. aureus* (phage ISP) and *P. aeruginosa* (phage PSP3) on a unique dual-species biofilm model, growing in artificial sputum media (ASM+ [289]), reflecting a clinically-relevant environment. Selected for their broad host range [339, 340] and demonstrated activity against single-species biofilms [340, 341]. Additionally, Phage ISP has been approved for use in clinical settings [342, 343], and there is potential for Phage PSP to be utilized on patients in the future due to its therapeutic efficacy against *P. aeruginosa* single-species biofilms and its strictly lysogenic character [340]. These phages are also combined with broad-spectrum antibiotics routinely used in patients with CF (ceftazidime, meropenem, ciprofloxacin, and tobramycin).

III. 3.c. Materials & Methods

Bacteria, phages and antibiotics

The reference strains *S. aureus* ATCC25923 and *P. aeruginosa* PAO1 were used. Phage isolation and propagation techniques were described elsewhere [340]. Phage PSP3 active on *P. aeruginosa* (de novo isolated at the Queen Astrid Military Hospital [340]) and Phage ISP active on *S. aureus* (Eliava Institute, Tbilisi, Georgia [339]) were selected as active on these strains. Ciprofloxacin, ceftazidime, meropenem and tobramycin (potency, 89%, 72%, 92% and 100%, respectively) were obtained from Bayer (Leverkusen, Germany), Panpharma (Luitré-Dompierre, France), Fresenius Kabi (Schelle, Belgium) and Galephar (Marche-en-Famenne, Belgium), respectively, and selected as representative broad-spectrum antibiotics active on both species.

Dual-species biofilms

Mature dual species biofilms were formed in artificial sputum medium (ASM+; see [289] for detailed composition) based on a previously published protocol [255]. In brief, *S. aureus* colonies from an overnight culture were suspended in Cation-adjusted Mueller Hinton Broth (MHB-ca; Sigma-Aldrich), adjusted to a turbidity of 2.6 McFarland units and diluted to achieve approx. 2.1 $\log10^7$ CFU/mL. Two hundred µL of this suspension were inoculated in 96-well plates, which were incubated at 37 °C for 2 h to allow bacterial adhesion. MHB-ca was then replaced with ASM+ and plates were further incubated at 37 °C for 24 hours. Medium was removed and replaced by 20 µL of *P. aeruginosa* (from an overnight culture diluted in MHB-Ca to approx. 1.35 10^7 CFU/mL) and 180 µL ASM+. Biofilms were then grown at 37 °C for 48 h with refreshment of the medium after 24 h, in order to obtain a mature, stable dual-species biofilm.

Antibiotic and phage activity on planktonic bacteria

MICs were determined in MHB-Ca according to CLSI guidelines. Phage activity was determined by spot assay and double agar assay [340]. The effect of phages on bacterial growth was further determined in liquid culture using a 96-well plate reader system, specifically the OmniLog® system (Biolog, Hayward, CA). This involved monitoring changes in color intensity resulting from the reduction of a tetrazolium dye, which occurs during active bacterial growth when cellular respiration reduces the tetrazolium dye and produces a color change that is measured automatically [344].

A bacterial suspension in PBS was adjusted to an OD_{600nm} of 0.5 and diluted 10-fold in lysogeny broth (LB) containing a 100-fold diluted tetrazolium dye (average inoculum, 10^7 CFU/mL). Individual phages were added at different Multiplicities of Infection (MOI; PFU/CFU ratio) and colour intensity was read every 15 minutes at 37 °C and converted in relative respiration units, with data analysis performed with the Omnilog Data Analysis Software 1.7.

Antibiotic and phage activity on dual species biofilms

ASM+ medium from mature biofilms was removed and replaced by ASM+ containing individual antibiotics alone or combined with a cocktail containing PSP3 and ISP each at 10^9 PFU/mL. After 24 h of incubation at 37 °C, the medium was removed, and biofilms were washed once with PBS. To measure residual CFU, biofilms were disrupted by mechanical scratching, resuspended in 200 µL of PBS and sonicated (30 s at 60% amplitude; Q700; QSonica, Newton, CT) to release cells and disaggregate the biofilm structure. Aliquots were serially diluted and plated onto Mannitol Salt Agar (MSA; peptone 5 g/L, NaCl 75 g/L, D-mannitol 10 g/L, agar 15 g/L) or *Pseudomonas* Isolation Agar (PIA; Sigma-Aldrich) to allow the selective counting of *S. aureus* and *P. aeruginosa* CFU, respectively. Residual biomass was measured after crystal violet staining as previously described [289].

Statistical analysis

Statistical analyses were performed with GraphPad Software (version 10.1.2; GraphPad Software, San Diego, CA).

III. 3.d. Results

Antibiotic susceptibility testing

Table 1 shows the MICs of antibiotics against *S. aureus* ATCC25923 and *P. aeruginosa* PAO1. In subsequent experiments, antibiotics were used at 1, 10 and 100-fold the MIC of the less susceptible isolate in this pair.

Activity of phages and antibiotics against dual species biofilms

Figure 1 shows the activity of individual antibiotics alone or combined with the phage cocktail against 48 h dual-species biofilms.

Considering first the treatment effects on biomass, ceftazidime was ineffective, while meropenem reduced it by approx. 20% (at concentrations ≥ 10-fold MIC), and tobramycin and ciprofloxacin, of approx. 50% (at concentrations ≥ 10- and 1-fold the MIC, respectively), with no improvement when their concentration was increased. Phages alone caused a 23% reduction in biomass. Phage-antibiotic combinations were more active than antibiotics or phages alone, with a drop of at least 70% of the biomass observed when phages where combined with ciprofloxacin at 1-fold its MIC and with other antibiotics, at 10-fold their MIC.

Considering then the treatment effects on bacterial counts, all antibiotics alone caused a concentration-dependent decrease in CFU, which was significant for concentrations ≥ 1-fold the MIC for ciprofloxacin but ≥ 10-fold the MIC for the other antibiotics, against both strains. At the highest concentration tested, reductions of

S. aureus and *P. aeruginosa* CFU reached -2.8 and -3.5 $\log_{10}$ for ciprofloxacin, -2.5 and -3.6 $\log_{10}$ for tobramycin, -2.3 and -3.1 $\log_{10}$ for meropenem, and -2.3 and -2.1 $\log_{10}$ for ceftazidime, respectively. Phages alone were inactive on *S. aureus* but reduced *P. aeruginosa* CFU of 2.1 $\log_{10}$. In combination with antibiotics, no improvement was observed against *S. aureus* (except with tobramycin at 10-fold the MIC), but a globally additive effect was observed against *P. aeruginosa* except with ciprofloxacin (at all concentrations) and tobramycin (at 100-fold the MIC), i.e. in conditions for which the antibiotic alone was already highly effective (decrease of 3.5 $\log_{10}$).

Inhibition by phages of bacterial respiration in planktonic cultures

As the phage cocktail improved antibiotic activity against *P. aeruginosa* but not *S. aureus,* we further characterized their activity against planktonic bacteria. To this effect, we followed the respiration rate of each bacterial strain over time in the presence of phage ISP (*S. aureus*) or PSP3 (*P. aeruginosa*) (Figure 2). Phage ISP completely inhibited the respiration of *S. aureus* ATCC25923 at MOI > 0.1 PFU/CFU. Its activity decreased progressively with dilution and vanished at MOI of 10^{-5} PFU/CFU. Phage PSP3 totally prevented PAO1 respiration during 14 h at MOI $\geqslant 10^{-4}$ PFU/CFU, after which bacteria recovered full metabolic activity, suggesting they developed resistance to the phage.

Table 1: MIC of antibiotics in MHB-ca (mg/L)

Antibiotics[a]	S. aureus ATCC25923	P. aeruginosa PAO1
Ciprofloxacin	8	0.25
Ceftazidime	0.5	2
Meropenem	0.03	1
Tobramycin	0.5	1

[a] EUCAST resistance breakpoints (R): > 8 mg/L for meropenem and ceftazidime against *P. aeruginosa* (no breakpoint set for beta-lactams against *S. aureus* but ATCC25923 is an MSSA and therefore considered as susceptible), > 0.5 and 1 mg/L for ciprofloxacin against *S. aureus* and *P. aeruginosa*, respectively, and > 2 mg/L against both species for tobramycin

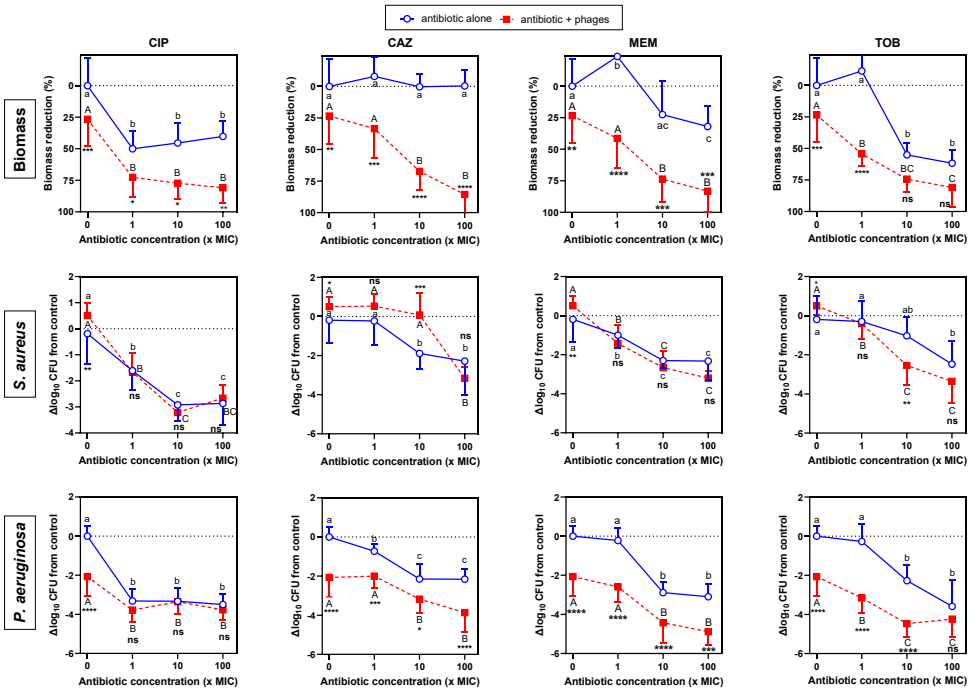

Figure 1**:** Activity of antibiotics and phages against 48 h dual species biofilms formed by reference strains *S. aureus* ATCC25923 and *P. aeruginosa* PAO1. Biofilms were incubated during 24 h in control conditions or with antibiotics at 1, 10 or 100 x MIC (ciprofloxacin [CIP], ceftazidime [CAZ], meropenem [MEM], or tobramycin [TOB], ISP and PSP3 phages each at 10^9 PFU/mL or their combinations. The successive rows show the reduction in biomass expressed in percentage of the crystal violet OD_{570nm} measured for non-treated biofilms (top), the reduction in viable counts of *S. aureus* (middle) or *P. aeruginosa* (bottom), both expressed in $\Delta\log_{10}$ CFU from control. Control values were 1.4 ± 0.35 (biomass), 5.8 ± 0.7 $\log_{10}$ CFU/mL for *S. aureus* and 8.7 ± 0.3 $\log_{10}$ CFU/mL for *P. aeruginosa.* Statistics: Two-way ANOVA analysis with Tukey post-test. Comparison between antibiotic concentrations: data points with different letters are statistically different from one another ($p < 0.05$; small letters: antibiotic alone; caps letters: antibiotic + phages). Comparison between antibiotic alone and antibiotic + phage at a given antibiotic concentration: ns, not significant; *, $p < 0.05$; **, $p < 0.01$; ***, $p<0.001$; ****, $p < 0.0001$. Data are mean ± SD (N≥3; n=8).

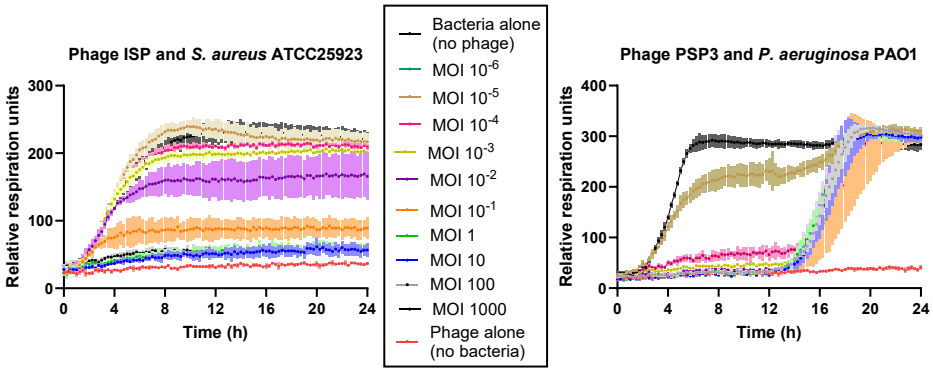

Figure 2: Activity of phages against planktonic cultures of reference strains *S. aureus* ATCC25923 and *P. aeruginosa* PAO1. Bacteria (initial inoculum: 10^7 CFU/mL) were incubated during 24 h in control conditions or with phages at different MOI. A negative control (phages in the absence of bacteria) and a positive control (bacteria in the absence of phages) were also included. Colour intensity was measured every 15 minutes to follow the reduction of a tetrazolium dye by metabolic active bacteria. Data are mean ± SD (n=3).

III.3.e. Discussion

Using a dual species biofilm cultivated in a highly viscous medium reminiscent of the conditions prevailing in the lungs of patients with CF [289], we found that antibiotics exhibit some degree of activity, particularly when used at elevated concentrations. Interestingly, this activity is higher than that observed in the corresponding mono-species biofilms [275, 289], as previously described for broad-spectrum antibiotics in a much simpler dual-species biofilm model [345]. When combined with a cocktail comprising one phage active on *S. aureus* and another one active on *P. aeruginosa,* antibiotic activity was further improved against biomass and against *P. aeruginosa* counts, but not against *S. aureus* counts. This lack of effect against *S. aureus* was unexpected, considering that the phage ISP was active on *S. aureus* ATCC25923 in double agar assay, and showed activity against single species biofilms grown in much less complex medium [341].

One potential reason for decreased phage activity against biofilms may be attributed to the barrier effect of the mucoid environment in the artificial sputum medium. To the best of our knowledge, phage activity against dual-species biofilms in this medium has not been previously evaluated and the influence of mucus on phage activity is still a topic of debate [338]. While one study indicates that a phage cocktail remains active against *P. aeruginosa* in sputum samples from patients with CF [335], there are no data for *S. aureus.* The presence of mucus is suggested to enhance phage proximity to bacteria and persistence at the infection site [346], while intestinal mucus has been reported to impair phage killing capacity [347]. The influence of ASM+ on phage activity remains unexplored. However, it is noteworthy that phage activity against *S. aureus* is hindered in human plasma. This is attributed to the plasmas tendency to promote bacterial aggregation, consequently masking phage surface receptors, a phenomenon that may also occur in biofilms [348].

Another factor contributing to reduced phage activity may arise from the biofilm lifestyle, known for conferring antibiotic tolerance due to decreased bacterial metabolism and to the protective matrix barrier. Phage activity against biofilms, particularly in dual-species biofilm models, is not well-characterized. Many studies primarily focus on *P. aeruginosa* using CF isolates, often cultivated in conventional bacterial culture media. Martin *et al.* observed enhanced reduction in biomass and bacterial counts with a combination of antibiotics and a four-phage cocktail [337]. In contrast, Fiscarelli *et al.* rather found stimulation of pseudomonal biofilms exposed to either sub-inhibitory concentrations of antibiotics or of several phages but significant reduction of biomass of biofilms treated by phages and tobramycin [243]. Chang *et al.* reported synergistic interactions between phage PEV20 and ciprofloxacin against *P. aeruginosa* biofilms while phages alone were not active [336]. Regarding staphylococci, studies mainly relate to implant-related biofilm infections, where the matrix effect impedes phage activity, particularly against *S. epidermidis* [349].

Few studies have examined *S. aureus* - *P. aeruginosa* dual-species biofilms, particularly in conditions resembling those found in patients with CF. Overall, these studies indicate that synergy between antibiotics and phages can occur, though not consistently, and is notably influenced by factors such as the concentrations of phages and antibiotics, their simultaneous or sequential administration, and the frequency of phage applications over time [350]. These studies also suggest that outcomes are generally less favourable against dual-species biofilms compared to mono-species biofilms of the same strains.

Our phage cocktail achieved a 20-25% reduction in biofilm biomass and a 2 $\log_{10}$ CFU reduction for PAO1 only, and these effects were markedly amplified when combined with antibiotics. Biomass reduction by phages is somehow surprising, considering that none of the two phages used produces depolymerases [339, 340],

i.e. enzymes hydrolyzing biofilm matrix polymers. A recent review compiling all existing data on phage activity against biofilms [351] suggests that increased burst size, phage inoculum, and infection time lead to more significant biomass reduction, which aligns with our findings. Conversely, CFU reduction is typically observed with phages possessing smaller genomes that can replicate more rapidly, a characteristic not met by our phages with genome sizes of 138,715 bp for ISP and 66,308 bp for PSP3 [339, 340].

In this context, the assessment of phage activity against planktonic cultures by continuous monitoring of bacterial respiration provides valuable insights. Previous research indicates that disparity might be observed between phage activity measured by plaque assay and their efficacy on biofilms [337]. We noticed that ISP requires higher MOI to prevent *S. aureus* ATCC25923 growth in planktonic cultures compared to PSP3 against *P. aeruginosa* PAO1. Given that MOI were ranging from 1000 to 10 PFU/CFU at the time of phage addition to biofilms (10^9 PFU added to biofilms containing ~10^6 and 10^8 CFU/mL of *S. aureus* and *P. aeruginosa*), our findings suggest that effective action on biofilms in ASM+ requires phages to exhibit efficacy at considerably lower MOI against planktonic bacteria, emphasizing the challenge of their low bioavailability in this complex biofilm model. This also suggests that the concept of tolerance in biofilms may extend to phages, not just antibiotics. Additionally, it is worth noting that the use of phage PSP3 at low titers and without simultaneous antibiotic quickly foster resistance development.

Our study has some limitations. Firstly, we only used two strains and two phages. This stems from the complexity and labor-intensive nature of our biofilm model, making high-throughput screening impractical. This also explain why we did not test various conditions of treatment applications, despite their potential impact on the results. Notwithstanding these limits, our data suggests a future experimental strategy could involve prescreening their effect on bacterial growth in planktonic

cultures before biofilm testing. Lastly, we did not extensively examine the biofilm matrix composition or the phage's ability to penetrate biofilms, as these complex analyses would represent an independent undertaking beyond the scope of the present study.

In a recent position paper [352], the taskforce of the Antibacterial Resistance Leadership Group (ARLG) in the US underscored a series of knowledge gaps in the field of phage therapy, including the lack of consensus on optimal evaluation methodologies to evaluate phages or phage-antibiotic combinations in order to predict their clinical efficacy, the needs to characterize their activity against biofilms, or the necessity to consider how the environment at the site of infection might influence their activity. These considerations are crucial as we await data from well-conducted clinical trials. In this context, our study pioneers the evaluation of phage-antibiotic combinations against relevant dual-species biofilms in an in-vitro model relevant of CF. The established model and evaluation process can now be applied to clinical isolates, and the identified pitfalls may guide further investigations to evaluate alternative phages or treatment protocols with optimized efficacy.

III.3.f. Acknowledgments and Conflicts of interest

Acknowledgments

This work was supported by the Belgian Fonds de la Recherche Scientifique (FNRS-FRS) grant J.0177.23 and by a grant from the King Baudouin Foundation (Fonds Forton) and the Belgian Mucovereniging/Association Muco. Z.W. is recipient of a Chinese Scholarship Council (CSC) PhD grant and was further supported by the King Baudouin Foundation (Fonds Forton) and the Belgian

Mucovereniging/Association Muco; S.D.S received a Doctiris doctoral fellowship from Innoviris (grant 2019-PHD-9). A. G. is supported by a grant from the King Baudouin Foundation (Fonds Forton) and the Belgian Mucovereniging/Association Muco. M.M. is supported by the Royal Higher Institute for Defence. F.V.B. is Research Director from the Belgian FNRS-FRS.

Conflicts of interest

The authors have no conflict of interest to declare.

Chapter IV. Discussion & Perspectives

IV.1. Main achievements of this work

Biofilm poses a significant health threat, contributing to as much as 80% of infections. Cystic fibrosis chronic infection exemplifies a typical case of biofilm, presenting as a multispecies-biofilm infection. However, the key pathogens driving lung deterioration in this context are *S. aureus* and *P. aeruginosa*. Treating biofilm infections proves challenging due to their high tolerance to antibiotics, necessitating ongoing efforts to discover and optimize strategies for combatting such infections.

The establishment of a robust in vitro biofilm model serves as the foundational and crucial first step in developing novel approaches to combat biofilm-related issues. In this thesis, we successfully attained our initial goals. Specifically, ① we developed a dual-species biofilm model that can be applicable to clinical isolates and used to screen novel therapy strategies. In addition, we investigated and revealed a cross-adaptation phenomenon between *S. aureus* and co-isolated *P. aeruginosa* from the same patients. Notably, the mechanism driving this cross-adaptation differs from the conventional explanations involving the interaction between *S. aureus* and *P. aeruginosa*. ② We utilized enzymes as an adjuvant of antibiotics to successfully improve the efficacy of eradicating biofilms. ③ We employed phages as an adjuvant to antibiotics to increase the efficacy of biofilm therapy.

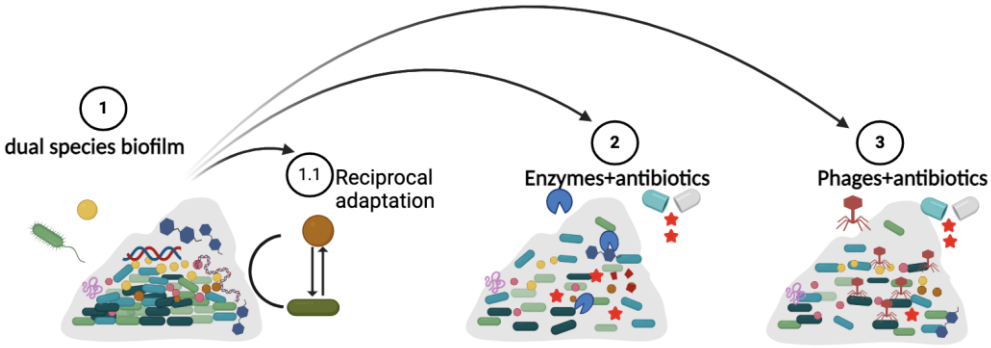

Figure 1: Schematic representation of main achievements of this thesis

Development of dual species biofilm model

The evaluation of the dual-species biofilm model in our conditions relies on several critical factors. Firstly, it depends on whether *S. aureus* and *P. aeruginosa* can form aggregates and produce EPS, marking the initial step. Secondly, successful coexistence of both species over an extended period is crucial, posing a significant challenge as laboratory *S. aureus* and *P. aeruginosa* often exhibit competitive behavior. Thirdly, it is essential for *S. aureus* and *P. aeruginosa* to remain stable over time. Lastly, and importantly, the model must be suitable for diverse clinical isolates from patients. Without a doubt, the model developed in this study meets all these conditions, except for the use of a unique phenotype of *S. aureus*. As the infection progresses, microorganisms adapt to the lung environment in patients with CF, exhibiting different genotypes and phenotypes. We have already confirmed that this model could be suitable for diverse *P. aeruginosa* based on its various phenotypes. Although we didn't test it for different phenotypes of *S. aureus* isolates, we believe that this model is also applicable to diverse isolates of *S. aureus* from patients with CF, such as mucoid *S. aureus* or SCVs. These *S. aureus* phenotypes are generally more advantageous for this pathogen survival in a hostile environment or when encountering competitive rivals like *P. aeruginosa*.

The highlight of this model is its reliance on the ASM+ medium, mimicking the average components found in the airways of patients with CF. Another crucial aspect is its ability to replicate the observed colonization order of *S. aureus* and *P. aeruginosa* in vivo, achieved through the inoculation of *S. aureus* before *P. aeruginosa*. Initially, we did not consider mimicking the colonization sequence of *S. aureus* and *P. aeruginosa* in the lungs of CF patients when constructing biofilms. This decision was based solely on the fact that *S. aureus* could not stably survive when both bacteria were cultured simultaneously, even with a minimal inoculum of *P. aeruginosa*. One possible explanation for the ability of *S. aureus* to remain stable over time when inoculated with *S. aureus* prior to *P. aeruginosa* is that a 24-hour incubation is adequate for the development of a biofilm, providing protection to *S. aureus* from the toxic metabolites produced by *P. aeruginosa*. The mechanism by which biofilms exhibit tolerance to antibiotics was discussed in the introduction to Chapter 1, and this mechanism also applies to preformed *S. aureus* biofilms exposed to toxic products from *P. aeruginosa*.

Additionally, this model is not confined to our current study; it can be extended to encompass any strategies or agents used for combating biofilm relevant to lung infections in CF patients. For instance, other anti-biofilm strategies including nanoparticle-metal treatment, Quorum Sensing Inhibitors, and Nano-Based Antibiotic Delivery. Meanwhile, it can also be further used for exploration about interaction between species due to the gown condition ASM+ close to sputum of patients.

It should be clarified that the ASM+ used in our study did not represent all types of mucus in CF patients. Previous studies in our laboratory have compared ASM+ with two groups of mucus samples classified according to their macroscopic appearance: purulent (uniformly green or yellow) and mucopurulent (a mixture of purulent and mucoid portions) [275]. Both purulent and mucopurulent mucus have distinct

viscoelastic properties. However, in both categories the elastic moduli were higher than the viscous moduli within the same range of shear strains [275]. Similarly, the artificial sputum medium has higher elasticity than viscosity, whereas ASM+ was closer to mucopurulent sputum and represents a portion of the mucus collected from CF patients [275]. The difference in mucus may enable biofilm to have a different response to antibiotic treatment. Thus, this model may not exactly cover all biofilm that infects patients with CF when screening anti-biofilm strategies or agents. Indeed, the replication of all mucus characteristics presents a significant challenge due to fluctuations observed between patients and even in the same patient over time. Moreover, with the introduction of new corrective therapies (such as CFTR modulators), mucus properties may undergo drastic changes.

Investigation of reciprocal adaptation between co-isolated *S. aureus* and *P. aeruginosa*

The initial observation of mutual adaptation was based on the similar CFUs between *S. aureus* and *P. aeruginosa*, as well as the spatial distribution of cross-aggregation between the two within the biofilm. Furthermore, this reciprocal relationship was further confirmed through experiments utilizing cross-strain cultures. The methods employed to evaluate cross-adaptation are practical and cost-effective, making them applicable to a broad spectrum of studies investigating bacterial interactions.

The interaction between *S. aureus* and *P. aeruginosa* is complex and diverse. Earlier in-vitro coculture studies, utilizing laboratory strains of *S. aureus* and *P. aeruginosa*, revealed the eradication of *S. aureus* by *P. aeruginosa*, leading to an initial characterization of their interaction as a competitive relationship. The mechanisms underlying this competition have been thoroughly studied and understood. However, these two microorganisms often co-infect patients with conditions such as CF or other infections, like wounds. This has prompted a reassessment of the interaction

between *S. aureus* and *P. aeruginosa*, leading to a consensus that competition is not the exclusive relationship between them; they also coexist, even within in-vitro coculture settings. Furthermore, longitudinal studies following patients have concluded that the interaction between *S. aureus* and *P. aeruginosa* undergoes a transition from competition in the early stages of infection to coexistence or even bacterial cooperation in the later stages [258, 263]. Studies on the mechanisms of coexistence between these two bacteria have been growing over time. Most investigations have focused on *P. aeruginosa*, suggesting that its adaptation to the lungs of CF patients leads to decreased virulence, thereby favoring the survival and coexistence of *S. aureus* and *P. aeruginosa* [272]. For instance, *P. aeruginosa* decreases the production of toxic metabolites like pyocyanin, HQNO, and rhamnolipids, which promote the survival of *S. aureus*.

A limited number of studies have focused on the bidirectional adaptation between these two bacteria. These limited studies currently emphasize trophic cooperation, specifically regarding carbon sources. For example, acetoin produced by *S. aureus* can be catabolized by *P. aeruginosa* as an alternative carbon source, and its accumulation is toxic to *S. aureus*. The catabolic ability of *P. aeruginosa* on acetoin was thought to favor the coexistence of *S. aureus* with *P. aeruginosa*. We also compared the expression of catabolic acetoin genes in biofilm formed by co-isolated *S. aureus* and *P. aeruginosa* pairs with reciprocal adaptation, as opposed to cross-strain pairs without reciprocal adaptation. However, no difference was observed between the two groups, suggesting that acetoin may not be a determining factor contributing to reciprocal adaptation between *S. aureus* and *P. aeruginosa* in our experimental conditions. This could be attributed to the rich nutrients present within ASM+. Once again, it emphasizes that growth conditions are crucial for the interaction between bacteria. Different media may lead to variations in metabolic products and gene expression.

A notable example is the secretion of siderophores pyoverdine and pyochelin by *P. aeruginosa* when iron is limited in growth conditions, while the production of siderophores is lacking in a rich iron medium. It's worth noting that the production of pyoverdine and pyochelin is not beneficial to the survival of *S. aureus* when co-cultured with *P. aeruginosa*. Thus, some mechanisms of interaction between *S. aureus* and *P. aeruginosa*, if not using a medium mimicking the in-vivo growth environment, may differ from the actual mechanisms involving cross-adaptation in the mucus within the airways of patients with CF.

Under conditions mimicking the growth environment and using co-isolated *S. aureus* and *P. aeruginosa* from the same patients, we proposed that the reciprocal adaptation between *S. aureus* and *P. aeruginosa* was attributed to the downregulation of harmful genes to each other, and *S. aureus* increased resistance to toxic metabolites produced by *P. aeruginosa*. In parallel, we found that *P. aeruginosa* secondary metabolites didn't have a major impact on mutual adaptation, as *S. aureus* thrived in the presence of co-isolated *P. aeruginosa* that produced abundant QS metabolites. Instead, the thriving of *S. aureus* was associated with the overexpression of genes involved in response to oxidant conditions (*crtN*) when cocultured with *P. aeruginosa* overproducing QS.

Still, the interaction between *S. aureus* and *P. aeruginosa* remains complex. Several seemingly minor factors may contribute to the reciprocal adaptation between the two. For example, the delayed production of QS secondary metabolites due to slow growth of *P. aeruginosa* can help *S. aureus* develop a defense mechanism. Additionally, *P. aeruginosa* with a mucoid phenotype has already been determined to have a reduced ability to compete with *S. aureus* due to the overproduction of alginate. The suggested mechanism indicates that alginate is involved in the downregulation of QS genes and the subsequent decrease in QS metabolites [214]. However, in our study, the mucoid phenotype in *P. aeruginosa* (UEQ310) did not

result in the inactivation of QS genes, and abundant QS metabolites were produced when co-cultured with co-isolated *S. aureus*. Therefore, additional mechanisms by which mucoid *P. aeruginosa*, overproducing alginate, contributes to the survival of *S. aureus* are yet to be determined.

Once again, the interaction between *S. aureus* and *P. aeruginosa* is diverse, even in cases of coinfection in the same patients. Therefore, the reciprocal adaptation observed in our study does not account for the fact that all co-infected *S. aureus* and *P. aeruginosa* pairs exhibit the similar behaviors (reciprocal adaptation). In a poster presented at the European Society of Clinical Microbiology and Infectious Diseases (refer to the appendix for the poster [**Chapter V**]), we had the opportunity to showcase dual-species biofilms separately formed by different phenotypes of *P. aeruginosa* and corresponding co-isolated *S. aureus* from the same patients. Notably, in this study, the non-mucoid *P. aeruginosa* (857JBJ) exhibited a competitive advantage over *S. aureus*, despite both species originating from the same patient. These co-isolated pairs may not yet exhibit reciprocal adaptation and could be in an evolutionary stage that is only a matter of time. Reciprocal adaptation is possibly a final evolutionary outcome in dual-species interactions.

In addition to nutritional factors influencing the interaction between *S. aureus* and *P. aeruginosa*, other microorganisms may play a role in the interplay between these two bacteria in co-infected patients with CF. These include bacteria such as *H. influenzae*, non-tuberculous mycobacteria, *S. maltophilia*, *A. xylosoxidans*, and *B. cepacia*, fungi such as *Aspergillus fumigatus*, *Candida albicans*, *Scedosporium spp*., *Pneumocystis jirovecii*, and *Exophiala dermatitidis*, as well as viruses. Most of these microorganisms interact with either *S. aureus* or *P. aeruginosa*. For instance, *H. influenzae* exposure significantly diminishes susceptibility to *P. aeruginosa* infection, likely by priming host innate immunity rather than through direct interspecies competition [353]. Interactions between *S. aureus* and NTM remain

unreported, but a limited study exists for *P. aeruginosa* and NTM. The two organisms can coexist in a dual-species biofilm, forming a "layered" structure with the *P. aeruginosa* biofilm atop the NTM biofilm, without *P. aeruginosa* directly inhibiting NTM [354]. Besides, *P. aeruginosa* has been reported to inhibit biofilm formation by *A. fumigatus* and kill its cells upon contact [355]. However, recent studies have shown a synergistic relationship where *P. aeruginosa* supports *A. fumigatus* growth beyond its immediate vicinity through volatile compounds usable by *A. fumigatus* as metabolites [354]. At present, little is known about viral-bacterial interactions in the CF respiratory tract and how viruses affect the interaction between *S. aureus* and *P. aeruginosa*.

Additionally, the presence of immune cell debris like neutrophil may impact the relationship between *S. aureus* and *P. aeruginosa* by fostering biofilm formation. Therefore, it is advisable to take into account the disease context and the environmental conditions conducive to bacterial growth or aggregation when investigating the interactions among these microorganisms.

Exploring the reciprocal adaptation between coisolated *S. aureus* and *P. aeruginosa* holds considerable significance, as heightened reciprocal adaptation could exacerbate the severity of infection and increase tolerance to antibiotic treatment. Our findings present an illustrative case: the co-isolated pair VBB496 demonstrated a comparable reciprocal adaptation, even in a commensal-like relationship where *P. aeruginosa* struggles to survive and form a biofilm when cultured alone. Furthermore, the biofilm formed by *P. aeruginosa* VBB496 in conjunction with co-isolated *S. aureus* was not as robust and abundant as that of another pair (UEQ310). However, intriguingly, the VBB496 biofilm exhibited significant tolerance to antibiotic treatment compared to the robust biofilm of UEQ310.

While our study did not systematically examine how the interaction influences therapy efficacy, it remains crucial to comprehend the impact of the interplay between *S. aureus* and *P. aeruginosa* on treatment outcomes. This understanding is vital for developing innovative strategies against biofilm infections. Exploring methods to disrupt or unbalance reciprocal adaptation could pave the way for more effective interventions, offering novel approaches to combat biofilm formation and enhance treatment effectiveness.

Potential of antimicrobials with an adjuvant

Enzymes and phages were separately utilized as adjuvants to antibiotics for treating biofilms grown in ASM+, mimicking sputum of patients with CF. Enzyme-antibiotic combinations demonstrated synergistic efficacy against biofilms of clinical isolates. Additionally, phage-antibiotic combinations exhibited additive efficacy against reference biofilms.

The treatment procedures were similar between enzyme-antibiotics and phage-antibiotics combinations for treating biofilm. Specifically, antibiotics and adjuvants (phages or enzymes) were incubated in parallel without washing the biofilm, mimicking the real-life scenario where biofilm cannot be washed before treatment in vivo. Additionally, the biofilms of reference strains or one pair of clinical isolates primarily grew in ASM+ rather than on the inner surface of wells, making washing of the biofilm impractical and potentially disruptive to the biofilm structure. Furthermore, the absence of antagonisms between the enzyme or phages and the antibiotics underscores the rationale for using both strategies in parallel. However, it should also be considered in the future to sequentially incubate with the adjuvant first and then antibiotics, as this may potentially enhance efficacy.

In the first strategy of enzyme-antibiotic combination, a significantly high concentration of DNase I and alginate lyase was required to achieve a dramatic

reduction in biomass and CFUs of the biofilm. The elevated enzyme concentration may indicate an abundant substrate of DNA and alginate within the biofilms. However, it also potentially suggests constrained enzymatic activity at such high concentrations. On one hand, DNA is one of the constituents within ASM+ and therefore a part of DNase I would degrade the DNA within the medium. This results in less abundant DNase I available to target the DNA within the biofilm. Consequently, an abundant substrate of DNA in ASM+ and the biofilm necessitates a corresponding higher concentration of DNase I to effectively treat the biofilm. Notably, it is impossible to directly bypass the DNA constituents of ASM+ or mucus to target the biofilm. The only potential improvement may involve finding a method for enzyme delivery.

On the other hand, the optimal activity of DNase I is obtained in the presence of magnesium ions. However, magnesium was also reported to increase biofilm formation [356], reason why didn't add magnesium ions during treatment with DNase I. Additionally, alginate lyase commonly exhibits optimal activity under acidic conditions. Clearly, the local conditions necessary for optimal enzyme activity were not met in our experiments. This could be another possible reason for the limited efficacy observed, which warrants further investigation in future studies.

In the second approach involving the combination of phages and antibiotics, an additional effectiveness was observed in targeting the biofilm of reference strains, yet further investigation is required for clinical isolates. The biomass of dual-species biofilm and the culturable cells of one species (*P. aeruginosa*) were significantly reduced compared to treatment with either phages or antibiotics alone, but there was limited activity against the other species (*S. aureus*) within the dual-species biofilm. Besides the potential influence of ASM+ (as presented in paper 3) on the activity of phage ISP (targeting *S. aureus*), interactions between *S. aureus* and *P. aeruginosa* may decrease the activity of phage ISP against *S. aureus*, resulting in less additive

efficacy against this species. One mechanism of bacteriophage resistance involves bacteria preventing phage adsorption to receptors located on the bacterial cell membrane or cell wall through receptor alteration or masking. It has been reported that *Staphylococcus aureus* protein A (SpA) is capable of blocking phage adsorption to receptors [357]. However, it's worth noting that the reference strain *P. aeruginosa* PAO1 maintains an advantage over *S. aureus*, despite both species coexisting well over time. Therefore, it is highly likely that *P. aeruginosa* induces the production of more proteins similar to SpA to further increase bacterial resistance to phages. Additionally, polysaccharide production also potentially blocks phage adsorption, further decreasing phage activity against bacteria.

An optimal therapeutic outcome for dual-species biofilms is the dramatic elimination of both species within the biofilm. In the strategy involving enzyme-antibiotic combinations, significant reductions were observed in both species compared to treatment with either enzymes or antibiotics alone. However, for the phage-antibiotic combination, a lesser improvement was noted against *S. aureus* within the biofilm compared to treatment with either phages or antibiotics alone. It is noteworthy that this strategy still exhibited additive activity against *S. aureus* when phages were combined with tobramycin at a 10-fold MIC. This underscores the importance of considering antibiotic selection and concentration screening for future applications. Therefore, the application of bacteriophages as potentiators of antibiotics remains promising for clinical isolates.

IV.2. Limitation of this work

Growth environment of biofilm

Different growth conditions, reference strains, as well as experimental designs may generate varying impacts on the response of biofilm to antibiotics. Simultaneously,

these factors could influence the interaction between *S. aureus* and *P. aeruginosa*, potentially leading to diverse responses and further enabling biofilms to exhibit different sensitivity to antibiotic treatment.

ASM+ mimics the viscoelasticity of mucopurulent sputum rather than purulent sputum, which allows it to represent a portion of the mucus collected from CF patients. Consequently, our model only depicted biofilms growing in partial mucus (mucopurulent mucus), while biofilms growing in purulent mucus were absent in this thesis. Despite ASM+ being similar to mucopurulent mucus, the growth environment of biofilm in vitro remains distinct from the real environment in vivo. On one hand, the in vitro culture environment for biofilm formation did not include other microorganisms such as *H. influenzae*, NTM, *S. maltophilia*, *A. xylosoxidans*, and *B. cepacia*. These microorganisms could compete for nutrition and space. In parallel, lung epithelial or immune cells such as neutrophils were also absent, whereas they likely influence biofilm formation and interactions between *S. aureus* and *P. aeruginosa*. On the other hand, while we considered the average composition and viscoelasticity of mucus present in the airways of CF patients for ASM+ to mimic partial mucus, we overlooked the oxygen and acidity levels during biofilm growth in vitro culture. Specifically, we did not take into account the oxygen and acidity levels of mucus occurring in the airways of CF patients when growing the biofilm in vitro.

The mucus found in the airways of patients with CF typically presents a slightly acidic environment (pH=6.6-7.0)[358]. Such acidic conditions have been suggested to promote the formation of *P. aeruginosa* single-species biofilm and accelerate its resistance development, yet this effect can also be reversed by restoring the acidic environment to physiologically neutral conditions [359]. However, the ASM+ utilized in this study exhibits slightly higher pH values ranging from 7.1 to 7.4 compared to the mucus of patients. This slight increase in pH in our medium

potentially influences the formation of dual-species biofilm and the biofilms' tolerance to antibiotics.

Additionally, oxygen is present at a steep concentration gradient, often hypoxic or microaerobic, in the deeper mucus of patients with CF [360]. It's worth noting that the surface of the CF airway is consistently exposed to high oxygen concentrations [358], resulting in only the interior of the mucus being an anaerobic or microaerobic environment. Although our medium may potentially exhibit a limited oxygen concentration due to its thick and high viscoelastic properties, we did not measure the oxygen level within ASM+.

The low level of oxygen has been found to reduce the sensitivity of the biofilm to antibiotics such as tobramycin, ciprofloxacin, carbenicillin, ceftazidime, chloramphenicol, and tetracycline [361]. Additionally, aside from directly increasing tolerance to antibiotics, these microenvironments with acidic and anaerobic or microaerobic characteristics also affect the interaction between *S. aureus* and *P. aeruginosa*, further diminishing the response to antibiotics. For instance, anaerobic conditions have been identified as promoting the coexistence of *S. aureus* and *P. aeruginosa*, potentially influencing disease progression [301, 362].

***In vivo* localization of dual-species biofilms**

25-30% of CF patients are co-infected with *S. aureus* and *P. aeruginosa* [33], and numerous in vitro dual-species biofilms of these pathogens have been established, primarily grown in conventional media [178, 363]. In our study, *S. aureus* and *P. aeruginosa*, co-isolated from the same patients, co-aggregated throughout the biofilm architecture, as confirmed by confocal laser microscopy. However, to date, there is no available evidence demonstrating simultaneous biofilm formation by *S. aureus* and *P. aeruginosa* at the same lung site in CF patients. One study indicated the presence of multiple biofilms in explanted CF lung tissue, where these species

typically aggregated separately in vivo [177]. When examining sputum samples, it remains challenging to directly observe the localization of *S. aureus* and co-infected *P. aeruginosa* because it is not possible in such samples to know if co-isolates species where originating from the same location in the lungs. Visualizing the localization of both species in explanted lungs, remains the only available option to ascertain if *S. aureus* and *P. aeruginosa* form biofilms in the same area in CF patients.

Experimental design and technique

Our reference model only confirmed its applicability to biofilms formed by different strains of *S. aureus* and *P. aeruginosa*. In these biofilms cultured in ASM+ mimicking the mucus environment found in patients, both species remain stable over time and produce abundant biomass. However, it's important to note that clinical isolates of both *S. aureus* and *P. aeruginosa* display diversity within patients with CF. Therefore, this reference model cannot fully replace the complexity of biofilms formed in vivo when optimizing and determining novel therapy strategies against such infections. For example, while the reference model demonstrated improved therapeutic efficacy with a phage-antibiotic combination, it was not effective against biofilms formed by two pairs of clinical isolates (UEQ310 and VBB496).

In our investigations of the interaction between *S. aureus* and *P. aeruginosa* within biofilms, we encountered limitations in the techniques available to us. We did not explore the various matrix compositions and their proportions within the biofilms due to these limitations. Additionally, we did not measure the heterogeneous microenvironment within the biofilm, including variations in acid and oxygen concentration. However, these differences in oxygen and pH levels, as well as the composition of the biofilm matrix, have the potential to influence the interaction between *S. aureus* and *P. aeruginosa*, thereby potentially impacting treatment efficacy in parallel.

Moreover, a comprehensive experimental design was challenging, particularly concerning mechanisms of cross adaptation between *S. aureus* and *P. aeruginosa*, as our initial focus was on developing a biofilm model. This primarily stems from several aspects. On one hand, we did not conduct a full transcriptomic analysis, as stated in paper 1. Instead, we directly examined the expression of genes associated with our hypothesis using RT-PCR techniques. The reciprocal adaptation between *S. aureus* and *P. aeruginosa* resulted from a decrease in the virulence of *P. aeruginosa* and an increase in the tolerance of *S. aureus* to *P. aeruginosa*. Therefore, we investigated specific genes potentially involved in this interaction using RT-PCR techniques, such as QS genes. However, the virulence factors of *P. aeruginosa* are not solely limited to the products of the genes quantified in this study. They may also be attributed to surface structure virulence factors, as depicted in Chapter 1, including lipopolysaccharides located on the outer face of the outer membrane and secretion systems, or genes associated with trophic processes. In fact, mutations in genes involved in lipopolysaccharide synthesis have been suggested to potentially play a role in the interaction between *S. aureus* and *P. aeruginosa*, although the precise nature of these interactions remains to be determined [217]. It may be more reasonable for transcriptomic analysis to be used initially to examine the expression of whole genoees, followed by the confirmation of altered gene expression through RT-PCR.

On the other hand, we employed LC-MS to detect secondary metabolites in the biofilm and discovered that *P. aeruginosa* is a key contributor to the production of these compounds in dual-species biofilm with *S. aureus*. However, volatile compounds secreted by bacteria could not be quantified or identified using this method [364]. For instance, a representative volatile compound produced by *P. aeruginosa*, hydrogen cyanide (HCN), was not detected in our study. HCN is a potential biomarker of *P. aeruginosa* infection in patients with CF and has been

identified to control *S. aureus* growth in a mouse model of airways coinfected by *P. aeruginosa* and *S. aureus* [365, 366]. Furthermore, the secondary metabolites identified in our studies were predominantly produced by *P. aeruginosa*, even in the presence of *S. aureus*. This indicates that the organic small molecules generated by *S. aureus* are extremely limited, and the detection technique is potentially constrained in identifying compounds with lower abundance. Additionally, the existing literature on secondary metabolites secreted by *S. aureus* is also sparse. It's noteworthy that *S. aureus* secretes virulence factors primarily composed of proteins, including adhesins, proteins evading host immunity such as SpA, and exotoxins like α-, β-, γ-hemolysin, PVL, and PSMs. These primary metabolites may play a role in the interaction between *S. aureus* and *P. aeruginosa*. However, we did not assess the primary metabolites produced by *S. aureus* or *P. aeruginosa* in their dual-species biofilm.

In our study on biofilm therapy, we did not systematically explore conditions for treating dual-species biofilms with enzyme- or phage-antibiotic combinations. For instance, therapy efficacy might vary between simultaneous incubation of adjuvants (enzymes/phages) with antibiotics and sequential incubation of adjuvants (enzymes/phages) with antibiotics. Additionally, our testing was limited to therapy strategies involving enzymes applied to biofilms separately formed by two pairs of co-isolated *S. aureus* and *P. aeruginosa* from two patients. Both strains of *P. aeruginosa* in these pairs exhibited similar mucoid phenotypes. However, other biofilms of clinical isolates with non-mucoid or SCVs phenotypes may respond differently to enzyme-antibiotic combinations. Furthermore, we did not investigate the use of phage-antibiotic combinations on biofilms of clinical isolates. Although this therapy demonstrated significant additive efficacy against reference dual-species biofilm, diverse clinical isolates may potentially respond differently to phage-antibiotic combinations in our study.

IV.3. Perspectives

The conditions and methodologies employed in our studies are open to further refinement, and there is potential for expanding upon our research findings.

Optimization of Biofilm Growth Environment

As previously described in the paragraph on Chapter IV, Part 2, Limitations of this Work, biofilm formation, the interaction between *S. aureus* and *P. aeruginosa*, as well as the response of biofilm to antibiotic treatment, can all be affected by a series of factors, including other species of microorganisms (such as *H. influenzae*, NTM, *S. maltophilia*, *A. xylosoxidans*, and *B. cepacia*), immune and epithelial cells, pH, and oxygen concentration in the growth environment. These factors were not addressed in this thesis but could be investigated in future research.

Addition of other microbial species

The key challenge lies in distinguishing and quantifying individual bacteria from a multi-species biofilm when introducing other microorganisms. The biomass of a multi-species biofilm can be easily characterized using crystal violet, while the viability of individual species can be quantified by plating on selective media. Eva et al. have developed six selective media to characterize individual bacteria from multi-species biofilms containing *P. aeruginosa*, *S. aureus*, *A. xylosoxidans*, *S. anginosus*, *Rothia mucilaginosa*, and *Gemella haemolysans* [367]. Among them, at least three selective media used for the selection of the former three bacteria are available for use in our future studies. The selection of other selective media for multiple-species cultures is still to be determined.

Addition of CF lung epithelial cells

It is feasible to introduce human CF lung cells when establishing multiple-species biofilms relevant to lung infections in patients with CF. Single-species biofilms with human airway epithelial cells have been established, whereas these biofilms were grown in conventional medium, such as minimal essential medium [368-370]. The CF lung model grown in artificial sputum medium was achieved by adding human A549 cells line [371]. The A549 cell line is derived from adenocarcinoma human alveolar basal epithelial cells. However, opportunistic species preferentially infect the bronchi rather than the alveoli [358]. Therefore, for future studies aiming to establish multiple-species biofilms, it is advisable to primarily consider using bronchial epithelial cell lines, such as BEAS-2B or the ATCC-approved cell line pair NuLi-1 and CuFi-1 monolayers. These choices would better represent the CF microenvironment.

Adjustment of H^+ and O_2 within Artificial Sputum Medium

The biofilm growth conditions in this thesis maintain a near-neutral pH and are aerobic. However, considering the weakly acidic and anaerobic or microaerobic environment that occurs in the airways of patients with CF, it is necessary to adjust the pH value and oxygen concentration within the artificial sputum medium (ASM+) to resemble the conditions of mucus in patients more closely. The pH value within ASM+ can be easily adjusted to a range of 6.6 to 7.0 using hydrochloric acid solution. Additionally, a microaerobic culture condition can be achieved using CampyGen gas generation packs in large anaerobic jars. These packs generate a microaerophilic environment composed of 5% oxygen, 10% carbon dioxide, and 85% nitrogen [372].

Consequence of reciprocal adaptation between *S. aureus* and *P. aeruginosa* and additional potential mechanisms

As already presented in "Chapter I, Part 2.3.3: Interactions Between *S. aureus* and *P. aeruginosa* within a Biofilm", the coexistence of *S. aureus* and *P. aeruginosa* within a biofilm can impact antimicrobial efficacy. This interaction can result in one species potentially demonstrating increased tolerance to antibiotics against the other, while at the same time, it may also lead to decreased tolerance. In our study, the representative co-isolate pair VBB496 demonstrated a significant enhancement of reciprocal adaptation between *S. aureus* and *P. aeruginosa* compared to another pair, UEQ310 (as referenced in Paper 1). Interestingly, the dual-species biofilm formed by VBB496 exhibited greater resilience to antibiotic eradication compared to the UEQ310 pair, as showed by the results from Paper 2. These findings suggest that the reciprocal adaptation between *S. aureus* and *P. aeruginosa* has the potential to increase the tolerance of dual-species biofilms to antibiotics. Therefore, the sensitivity of dual-species biofilms to antibiotics may depend on the nature of their interaction between *S. aureus* and *P. aeruginosa*. Certainly, additional experimental research is warranted to validate this observation.

The future study could involve additional co-isolated pairs exhibiting reciprocal adaptation, such as SCVs and similar non-pigmented mucoid strains of *P. aeruginosa*. If all dual-species biofilms demonstrate that reciprocal adaptation between *S. aureus* and *P. aeruginosa* enhances tolerance to antibiotics, it would be valuable to investigate mechanisms for further understanding this adaptation and its implications for antibiotic treatment. Moreover, it is crucial to prioritize the development of strategies aimed at disrupting the balance between *S. aureus* and *P. aeruginosa*, thereby enhancing the efficacy of antibiotic treatments.

Additional mechanisms involving reciprocal interactions between *S. aureus* and *P. aeruginosa* could be explored from several perspectives. Firstly, by comparing the cell surface structures of clinical isolates exhibiting reciprocal and non-reciprocal adaptation, including flagella and pili IV associated with motility. This comparison aims to understand how these differences contribute to cross-adaptation between *S. aureus* and *P. aeruginosa*, focusing on surface structure virulence factors of *P. aeruginosa*, such as secretion systems and lipopolysaccharides. Secondly, investigating the interactions between a series of virulence proteins secreted by *S. aureus* and *P. aeruginosa*, including adhesin proteins or exotoxins such as α-, β-, and γ-hemolysin, PVL, and PSMs produced by *S. aureus*. Thirdly, exploring how volatile organic small molecules produced by both species influence their interaction. Lastly, the trophic cooperation between *S. aureus* and *P. aeruginosa* will be investigated and the composition of the biofilm matrix will be analysed, as most studies have used conventional media. These potential mechanisms can be studied using techniques such as transcriptomic analysis and proteomic analysis, either individually or in combination.

Extension of clinical isolates and antibiotics

Clinical isolates

All clinical isolates of *S. aureus* and *P. aeruginosa* recovered from CF patients tested in this thesis were found to be susceptible to the antibiotics examined. However, it's worth noting that methicillin-resistant *S. aureus* (MRSA) accounts for a prevalence ranging between 10% and 20% in CF patients. Additionally, the Patient Registry Annual Data Report from the Cystic Fibrosis Foundation in the United States in 2022 revealed that 12.7% of *P. aeruginosa* isolates exhibited multidrug resistance (MDR-PA) among individuals with CF and cultures growing *P. aeruginosa*. Therefore, the biofilm model holds promise for studying these multiple resistant clinical isolates

and exploring alternative strategies, such as phages in combination with antibiotics like vancomycin. Successful cases of phage therapy targeting single-species infections of MRSA and MDR-PA have been documented. Abd-Allah, Israa M., et al., isolated five phages belonging to the Siphoviridae family, order Caudovirales, which exhibited lytic activity against a set of 23 MRSA strains [373]. Another phage, vFB297, a member of the genus Pakpunaviru, has been identified and successfully treated a clinical patient infected with MDR-PA [374]. Thus, the development and eradication of *S. aureus* and *P. aeruginosa* dual-species biofilms with multiple resistant clinical isolates hold promise through the use of phages specifically targeting the multiple resistant bacteria, in combination with antibiotic therapy.

Antibiotics

The treatment with individual antibiotics needs to consider the activity of each antibiotic against both *S. aureus* and *P. aeruginosa* within the biofilm. Thus, the selection of antibiotics was limited in our study. Only ciprofloxacin, meropenem, ceftazidime, and tobramycin met this condition in which individual antibiotics simultaneously act on *S. aureus* and *P. aeruginosa*. Moreover, ceftazidime and meropenem showed less effectiveness against biofilms of reference strains and clinical isolates even in combination with adjuvants. Considering the limitation of single antibiotics that can simultaneously act on both species, individual antibiotics either acting on *S. aureus* or *P. aeruginosa* can be combined to treat dual species biofilm, which offers more therapeutic options. Using combination antibiotics with adjuvants such as enzymes or bacteriophages again can maximize therapeutic efficacy. In our experimental work, the combination of meropenem and tobramycin showed higher efficacy than individual antibiotics. This opens a door for other combinations of antibiotics to treat dual species biofilm in context of CF. Moreover, a more significant efficacy was obtained when two antibiotics were combined with enzymes to treat dual species biofilm. Another interest of combining antibiotics has

the potential to decrease the rate of resistance and might result in synergistic effects. Some common combinations of antibiotics are already used to treat single-species biofilm infection. For instance, a synergistic efficacy was observed when rifampicin was combined separately with vancomycin, linezolid, and daptomycin to treat *S. aureus* single-species biofilm [375]. Tobramycin-ceftazidime combination was used to treat *P. aeruginosa* single-species biofilm, which also showed the most efficacy [376]. Lastly, based on antibiotic combination, antibiotic combination plus adjuvants is a potentially promising strategy.

Optimization of treatment strategies

In our efforts to treat dual-species biofilms, we applied a combination of antibiotics and adjuvants (phages or enzymes) simultaneously. However, altering the sequence of therapy by initially using enzymes or phages followed by incubation with antibiotics might yield different efficacy outcomes, as previously illustrated. Hence, optimizing treatment protocols could lead to promising therapeutic outcomes.

Regarding enzymes as adjuvants to enhance antibiotic activity (as presented in Paper 2), our focus was solely on degrading DNA and alginate within the biofilm matrix, overlooking another essential component, namely proteins. Proteins within the matrix can increase viscoelasticity and physically limit the penetration of antibiotics, potentially reducing treatment efficacy. A combination of protease and antibiotics was reported to significantly increase antibiotics targeting bacteria within biofilm in some in vitro studies [228]. However, considering its toxicity to host cells, implementing this approach in our situation may not be practical.

Additionally, recent research has demonstrated that extracellular RNA (eRNA) associates with eDNA to form matrix fibers in biofilms. Degradation of eRNA associated with eDNA results in a loss of eDNA fibers and biofilm viscoelasticity [377]. Therefore, additional degradation of RNA to decrease biofilm viscoelasticity

and enhance the efficacy of antimicrobial agents may prove to be a promising strategy.

In the context of phage-antibiotic combination therapy, only reference strains were tested. However, this therapeutic approach could be extended to clinical isolates of CF patients, especially those of *P. aeruginosa* with a pigmented non-mucoid phenotype, as they closely resemble our reference strains. Additionally, this strategy could be be applied to other respiratory diseases such as chronic obstructive pulmonary disease (COPD) and bronchiectasis, where *P. aeruginosa* is a dominant pathogen [30]. Conversely, conditions like asthma, pulmonary fibrosis, and pneumonia are primarily associated with pathogens other than *P. aeruginosa*, such as *Haemophilus*, *Moraxella*, and *Neisseriaceae* in the case of asthma [30]. These respiratory infections require new phages to target the specific pathogens involved and also to isolates phages which target a broader range of clinical isolates from CF patients.

While enzyme-antibiotics combination therapy almost eliminated *S. aureus* but not *P. aeruginosa*, and phage-antibiotics combination therapy showed limited activity against *S. aureus* but effective efficacy against *P. aeruginosa* in dual-species biofilms, a combination therapy involving enzymes, phages, and antibiotics is worth considering. For example, alginate lyase can degrade alginate, potentially enhancing phage activity. Therefore, incorporating enzymes, phages, and antibiotics into a combination therapy could potentially yield significant therapeutic outcomes.

Once an effective strategy for combating biofilms is established, it's crucial to further investigate the underlying mechanisms by which antibiotics and adjuvants exert their effects on biofilms. This includes examining changes in gene expression, metabolite production, interactions between antibiotics and matrices, and the heterogeneous microenvironment within the biofilm.

The entire work in this thesis is systematically designed, covering aspects from the model and the interaction between bacteria to the therapy of biofilm infections. Despite some limitations and potential oversights, our investigation paves the way for a comprehensive study regarding lung infections in CF patients. The results and ideas presented in this thesis will inspire further research aimed at developing a dynamic multi-species biofilm model that closely mimics the situation in CF patients. New insights gained from this work can inject fresh perspectives into the study of dynamic interactions between microorganisms in the future. The novel strategies incorporating enzyme-antibiotic or phage-antibiotic combinations show promise for application in CF patients. In particular, the enzyme-antibiotic combination containing DNase I and alginate lyase holds potential to treat CF infections in the near future. We hope and believe that our study can ultimately benefit CF patients by eradicating biofilm infections and alleviating their pulmonary lung deterioration.

Chapter V: Annexes

Poster presentation at the 'European Society of Clinical Microbiology and Infectious Diseases' on April 28, 2022.

Lisbon, Portugal
23–26 April 2022
32nd ECCMID
ESCMID

In-Vitro Study of Dual Species Biofilm Formed by Clinical Isolates of *S. aureus* and Different Phenotypes *P. aeruginosa* Collected as Pairs from Patients with Cystic Fibrosis

Zhifen Wang, Christiane Knoop, Albert Ruiz-Sorribas, Françoise Van Bambeke

[1]Université catholique de Louvain, [2]Hôpital Erasme, Université libre de Bruxelles - Brussels (Belgium)

Contact: zhifen.wang@uclouvain.be

UCLouvain
LDRI
Hôpital Erasme
ULB

INTRODUCTION

The sticky mucus in airways of CF patients favors the colonization by bacteria [1] that tend to form difficult to-treat biofilms [2]. Although ***S. aureus*** **(SA)** and ***P. aeruginosa*** **(PA)** can be isolated concomitantly in the sputum of these patients, in-vitro biofilm models with reference strains often claim that PA overgrows SA [3].

ASM: mimics the viscoelastic properties of the mucus found in the airways of CF patients [5]

- ✓**higher elasticity than viscosity**
- ✓**Composition** (per liter)**:** 10 g mucin; 4 g DNA; , 5.9 mg DTPA ; 5 g NaCl; 2.2 g KCl; 3 g agar; 5 g amino acids; 1.81 g Tris; 5 ml egg yolk emulsion

OBJECT

- Establish dual-species biofilms using artificial sputum (ASM)
- Characterise the resulting biofilms for different phenotypes of PA

METHODS

classification of PA

all SA → same phenotype

biofilm growth process

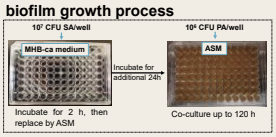

characterization of biofilms

- The **biomass** was quantified by **crystal violet staining**
- **CFUs** were counted on **species-specific agar media**

- The **distribution of PA and SA** was observed in confocal microscopy after **fluorescence in situ hybridization**

RESULTS AND CONCLUSION

- SA remained steady in all dual-species biofilms over time (mucoid or SCV PA) or after 72 h (non mucoid PA).
- PA was stable over time (non-mucoid or SCV) or after 72h (mucoid)
- Biomass was stable over time for all biofilms

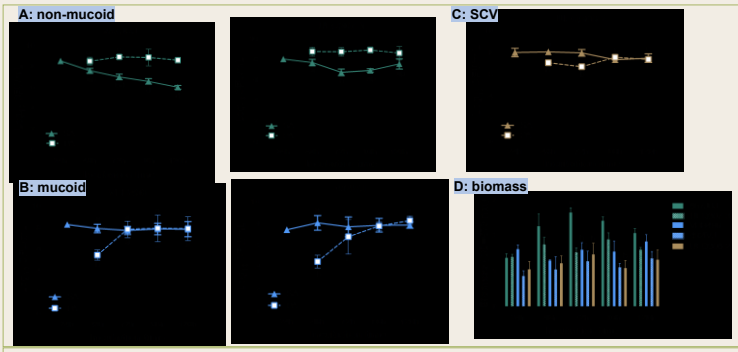

Fig. 1. Evolution over time of CFUs (A-C) or biomass (D) in dual species biofilms of clinical isolates of PA and SA for different phenotypes of PA (A: non-mucoid; B: mucoid; C: SCV). Values are means ± SEM from 3 or 4 independent experiments performed in more than triplicates; values with different letters are significantly different from each other ($P<0.05$). 2-way ANOVA followed by Tukey's multiple comparisons test of pairs of isolates. In panel D, statistics are indicated only for time points for which some differences are seen.

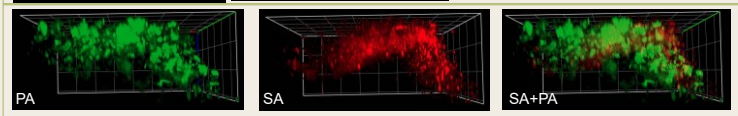

Fig. 2. illustrates for a representative pair of isolates with mucoid PA (VBB496) that SA and PA aggregated with each other in biofilms.

- **Dual-species biofilms easily form in ASM with isolates obtained from the same patients, and SA is not outcompeted by PA, whatever its phenotype. Furthermore, SA and PA can grow in common aggregates. This is consistent with the cross-adaptation of PA and SA observed for isolates collected after several years in CF patients [4].**

REFERENCES

[1] Ratjen *et al.* 2015 Nat Rev Dis Primers 1: 15010.
[2] Høiby *et al.* 2015 Clin Microbiol Infect 21: S1-S25.
[3] Filkins *et al.* 2015 J Bacteriol 197(14):2252-64.
[4] Baldan *et al. 2014 PLoS One 9 (3): e89614.*
[5] Diaz Iglesias *et al. 2019 Antimicrob Agents Chemother 63: e02204-19*

Acknowledgements: fnrs

A copy of this poster will be made available after the meeting at http://www.facm.ucl.ac.be/posters.htm

Bibliography

1. Cohen, T.S. and A. Prince, *Cystic fibrosis: a mucosal immunodeficiency syndrome.* Nat Med, 2012. **18**(4): p. 509-19.
2. Lubamba, B., et al., *Cystic fibrosis: insight into CFTR pathophysiology and pharmacotherapy.* Clin Biochem, 2012. **45**(15): p. 1132-44.
3. Zolin A, O.A., Jung A, van Rens J et al, *ECFSPR Annual Report 2021*. 2023.
4. Registry, C.F.F.P., *2021 Cystic Fibrosis Foundation Patient Registry Highlights*. 2021.
5. Guo, J., A. Garratt, and A. Hill, *Worldwide rates of diagnosis and effective treatment for cystic fibrosis.* J Cyst Fibros, 2022. **21**(3): p. 456-462.
6. Mirtajani, S.B., et al., *Geographical distribution of cystic fibrosis; The past 70 years of data analyzis.* Biomedical and Biotechnology Research Journal (BBRJ), 2017. **1**: p. 105-112.
7. Taylor-Cousar, J.L., et al., *The Impact of Highly Effective Cystic Fibrosis Transmembrane Conductance Regulator Modulators on the Health of Female Subjects With Cystic Fibrosis.* Clin Ther, 2023. **45**(3): p. 278-289.
8. Busch, R., *On the history of cystic fibrosis.* Acta Univ Carol Med (Praha), 1990. **36**(1-4): p. 13-5.
9. Barben, J., *First description of cystic fibrosis.* J Cyst Fibros, 2021. **20**(1): p. 183.
10. Andersen, D.H. and R.G. Hodges, *Celiac syndrome; genetics of cystic fibrosis of the pancreas, with a consideration of etiology.* Am J Dis Child (1911), 1946. **72**: p. 62-80.
11. Clague, S., *Dorothy Hansine Andersen.* Lancet Respir Med, 2014. **2**(3): p. 184-5.
12. Gibson, L.E. and R.E. Cooke, *A test for concentration of electrolytes in sweat in cystic fibrosis of the pancreas utilizing pilocarpine by iontophoresis.* Pediatrics, 1959. **23**(3): p. 545-9.
13. Szaff, M., N. Hoiby, and E.W. Flensborg, *Frequent antibiotic therapy improves survival of cystic fibrosis patients with chronic Pseudomonas aeruginosa infection.* Acta Paediatr Scand, 1983. **72**(5): p. 651-7.
14. Knowles, M., J. Gatzy, and R. Boucher, *Increased bioelectric potential difference across respiratory epithelia in cystic fibrosis.* N Engl J Med, 1981. **305**(25): p. 1489-95.
15. Kerem, B., et al., *Identification of the cystic fibrosis gene: genetic analysis.* Science, 1989. **245**(4922): p. 1073-80.
16. Hanssens, L.S., J. Duchateau, and G.J. Casimir, *CFTR Protein: Not Just a Chloride Channel?* Cells, 2021. **10**(11): p. 2844.

17. Ellsworth, R.E., et al., *Comparative genomic sequence analysis of the human and mouse cystic fibrosis transmembrane conductance regulator genes.* Proc Natl Acad Sci U S A, 2000. **97**(3): p. 1172-7.
18. Bareil, C. and A. Bergougnoux, *CFTR gene variants, epidemiology and molecular pathology.* Arch Pediatr, 2020. **27 Suppl 1**: p. eS8-eS12.
19. Ong, T. and B.W. Ramsey, *Cystic Fibrosis: A Review.* JAMA, 2023. **329**(21): p. 1859-1871.
20. Lucarelli, M., et al., *A new complex allele of the CFTR gene partially explains the variable phenotype of the L997F mutation.* Genet Med, 2010. **12**(9): p. 548-55.
21. Lopes-Pacheco, M., *CFTR Modulators: Shedding Light on Precision Medicine for Cystic Fibrosis.* Front Pharmacol, 2016. **7**: p. 275.
22. Dickinson, K.M. and J.M. Collaco, *Cystic Fibrosis.* Pediatr Rev, 2021. **42**(2): p. 55-67.
23. Sathe, M. and R. Houwen, *Meconium ileus in Cystic Fibrosis.* J Cyst Fibros, 2017. **16 Suppl 2**: p. S32-S39.
24. Udefiagbon, O., *Meconium Ileus*, in *Pediatric Surgery, Flowcharts and Clinical Algorithms*, S. Sameh, Editor. 2019, IntechOpen: Rijeka. p. Ch. 4.
25. Minasian, C., A. McCullagh, and A. Bush, *Cystic fibrosis in neonates and infants.* Early Hum Dev, 2005. **81**(12): p. 997-1004.
26. Wilschanski, M. and I. Novak, *The cystic fibrosis of exocrine pancreas.* Cold Spring Harb Perspect Med, 2013. **3**(5): p. a009746.
27. Kobelska-Dubiel, N., B. Klincewicz, and W. Cichy, *Liver disease in cystic fibrosis.* Prz Gastroenterol, 2014. **9**(3): p. 136-41.
28. de Souza, D.A.S., et al., *Congenital bilateral absence of the vas deferens as an atypical form of cystic fibrosis: reproductive implications and genetic counseling.* Andrology, 2018. **6**(1): p. 127-135.
29. Ahmad, A., A. Ahmed, and P. Patrizio, *Cystic fibrosis and fertility.* Curr Opin Obstet Gynecol, 2013. **25**(3): p. 167-72.
30. Li, R., J. Li, and X. Zhou, *Lung microbiome: new insights into the pathogenesis of respiratory diseases.* Signal Transduct Target Ther, 2024. **9**(1): p. 19.
31. Natalini, J.G., S. Singh, and L.N. Segal, *The dynamic lung microbiome in health and disease.* Nat Rev Microbiol, 2023. **21**(4): p. 222-235.
32. Yagi, K., et al., *The Lung Microbiome during Health and Disease.* Int J Mol Sci, 2021. **22**(19): p. 10872.
33. Marshall, B., A. Faro, and W. Brown, *Cystic fibrosis foundation patient registry 2020 annual data report; 2020*. 2022.
34. Adjemian, J., et al., *Prevalence of nontuberculous mycobacterial lung disease in U.S. Medicare beneficiaries.* Am J Respir Crit Care Med, 2012. **185**(8): p. 881-6.

35. Marshall, B., *2022 Patient Registry Annual Data Report*. 2022.
36. Rodman, D.M., et al., *Late diagnosis defines a unique population of long-term survivors of cystic fibrosis.* Am J Respir Crit Care Med, 2005. **171**(6): p. 621-6.
37. Wilson, L.M., L. Morrison, and K.A. Robinson, *Airway clearance techniques for cystic fibrosis: an overview of Cochrane systematic reviews.* Cochrane Database Syst Rev, 2019. **1**(1): p. CD011231.
38. Yang, C. and M. Montgomery, *Dornase alfa for cystic fibrosis.* Cochrane Database Syst Rev, 2021. **3**(3): p. CD001127.
39. Wark, P. and V.M. McDonald, *Nebulised hypertonic saline for cystic fibrosis.* Cochrane Database Syst Rev, 2009(2): p. CD001506.
40. Flume, P.A., et al., *Efficacy and safety of inhaled dry-powder mannitol in adults with cystic fibrosis: An international, randomized controlled study.* J Cyst Fibros, 2021. **20**(6): p. 1003-1009.
41. Schluchter, M., et al., *Relationship between high-dose ibuprofen use and rate of decline in FEV1 among young patients with mild lung disease in the CFF Registry.* Pediatr Pulmonol, 2004. **27**: p. 322.
42. Mogayzel, P.J., Jr., et al., *Cystic fibrosis pulmonary guidelines. Chronic medications for maintenance of lung health.* Am J Respir Crit Care Med, 2013. **187**(7): p. 680-9.
43. Zimmermann, P., et al., *The Immunomodulatory Effects of Macrolides-A Systematic Review of the Underlying Mechanisms.* Front Immunol, 2018. **9**: p. 302.
44. Stick, S.M., et al., *The effect of azithromycin on structural lung disease in infants with cystic fibrosis (COMBAT CF): a phase 3, randomised, double-blind, placebo-controlled clinical trial.* Lancet Respir Med, 2022. **10**(8): p. 776-784.
45. Ciuca, I.M., et al., *Antibiotherapy in Children with Cystic Fibrosis-An Extensive Review.* Children (Basel), 2022. **9**(8): p. 1258.
46. Smyth, A.R. and M. Rosenfeld, *Prophylactic anti-staphylococcal antibiotics for cystic fibrosis.* Cochrane Database Syst Rev, 2017. **4**(4): p. CD001912.
47. Stutman, H.R., et al., *Antibiotic prophylaxis in infants and young children with cystic fibrosis: a randomized controlled trial.* J Pediatr, 2002. **140**(3): p. 299-305.
48. Ratjen, F., et al., *Effect of continuous antistaphylococcal therapy on the rate of P. aeruginosa acquisition in patients with cystic fibrosis.* Pediatr Pulmonol, 2001. **31**(1): p. 13-6.
49. Denton, M., *Re: "Methicillin-resistant Staphylococcus aureus in children with cystic fibrosis: an eradication protocol" Solis et al. (Pediatr Pulmonol 2003;36: 189-195).* Pediatr Pulmonol, 2004. **38**(3): p. 272-3.

50. Mogayzel, P.J., Jr., et al., *Cystic Fibrosis Foundation pulmonary guideline. pharmacologic approaches to prevention and eradication of initial Pseudomonas aeruginosa infection.* Ann Am Thorac Soc, 2014. **11**(10): p. 1640-50.
51. Edmondson, C. and J.C. Davies, *Current and future treatment options for cystic fibrosis lung disease: latest evidence and clinical implications.* Ther Adv Chronic Dis, 2016. **7**(3): p. 170-83.
52. Castellani, C., et al., *ECFS best practice guidelines: the 2018 revision.* J Cyst Fibros, 2018. **17**(2): p. 153-178.
53. Esposito, S., et al., *Antimicrobial Treatment of Staphylococcus aureus in Patients With Cystic Fibrosis.* Front Pharmacol, 2019. **10**: p. 849.
54. Flume, P.A., et al., *Cystic fibrosis pulmonary guidelines: treatment of pulmonary exacerbations.* Am J Respir Crit Care Med, 2009. **180**(9): p. 802-8.
55. Fajac, I. and C.E. Wainwright, *New treatments targeting the basic defects in cystic fibrosis.* Presse Med, 2017. **46**(6 Pt 2): p. e165-e175.
56. Regard, L., et al., *CFTR Modulators in People with Cystic Fibrosis: Real-World Evidence in France.* Cells, 2022. **11**(11): p. 1769.
57. Dittrich, A.M., et al., *Use of elexacaftor/tezacaftor/ivacaftor leads to changes in detection frequencies of Staphylococcus aureus and Pseudomonas aeruginosa dependent on age and lung function in people with cystic fibrosis.* Int J Infect Dis, 2024. **139**: p. 124-131.
58. Dagenais, R.V.E., V.C.H. Su, and B.S. Quon, *Real-World Safety of CFTR Modulators in the Treatment of Cystic Fibrosis: A Systematic Review.* J Clin Med, 2020. **10**(1): p. 23.
59. Foster, T.J., et al., *Adhesion, invasion and evasion: the many functions of the surface proteins of Staphylococcus aureus.* Nat Rev Microbiol, 2014. **12**(1): p. 49-62.
60. Foster, T.J., *Surface Proteins of Staphylococcus aureus.* Microbiol Spectr, 2019. **7**(4).
61. Xue, L., et al., *Staphyloxanthin: a potential target for antivirulence therapy.* Infect Drug Resist, 2019. **12**: p. 2151-2160.
62. O'Riordan, K. and J.C. Lee, *Staphylococcus aureus capsular polysaccharides.* Clin Microbiol Rev, 2004. **17**(1): p. 218-34.
63. Thammavongsa, V., et al., *Staphylococcal manipulation of host immune responses.* Nat Rev Microbiol, 2015. **13**(9): p. 529-43.
64. Kuipers, A., et al., *The Staphylococcus aureus polysaccharide capsule and Efb-dependent fibrinogen shield act in concert to protect against phagocytosis.* Microbiology (Reading), 2016. **162**(7): p. 1185-1194.
65. Foster, T.J., *Immune evasion by staphylococci.* Nat Rev Microbiol, 2005. **3**(12): p. 948-58.

66. Jusko, M., et al., *Staphylococcal proteases aid in evasion of the human complement system.* J Innate Immun, 2014. **6**(1): p. 31-46.
67. Oliveira, D., A. Borges, and M. Simoes, *Staphylococcus aureus Toxins and Their Molecular Activity in Infectious Diseases.* Toxins (Basel), 2018. **10**(6): p. 252.
68. Ahmad-Mansour, N., et al., *Staphylococcus aureus Toxins: An Update on Their Pathogenic Properties and Potential Treatments.* Toxins (Basel), 2021. **13**(10): p. 677.
69. Otter, J.A., et al., *Panton-Valentine leukocidin-encoding bacteriophage and gene sequence variation in community-associated methicillin-resistant Staphylococcus aureus.* Clin Microbiol Infect, 2010. **16**(1): p. 68-73.
70. Joo, H.S. and M. Otto, *Molecular basis of in vivo biofilm formation by bacterial pathogens.* Chem Biol, 2012. **19**(12): p. 1503-13.
71. Lange, J., et al., *Staphylococcus aureus Pathogenicity in Cystic Fibrosis Patients-Results from an Observational Prospective Multicenter Study Concerning Virulence Genes, Phylogeny, and Gene Plasticity.* Toxins (Basel), 2020. **12**(5): p. 279.
72. Castillo-Juarez, I., et al., *Role of quorum sensing in bacterial infections.* World J Clin Cases, 2015. **3**(7): p. 575-98.
73. Tan, L., et al., *Therapeutic Targeting of the Staphylococcus aureus Accessory Gene Regulator (agr) System.* Front Microbiol, 2018. **9**: p. 55.
74. Peng, H.L., et al., *Cloning, characterization, and sequencing of an accessory gene regulator (agr) in Staphylococcus aureus.* J Bacteriol, 1988. **170**(9): p. 4365-72.
75. Doherty, N., et al., *Functional analysis of luxS in Staphylococcus aureus reveals a role in metabolism but not quorum sensing.* J Bacteriol, 2006. **188**(8): p. 2885-97.
76. Zhao, L., et al., *Staphylococcus aureus AI-2 quorum sensing associates with the KdpDE two-component system to regulate capsular polysaccharide synthesis and virulence.* Infect Immun, 2010. **78**(8): p. 3506-15.
77. Le, K.Y. and M. Otto, *Quorum-sensing regulation in staphylococci-an overview.* Front Microbiol, 2015. **6**: p. 1174.
78. Jenul, C. and A.R. Horswill, *Regulation of Staphylococcus aureus Virulence.* Microbiol Spectr, 2019. **7**(2): p. 10.
79. Goerke, C. and C. Wolz, *Adaptation of Staphylococcus aureus to the cystic fibrosis lung.* Int J Med Microbiol, 2010. **300**(8): p. 520-5.
80. Goerke, C., et al., *Direct quantitative transcript analysis of the agr regulon of Staphylococcus aureus during human infection in comparison to the expression profile in vitro.* Infect Immun, 2000. **68**(3): p. 1304-11.

81. Hirschhausen, N., et al., *Extended Staphylococcus aureus persistence in cystic fibrosis is associated with bacterial adaptation.* Int J Med Microbiol, 2013. **303**(8): p. 685-92.
82. Langhanki, L., et al., *In vivo competition and horizontal gene transfer among distinct Staphylococcus aureus lineages as major drivers for adaptational changes during long-term persistence in humans.* BMC Microbiol, 2018. **18**(1): p. 152.
83. Besier, S., et al., *Prevalence and clinical significance of Staphylococcus aureus small-colony variants in cystic fibrosis lung disease.* J Clin Microbiol, 2007. **45**(1): p. 168-72.
84. Junge, S., et al., *Factors Associated with Worse Lung Function in Cystic Fibrosis Patients with Persistent Staphylococcus aureus.* PLoS One, 2016. **11**(11): p. e0166220.
85. Proctor, R.A., et al., *Small colony variants: a pathogenic form of bacteria that facilitates persistent and recurrent infections.* Nat Rev Microbiol, 2006. **4**(4): p. 295-305.
86. Rumpf, C., et al., *Staphylococcus aureus and Cystic Fibrosis-A Close Relationship. What Can We Learn from Sequencing Studies?* Pathogens, 2021. **10**(9): p. 1769.
87. Arai, H., *Regulation and Function of Versatile Aerobic and Anaerobic Respiratory Metabolism in Pseudomonas aeruginosa.* Front Microbiol, 2011. **2**: p. 103.
88. Sadikot, R.T., et al., *Pathogen-host interactions in Pseudomonas aeruginosa pneumonia.* Am J Respir Crit Care Med, 2005. **171**(11): p. 1209-23.
89. Lopez-Causape, C., et al., *The Versatile Mutational Resistome of Pseudomonas aeruginosa.* Front Microbiol, 2018. **9**: p. 685.
90. Dingemans, J., et al., *Effect of Shear Stress on Pseudomonas aeruginosa Isolated from the Cystic Fibrosis Lung.* mBio, 2016. **7**(4): p. e00813-16.
91. Klockgether, J., et al., *Pseudomonas aeruginosa Genomic Structure and Diversity.* Front Microbiol, 2011. **2**: p. 150.
92. Wagener, B.M., et al., *The Role of Pseudomonas aeruginosa Virulence Factors in Cytoskeletal Dysregulation and Lung Barrier Dysfunction.* Toxins (Basel), 2021. **13**(11): p. 776.
93. Al-Otaibi, N.S. and J.R.C. Bergeron, *Structure and Assembly of the Bacterial Flagellum.* Subcell Biochem, 2022. **99**: p. 395-420.
94. Kearns, D.B., *A field guide to bacterial swarming motility.* Nat Rev Microbiol, 2010. **8**(9): p. 634-44.
95. Drake, D. and T.C. Montie, *Flagella, motility and invasive virulence of Pseudomonas aeruginosa.* J Gen Microbiol, 1988. **134**(1): p. 43-52.
96. Haiko, J. and B. Westerlund-Wikstrom, *The role of the bacterial flagellum in adhesion and virulence.* Biology (Basel), 2013. **2**(4): p. 1242-67.

97. Fleiszig, S.M.J., et al., *Contact lens-related corneal infection: Intrinsic resistance and its compromise.* Prog Retin Eye Res, 2020. **76**: p. 100804.
98. Bystrova, O.V., et al., *Full structure of the lipopolysaccharide of Pseudomonas aeruginosa immunotype 5.* Biochemistry (Mosc), 2004. **69**(2): p. 170-5.
99. Pier, G.B., *Pseudomonas aeruginosa lipopolysaccharide: a major virulence factor, initiator of inflammation and target for effective immunity.* Int J Med Microbiol, 2007. **297**(5): p. 277-95.
100. Hajjar, A.M., et al., *Human Toll-like receptor 4 recognizes host-specific LPS modifications.* Nat Immunol, 2002. **3**(4): p. 354-9.
101. Huszczynski, S.M., J.S. Lam, and C.M. Khursigara, *The Role of Pseudomonas aeruginosa Lipopolysaccharide in Bacterial Pathogenesis and Physiology.* Pathogens, 2019. **9**(1): p. 6.
102. Kipnis, E., T. Sawa, and J. Wiener-Kronish, *Targeting mechanisms of Pseudomonas aeruginosa pathogenesis.* Med Mal Infect, 2006. **36**(2): p. 78-91.
103. Faure, E., K. Kwong, and D. Nguyen, *Pseudomonas aeruginosa in Chronic Lung Infections: How to Adapt Within the Host?* Front Immunol, 2018. **9**: p. 2416.
104. Bleves, S., et al., *Protein secretion systems in Pseudomonas aeruginosa: A wealth of pathogenic weapons.* Int J Med Microbiol, 2010. **300**(8): p. 534-43.
105. Han, Y., et al., *A Pseudomonas aeruginosa type VI secretion system regulated by CueR facilitates copper acquisition.* PLoS Pathog, 2019. **15**(12): p. e1008198.
106. Juhas, M., D.W. Crook, and D.W. Hood, *Type IV secretion systems: tools of bacterial horizontal gene transfer and virulence.* Cell Microbiol, 2008. **10**(12): p. 2377-86.
107. Qin, S., et al., *Pseudomonas aeruginosa: pathogenesis, virulence factors, antibiotic resistance, interaction with host, technology advances and emerging therapeutics.* Signal Transduct Target Ther, 2022. **7**(1): p. 199.
108. Alcorn, J.F. and J.R. Wright, *Degradation of pulmonary surfactant protein D by Pseudomonas aeruginosa elastase abrogates innate immune function.* J Biol Chem, 2004. **279**(29): p. 30871-9.
109. Audia, J.P., et al., *In the absence of effector proteins, the Pseudomonas aeruginosa type three secretion system needle tip complex contributes to lung injury and systemic inflammatory responses.* PLoS One, 2013. **8**(11): p. e81792.
110. Xie, Y., et al., *Signal transduction schemes in Pseudomonas syringae.* Comput Struct Biotechnol J, 2020. **18**: p. 3415-3424.

111. Mann, E.E. and D.J. Wozniak, *Pseudomonas biofilm matrix composition and niche biology.* FEMS Microbiol Rev, 2012. **36**(4): p. 893-916.
112. Chatterjee, M., et al., *Antibiotic resistance in Pseudomonas aeruginosa and alternative therapeutic options.* Int J Med Microbiol, 2016. **306**(1): p. 48-58.
113. Le Mauff, F., et al., *The Pel polysaccharide is predominantly composed of a dimeric repeat of alpha-1,4 linked galactosamine and N-acetylgalactosamine.* Commun Biol, 2022. **5**(1): p. 502.
114. Franklin, M.J., et al., *Biosynthesis of the Pseudomonas aeruginosa Extracellular Polysaccharides, Alginate, Pel, and Psl.* Front Microbiol, 2011. **2**: p. 167.
115. Laarman, A.J., et al., *Pseudomonas aeruginosa alkaline protease blocks complement activation via the classical and lectin pathways.* J Immunol, 2012. **188**(1): p. 386-93.
116. Kharazmi, A., et al., *Pseudomonas aeruginosa exoproteases inhibit human neutrophil chemiluminescence.* Infect Immun, 1984. **44**(3): p. 587-91.
117. Galdino, A.C.M., et al., *Pseudomonas aeruginosa and Its Arsenal of Proteases: Weapons to Battle the Host*, in *Pathophysiological Aspects of Proteases*, S. Chakraborti and N.S. Dhalla, Editors. 2017, Springer Singapore: Singapore. p. 381-397.
118. Toder, D.S., et al., *lasA and lasB genes of Pseudomonas aeruginosa: analysis of transcription and gene product activity.* Infect Immun, 1994. **62**(4): p. 1320-7.
119. Kessler, E., et al., *Secreted LasA of Pseudomonas aeruginosa is a staphylolytic protease.* J Biol Chem, 1993. **268**(10): p. 7503-8.
120. Lache, M., et al., *Specificity of a bacteriolytic enzyme from Pseudomonas aeruginosa.* J Bacteriol, 1969. **100**(1): p. 254-9.
121. Mackinder, J.R., et al., *Sphingosine induction of the Pseudomonas aeruginosa hemolytic phospholipase C/sphingomyelinase, PlcH.* bioRxiv, 2023: p. 2023.11.06.565848.
122. Prasad, A.S.B., et al., *Pseudomonas aeruginosa virulence proteins pseudolysin and protease IV impede cutaneous wound healing.* Lab Invest, 2020. **100**(12): p. 1532-1550.
123. Rosenau, F., et al., *Lipase LipC affects motility, biofilm formation and rhamnolipid production in Pseudomonas aeruginosa.* FEMS Microbiol Lett, 2010. **309**(1): p. 25-34.
124. Javanmardi, F., et al., *A systematic review and meta-analysis on Exo-toxins prevalence in hospital acquired Pseudomonas aeruginosa isolates.* Infect Genet Evol, 2019. **75**: p. 104037.
125. Wood, S.J., et al., *Pseudomonas aeruginosa Cytotoxins: Mechanisms of Cytotoxicity and Impact on Inflammatory Responses.* Cells, 2023. **12**(1): p. 195.

126. Barr, H.L., et al., *Pseudomonas aeruginosa quorum sensing molecules correlate with clinical status in cystic fibrosis.* Eur Respir J, 2015. **46**(4): p. 1046-54.
127. Das, T., et al., *Pyocyanin facilitates extracellular DNA binding to Pseudomonas aeruginosa influencing cell surface properties and aggregation.* PLoS One, 2013. **8**(3): p. e58299.
128. Moayedi, A., J. Nowroozi, and A. Akhavan Sepahy, *Cytotoxic effect of pyocyanin on human pancreatic cancer cell line (Panc-1).* Iran J Basic Med Sci, 2018. **21**(8): p. 794-799.
129. Banin, E., M.L. Vasil, and E.P. Greenberg, *Iron and Pseudomonas aeruginosa biofilm formation.* Proc Natl Acad Sci U S A, 2005. **102**(31): p. 11076-81.
130. Kang, D., et al., *Pyoverdine, a siderophore from Pseudomonas aeruginosa, translocates into C. elegans, removes iron, and activates a distinct host response.* Virulence, 2018. **9**(1): p. 804-817.
131. Nickzad, A. and E. Déziel, *The involvement of rhamnolipids in microbial cell adhesion and biofilm development – an approach for control?* Letters in Applied Microbiology, 2014. **58**(5): p. 447-453.
132. Soberon-Chavez, G., F. Lepine, and E. Deziel, *Production of rhamnolipids by Pseudomonas aeruginosa.* Appl Microbiol Biotechnol, 2005. **68**(6): p. 718-25.
133. Reis, R.S., et al., *Gene regulation of rhamnolipid production in Pseudomonas aeruginosa--a review.* Bioresour Technol, 2011. **102**(11): p. 6377-84.
134. Tashiro, Y., et al., *Interspecies interaction between Pseudomonas aeruginosa and other microorganisms.* Microbes Environ, 2013. **28**(1): p. 13-24.
135. Hazan, R., et al., *Auto Poisoning of the Respiratory Chain by a Quorum-Sensing-Regulated Molecule Favors Biofilm Formation and Antibiotic Tolerance.* Curr Biol, 2016. **26**(2): p. 195-206.
136. Bru, J.L., et al., *PQS Produced by the Pseudomonas aeruginosa Stress Response Repels Swarms Away from Bacteriophage and Antibiotics.* J Bacteriol, 2019. **201**(23): p. e00383-19.
137. Ryall, B., et al., *Pseudomonas aeruginosa, cyanide accumulation and lung function in CF and non-CF bronchiectasis patients.* Eur Respir J, 2008. **32**(3): p. 740-7.
138. Blier, A.S., et al., *Quantification of Pseudomonas aeruginosa hydrogen cyanide production by a polarographic approach.* J Microbiol Methods, 2012. **90**(1): p. 20-4.

139. Sousa, A.M. and M.O. Pereira, *Pseudomonas aeruginosa Diversification during Infection Development in Cystic Fibrosis Lungs-A Review.* Pathogens, 2014. **3**(3): p. 680-703.
140. Burke, V., et al., *Longitudinal studies of virulence factors of Pseudomonas aeruginosa in cystic fibrosis.* Pathology, 1991. **23**(2): p. 145-8.
141. Jurado-Martin, I., M. Sainz-Mejias, and S. McClean, *Pseudomonas aeruginosa: An Audacious Pathogen with an Adaptable Arsenal of Virulence Factors.* Int J Mol Sci, 2021. **22**(6).
142. Fux, C.A., et al., *Survival strategies of infectious biofilms.* Trends Microbiol, 2005. **13**(1): p. 34-40.
143. Rutherford, S.T. and B.L. Bassler, *Bacterial quorum sensing: its role in virulence and possibilities for its control.* Cold Spring Harb Perspect Med, 2012. **2**(11): p. a012427.
144. Schuster, M., et al., *Acyl-homoserine lactone quorum sensing: from evolution to application.* Annu Rev Microbiol, 2013. **67**: p. 43-63.
145. Scoffone, V.C., et al., *Quorum Sensing as Antivirulence Target in Cystic Fibrosis Pathogens.* Int J Mol Sci, 2019. **20**(8): p. 1838.
146. Lee, J. and L. Zhang, *The hierarchy quorum sensing network in Pseudomonas aeruginosa.* Protein Cell, 2015. **6**(1): p. 26-41.
147. Schutz, C. and M. Empting, *Targeting the Pseudomonas quinolone signal quorum sensing system for the discovery of novel anti-infective pathoblockers.* Beilstein J Org Chem, 2018. **14**: p. 2627-2645.
148. Li, Y., et al., *Correlation between group behavior and quorum sensing in Pseudomonas aeruginosa isolated from patients with hospital-acquired pneumonia.* J Thorac Dis, 2014. **6**(6): p. 810-7.
149. Pena, R.T., et al., *Relationship Between Quorum Sensing and Secretion Systems.* Front Microbiol, 2019. **10**: p. 1100.
150. Kamal, A.A.M., et al., *Quorum Sensing Inhibitors as Pathoblockers for Pseudomonas aeruginosa Infections: A New Concept in Anti-Infective Drug Discovery*, in *Antibacterials: Volume II*, J.F. Fisher, S. Mobashery, and M.J. Miller, Editors. 2018, Springer International Publishing: Cham. p. 185-210.
151. Camus, L., F. Vandenesch, and K. Moreau, *From genotype to phenotype: adaptations of Pseudomonas aeruginosa to the cystic fibrosis environment.* Microb Genom, 2021. **7**(3): p. mgen000513.
152. Russell, N.J. and P. Gacesa, *Chemistry and biology of the alginate of mucoid strains of Pseudomonas aeruginosa in cystic fibrosis.* Mol Aspects Med, 1988. **10**(1): p. 1-91.
153. Malone, J.G., *Role of small colony variants in persistence of Pseudomonas aeruginosa infections in cystic fibrosis lungs.* Infect Drug Resist, 2015. **8**: p. 237-47.

154. Smith, E.E., et al., *Genetic adaptation by Pseudomonas aeruginosa to the airways of cystic fibrosis patients.* Proc Natl Acad Sci U S A, 2006. **103**(22): p. 8487-92.
155. Mateu-Borras, M., et al., *Pseudomonas aeruginosa adaptation in cystic fibrosis patients increases C5a levels and promotes neutrophil recruitment.* Virulence, 2022. **13**(1): p. 215-224.
156. Yin, W., et al., *Biofilms: The Microbial "Protective Clothing" in Extreme Environments.* Int J Mol Sci, 2019. **20**(14): p. 3423.
157. Wang, X., et al., *Biofilm formation: mechanistic insights and therapeutic targets.* Mol Biomed, 2023. **4**(1): p. 49.
158. Lin, M.H., et al., *Elucidating the crucial role of poly N-acetylglucosamine from Staphylococcus aureus in cellular adhesion and pathogenesis.* PLoS One, 2015. **10**(4): p. e0124216.
159. Colvin, K.M., et al., *The Pel and Psl polysaccharides provide Pseudomonas aeruginosa structural redundancy within the biofilm matrix.* Environ Microbiol, 2012. **14**(8): p. 1913-28.
160. Muszanska, A.K., et al., *Bacterial adhesion forces with substratum surfaces and the susceptibility of biofilms to antibiotics.* Antimicrob Agents Chemother, 2012. **56**(9): p. 4961-4.
161. Muhammad, M.H., et al., *Beyond Risk: Bacterial Biofilms and Their Regulating Approaches.* Front Microbiol, 2020. **11**: p. 928.
162. Laverty, G., S.P. Gorman, and B.F. Gilmore, *Biomolecular Mechanisms of Pseudomonas aeruginosa and Escherichia coli Biofilm Formation.* Pathogens, 2014. **3**(3): p. 596-632.
163. Rossi, E., M. Paroni, and P. Landini, *Biofilm and motility in response to environmental and host-related signals in Gram negative opportunistic pathogens.* J Appl Microbiol, 2018: p. 1769.
164. Schilcher, K. and A.R. Horswill, *Staphylococcal Biofilm Development: Structure, Regulation, and Treatment Strategies.* Microbiol Mol Biol Rev, 2020. **84**(3): p. e00026-19.
165. Campoccia, D., L. Montanaro, and C.R. Arciola, *Extracellular DNA (eDNA). A Major Ubiquitous Element of the Bacterial Biofilm Architecture.* Int J Mol Sci, 2021. **22**(16): p. 9100.
166. Latasa, C., et al., *Biofilm-associated proteins.* C R Biol, 2006. **329**(11): p. 849-57.
167. Stewart, P.S. and M.J. Franklin, *Physiological heterogeneity in biofilms.* Nat Rev Microbiol, 2008. **6**(3): p. 199-210.
168. Kaplan, J.B., *Biofilm dispersal: mechanisms, clinical implications, and potential therapeutic uses.* J Dent Res, 2010. **89**(3): p. 205-18.

169. Wood, T.L., et al., *Rhamnolipids from Pseudomonas aeruginosa disperse the biofilms of sulfate-reducing bacteria.* NPJ Biofilms Microbiomes, 2018. **4**: p. 22.
170. Otto, M., *Staphylococcal Biofilms.* Microbiol Spectr, 2018. **6**(4): p. 10.
171. Sauer, K., et al., *The biofilm life cycle: expanding the conceptual model of biofilm formation.* Nat Rev Microbiol, 2022. **20**(10): p. 608-620.
172. Lam, J., et al., *Production of mucoid microcolonies by Pseudomonas aeruginosa within infected lungs in cystic fibrosis.* Infect Immun, 1980. **28**(2): p. 546-56.
173. Bjarnsholt, T., et al., *Pseudomonas aeruginosa biofilms in the respiratory tract of cystic fibrosis patients.* Pediatr Pulmonol, 2009. **44**(6): p. 547-58.
174. Ulrich, M., et al., *Localization of Staphylococcus aureus in infected airways of patients with cystic fibrosis and in a cell culture model of S. aureus adherence.* Am J Respir Cell Mol Biol, 1998. **19**(1): p. 83-91.
175. Bjarnsholt, T., et al., *The in vivo biofilm.* Trends in Microbiology, 2013. **21**(9): p. 466-474.
176. Diaz Iglesias, I., *PhD thesis: Activity of antibiotics against in vitro mono-species biofilms of P. aeruginosa and S. aureus in the context of cystic fibrosis : the influence of the culture medium.* 2020, UCLouvain.
177. Rudkjobing, V.B., et al., *The microorganisms in chronically infected end-stage and non-end-stage cystic fibrosis patients.* FEMS Immunol Med Microbiol, 2012. **65**(2): p. 236-44.
178. Magalhaes, A.P., et al., *Unveiling Co-Infection in Cystic Fibrosis Airways: Transcriptomic Analysis of Pseudomonas aeruginosa and Staphylococcus aureus Dual-Species Biofilms.* Front Genet, 2022. **13**: p. 883199.
179. Gomes-Fernandes, M., et al., *Strain-specific interspecies interactions between co-isolated pairs of Staphylococcus aureus and Pseudomonas aeruginosa from patients with tracheobronchitis or bronchial colonization.* Sci Rep, 2022. **12**(1): p. 3374.
180. Monteiro, R., et al., *Long-term coexistence of Pseudomonas aeruginosa and Staphylococcus aureus using an in vitro cystic fibrosis model.* Future Microbiol, 2021. **16**: p. 879-893.
181. Gloag, E.S., et al., *Biofilm mechanics: Implications in infection and survival.* Biofilm, 2020. **2**: p. 100017.
182. Kovach, K., et al., *Evolutionary adaptations of biofilms infecting cystic fibrosis lungs promote mechanical toughness by adjusting polysaccharide production.* NPJ Biofilms Microbiomes, 2017. **3**: p. 1.
183. Suci, P.A., et al., *Investigation of ciprofloxacin penetration into Pseudomonas aeruginosa biofilms.* Antimicrob Agents Chemother, 1994. **38**(9): p. 2125-33.

184. Ciofu, O. and T. Tolker-Nielsen, *Tolerance and Resistance of Pseudomonas aeruginosa Biofilms to Antimicrobial Agents-How P. aeruginosa Can Escape Antibiotics.* Front Microbiol, 2019. **10**: p. 913.
185. Thomsen, K., et al., *Immune Response to Biofilm Growing Pulmonary Pseudomonas aeruginosa Infection.* Biomedicines, 2022. **10**(9): p. 2064.
186. Flemming, H.C. and J. Wingender, *The biofilm matrix.* Nat Rev Microbiol, 2010. **8**(9): p. 623-33.
187. Stewart, P.S., *Diffusion in biofilms.* J Bacteriol, 2003. **185**(5): p. 1485-91.
188. Sharma, S., et al., *Microbial Biofilm: A Review on Formation, Infection, Antibiotic Resistance, Control Measures, and Innovative Treatment.* Microorganisms, 2023. **11**(6): p. 1614.
189. Lewis, K., *Multidrug tolerance of biofilms and persister cells.* Curr Top Microbiol Immunol, 2008. **322**: p. 107-31.
190. Vega, N.M. and J. Gore, *Collective antibiotic resistance: mechanisms and implications.* Curr Opin Microbiol, 2014. **21**: p. 28-34.
191. Anderl, J.N., M.J. Franklin, and P.S. Stewart, *Role of antibiotic penetration limitation in Klebsiella pneumoniae biofilm resistance to ampicillin and ciprofloxacin.* Antimicrob Agents Chemother, 2000. **44**(7): p. 1818-24.
192. Bowler, L.L., et al., *Mature Pseudomonas aeruginosa biofilms prevail compared to young biofilms in the presence of ceftazidime.* Antimicrob Agents Chemother, 2012. **56**(9): p. 4976-9.
193. Ryder, V.J., I. Chopra, and A.J. O'Neill, *Increased mutability of Staphylococci in biofilms as a consequence of oxidative stress.* PLoS One, 2012. **7**(10): p. e47695.
194. Driffield, K., et al., *Increased mutability of Pseudomonas aeruginosa in biofilms.* J Antimicrob Chemother, 2008. **61**(5): p. 1053-6.
195. Conibear, T.C., S.L. Collins, and J.S. Webb, *Role of mutation in Pseudomonas aeruginosa biofilm development.* PLoS One, 2009. **4**(7): p. e6289.
196. Zhang, L. and T.F. Mah, *Involvement of a novel efflux system in biofilm-specific resistance to antibiotics.* J Bacteriol, 2008. **190**(13): p. 4447-52.
197. Chambers, J.R. and K. Sauer, *The MerR-like regulator BrlR impairs Pseudomonas aeruginosa biofilm tolerance to colistin by repressing PhoPQ.* J Bacteriol, 2013. **195**(20): p. 4678-88.
198. Molin, S. and T. Tolker-Nielsen, *Gene transfer occurs with enhanced efficiency in biofilms and induces enhanced stabilisation of the biofilm structure.* Curr Opin Biotechnol, 2003. **14**(3): p. 255-61.
199. Reisner, A., et al., *Synergistic effects in mixed Escherichia coli biofilms: conjugative plasmid transfer drives biofilm expansion.* J Bacteriol, 2006. **188**(10): p. 3582-8.

200. Hughes, D. and D.I. Andersson, *Selection of resistance at lethal and non-lethal antibiotic concentrations.* Curr Opin Microbiol, 2012. **15**(5): p. 555-60.
201. Lebeaux, D., J.M. Ghigo, and C. Beloin, *Biofilm-related infections: bridging the gap between clinical management and fundamental aspects of recalcitrance toward antibiotics.* Microbiol Mol Biol Rev, 2014. **78**(3): p. 510-43.
202. Niggli, S. and R. Kummerli, *Strain Background, Species Frequency, and Environmental Conditions Are Important in Determining Pseudomonas aeruginosa and Staphylococcus aureus Population Dynamics and Species Coexistence.* Appl Environ Microbiol, 2020. **86**(18): p. e00962-20.
203. Mashburn, L.M., et al., *Staphylococcus aureus serves as an iron source for Pseudomonas aeruginosa during in vivo coculture.* J Bacteriol, 2005. **187**(2): p. 554-66.
204. Ghssein, G. and Z. Ezzeddine, *A Review of Pseudomonas aeruginosa Metallophores: Pyoverdine, Pyochelin and Pseudopaline.* Biology (Basel), 2022. **11**(12): p. 1711.
205. Diggle, S.P., et al., *The Pseudomonas aeruginosa 4-quinolone signal molecules HHQ and PQS play multifunctional roles in quorum sensing and iron entrapment.* Chem Biol, 2007. **14**(1): p. 87-96.
206. Biswas, L. and F. Gotz, *Molecular Mechanisms of Staphylococcus and Pseudomonas Interactions in Cystic Fibrosis.* Front Cell Infect Microbiol, 2021. **11**: p. 824042.
207. Biswas, L., et al., *Small-colony variant selection as a survival strategy for Staphylococcus aureus in the presence of Pseudomonas aeruginosa.* Appl Environ Microbiol, 2009. **75**(21): p. 6910-2.
208. Hotterbeekx, A., et al., *In vivo and In vitro Interactions between Pseudomonas aeruginosa and Staphylococcus spp.* Front Cell Infect Microbiol, 2017. **7**: p. 106.
209. Korgaonkar, A.K. and M. Whiteley, *Pseudomonas aeruginosa enhances production of an antimicrobial in response to N-acetylglucosamine and peptidoglycan.* J Bacteriol, 2011. **193**(4): p. 909-17.
210. Kvich, L., et al., *Investigation of the Mechanism and Chemistry Underlying Staphylococcus aureus' Ability to Inhibit Pseudomonas aeruginosa Growth In Vitro.* J Bacteriol, 2022. **204**(11): p. e0017422.
211. Frydenlund Michelsen, C., et al., *Evolution of metabolic divergence in Pseudomonas aeruginosa during long-term infection facilitates a proto-cooperative interspecies interaction.* ISME J, 2016. **10**(6): p. 1323-36.
212. Radlinski, L., et al., *Pseudomonas aeruginosa exoproducts determine antibiotic efficacy against Staphylococcus aureus.* PLoS Biol, 2017. **15**(11): p. e2003981.

213. Barraza, J.P. and M. Whiteley, *A Pseudomonas aeruginosa Antimicrobial Affects the Biogeography but Not Fitness of Staphylococcus aureus during Coculture.* mBio, 2021. **12**(2): p. e00047-21.
214. Limoli, D.H., et al., *Pseudomonas aeruginosa Alginate Overproduction Promotes Coexistence with Staphylococcus aureus in a Model of Cystic Fibrosis Respiratory Infection.* mBio, 2017. **8**(2): p. e00186-17.
215. Price, C.E., et al., *Exogenous Alginate Protects Staphylococcus aureus from Killing by Pseudomonas aeruginosa.* J Bacteriol, 2020. **202**(8): p. e00559-19.
216. Barequet, I.S., et al., *Evaluation of Pseudomonas aeruginosa staphylolysin (LasA protease) in the treatment of methicillin-resistant Staphylococcus aureus endophthalmitis in a rat model.* Graefes Arch Clin Exp Ophthalmol, 2009. **247**(7): p. 913-7.
217. Tognon, M., et al., *Co-evolution with Staphylococcus aureus leads to lipopolysaccharide alterations in Pseudomonas aeruginosa.* ISME J, 2017. **11**(10): p. 2233-2243.
218. Michelsen, C.F., et al., *Staphylococcus aureus alters growth activity, autolysis, and antibiotic tolerance in a human host-adapted Pseudomonas aeruginosa lineage.* J Bacteriol, 2014. **196**(22): p. 3903-11.
219. Hogan, S., et al., *Potential use of targeted enzymatic agents in the treatment of Staphylococcus aureus biofilm-related infections.* J Hosp Infect, 2017. **96**(2): p. 177-182.
220. Little, D.J., et al., *PgaB orthologues contain a glycoside hydrolase domain that cleaves deacetylated poly-beta(1,6)-N-acetylglucosamine and can disrupt bacterial biofilms.* PLoS Pathog, 2018. **14**(4): p. e1006998.
221. Baker, P., et al., *Exopolysaccharide biosynthetic glycoside hydrolases can be utilized to disrupt and prevent Pseudomonas aeruginosa biofilms.* Sci Adv, 2016. **2**(5): p. e1501632.
222. Ebeling, W., et al., *Proteinase K from Tritirachium album Limber.* Eur J Biochem, 1974. **47**(1): p. 91-7.
223. Deusenbery, C., et al., *Synergy of Antibiotics and Antibiofilm Agents against Methicillin-Resistant Staphylococcus aureus Biofilms.* ACS Infect Dis, 2023. **9**(10): p. 1949-1963.
224. Banar, M., et al., *Evaluation of Mannosidase and Trypsin Enzymes Effects on Biofilm Production of Pseudomonas aeruginosa Isolated from Burn Wound Infections.* PLoS One, 2016. **11**(10): p. e0164622.
225. Mugita, N., et al., *Proteases, actinidin, papain and trypsin reduce oral biofilm on the tongue in elderly subjects and in vitro.* Arch Oral Biol, 2017. **82**: p. 233-240.
226. Wang, S., et al., *Strategy to combat biofilms: a focus on biofilm dispersal enzymes.* npj Biofilms and Microbiomes, 2023. **9**(1): p. 63.

227. Mechmechani, S., et al., *Pepsin and Trypsin Treatment Combined with Carvacrol: An Efficient Strategy to Fight Pseudomonas aeruginosa and Enterococcus faecalis Biofilms.* Microorganisms, 2023. **11**(1): p. 143.
228. Saggu, S.K., G. Jha, and P.C. Mishra, *Enzymatic Degradation of Biofilm by Metalloprotease From Microbacterium sp. SKS10.* Front Bioeng Biotechnol, 2019. **7**: p. 192.
229. Laarman, A.J., et al., *Staphylococcus aureus metalloprotease aureolysin cleaves complement C3 to mediate immune evasion.* J Immunol, 2011. **186**(11): p. 6445-53.
230. Loughran, A.J., et al., *Impact of individual extracellular proteases on Staphylococcus aureus biofilm formation in diverse clinical isolates and their isogenic sarA mutants.* Microbiologyopen, 2014. **3**(6): p. 897-909.
231. Mootz, J.M., et al., *Staphopains modulate Staphylococcus aureus biofilm integrity.* Infect Immun, 2013. **81**(9): p. 3227-38.
232. Shak, S., et al., *Recombinant human DNase I reduces the viscosity of cystic fibrosis sputum.* Proc Natl Acad Sci U S A, 1990. **87**(23): p. 9188-92.
233. Mayer-Hamblett, N., et al., *Discontinuation versus continuation of hypertonic saline or dornase alfa in modulator treated people with cystic fibrosis (SIMPLIFY): results from two parallel, multicentre, open-label, randomised, controlled, non-inferiority trials.* Lancet Respir Med, 2023. **11**(4): p. 329-340.
234. Donaldson, S.H., et al., *The effect of discontinuing hypertonic saline or dornase alfa on mucociliary clearance in elexacaftor/tezacaftor/ivacaftor treated people with cystic fibrosis: The SIMPLIFY-MCC Study.* J Cyst Fibros, 2024. **Feb13**: p. S1569-1993(24)00018-3.
235. Seper, A., et al., *Extracellular nucleases and extracellular DNA play important roles in Vibrio cholerae biofilm formation.* Mol Microbiol, 2011. **82**(4): p. 1015-37.
236. Basle, A., et al., *Crystal structure of NucB, a biofilm-degrading endonuclease.* Nucleic Acids Res, 2018. **46**(1): p. 473-484.
237. Shields, R.C., et al., *Efficacy of a marine bacterial nuclease against biofilm forming microorganisms isolated from chronic rhinosinusitis.* PLoS One, 2013. **8**(2): p. e55339.
238. Ofir, G. and R. Sorek, *Contemporary Phage Biology: From Classic Models to New Insights.* Cell, 2018. **172**(6): p. 1260-1270.
239. Summers, W.C., *The strange history of phage therapy.* Bacteriophage, 2012. **2**(2): p. 130-133.
240. Strathdee, S.A., et al., *Phage therapy: From biological mechanisms to future directions.* Cell, 2023. **186**(1): p. 17-31.
241. Chang, C., et al., *Bacteriophage-Mediated Control of Biofilm: A Promising New Dawn for the Future.* Front Microbiol, 2022. **13**: p. 825828.

242. Maffei, E., et al., *Phage Paride can kill dormant, antibiotic-tolerant cells of Pseudomonas aeruginosa by direct lytic replication.* Nat Commun, 2024. **15**(1): p. 175.
243. Fiscarelli, E.V., et al., *In Vitro Newly Isolated Environmental Phage Activity against Biofilms Preformed by Pseudomonas aeruginosa from Patients with Cystic Fibrosis.* Microorganisms, 2021. **9**(3): p. 478.
244. Lusiak-Szelachowska, M., B. Weber-Dabrowska, and A. Gorski, *Bacteriophages and Lysins in Biofilm Control.* Virol Sin, 2020. **35**(2): p. 125-133.
245. Mishra, S., et al., *Therapeutic Strategies against Biofilm Infections.* Life (Basel), 2023. **13**(1): p. 172.
246. Hu, X., et al., *Antimicrobial Photodynamic Therapy to Control Clinically Relevant Biofilm Infections.* Front Microbiol, 2018. **9**: p. 1299.
247. Asfour, H.Z., *Anti-Quorum Sensing Natural Compounds.* J Microsc Ultrastruct, 2018. **6**(1): p. 1-10.
248. Paluch, E., et al., *Prevention of biofilm formation by quorum quenching.* Appl Microbiol Biotechnol, 2020. **104**(5): p. 1871-1881.
249. Shahverdi, A.R., et al., *Synthesis and effect of silver nanoparticles on the antibacterial activity of different antibiotics against Staphylococcus aureus and Escherichia coli.* Nanomedicine, 2007. **3**(2): p. 168-71.
250. Caly, D.L., et al., *Targeting cyclic di-GMP signalling: a strategy to control biofilm formation?* Curr Pharm Des, 2015. **21**(1): p. 12-24.
251. Rouillard, K.R., et al., *Exogenous Nitric Oxide Improves Antibiotic Susceptibility in Resistant Bacteria.* ACS Infect Dis, 2021. **7**(1): p. 23-33.
252. Martin, I., V. Waters, and H. Grasemann, *Approaches to Targeting Bacterial Biofilms in Cystic Fibrosis Airways.* Int J Mol Sci, 2021. **22**(4): p. 2155.
253. Ratjen, F., et al., *Cystic fibrosis.* Nat Rev Dis Primers, 2015. **1**: p. 15010.
254. Shteinberg, M., et al., *Cystic fibrosis.* Lancet, 2021. **397**(10290): p. 2195-2211.
255. Woods, P.W., et al., *Maintenance of S. aureus in Co-culture With P. aeruginosa While Growing as Biofilms.* Front Microbiol, 2018. **9**: p. 3291.
256. Filkins, L.M., et al., *Coculture of Staphylococcus aureus with Pseudomonas aeruginosa drives S. aureus towards fermentative metabolism and reduced viability in a cystic fibrosis model.* Journal of bacteriology, 2015. **197**(14): p. 2252-2264.
257. Orazi, G., K.L. Ruoff, and G.A. O'Toole, *Pseudomonas aeruginosa Increases the Sensitivity of Biofilm-Grown Staphylococcus aureus to Membrane-Targeting Antiseptics and Antibiotics.* mBio, 2019. **10**(4): p. e01501-19.

258. Fischer, A.J., et al., *Sustained Coinfections with Staphylococcus aureus and Pseudomonas aeruginosa in Cystic Fibrosis.* Am J Respir Crit Care Med, 2021. **203**(3): p. 328-338.
259. Jean-Pierre, V., et al., *Biofilm Formation by Staphylococcus aureus in the Specific Context of Cystic Fibrosis.* Int J Mol Sci, 2022. **24**(1): p. 597.
260. Boudet, A., et al., *Biofilm Formation in Methicillin-Resistant Staphylococcus aureus Isolated in Cystic Fibrosis Patients Is Strain-Dependent and Differentially Influenced by Antibiotics.* Front Microbiol, 2021. **12**: p. 750489.
261. Ferguson, D.L., et al., *Extracellular DNA enhances biofilm integrity and mechanical properties of mucoid Pseudomonas aeruginosa.* J Bacteriol, 2023. **205**(10): p. e0023823.
262. Liang, Z., et al., *The role of individual exopolysaccharides in antibiotic tolerance of Pseudomonas aeruginosa aggregates.* Front Microbiol, 2023. **14**: p. 1187708.
263. Camus, L., et al., *Mixed Populations and Co-Infection: Pseudomonas aeruginosa and Staphylococcus aureus.* Adv Exp Med Biol, 2022. **1386**: p. 397-424.
264. Limoli, D.H. and L.R. Hoffman, *Help, hinder, hide and harm: what can we learn from the interactions between Pseudomonas aeruginosa and Staphylococcus aureus during respiratory infections?* Thorax, 2019. **74**(7): p. 684-692.
265. Limoli, D.H., et al., *Staphylococcus aureus and Pseudomonas aeruginosa co-infection is associated with cystic fibrosis-related diabetes and poor clinical outcomes.* European Journal of Clinical Microbiology & Infectious Diseases, 2016. **35**(6): p. 947-953.
266. Briaud, P., et al., *Impact of Coexistence Phenotype Between Staphylococcus aureus and Pseudomonas aeruginosa Isolates on Clinical Outcomes Among Cystic Fibrosis Patients.* Front Cell Infect Microbiol, 2020. **10**: p. 266.
267. Orazi, G. and G.A. O'Toole, *Pseudomonas aeruginosa alters Staphylococcus aureus sensitivity to vancomycin in a biofilm model of cystic fibrosis infection.* MBio, 2017. **8**(4): p. e00873-17.
268. Magalhaes, A.P., S.P. Lopes, and M.O. Pereira, *Insights into Cystic Fibrosis Polymicrobial Consortia: The Role of Species Interactions in Biofilm Development, Phenotype, and Response to In-Use Antibiotics.* Front Microbiol, 2016. **7**: p. 2146.
269. Magalhaes, A.P., et al., *Viable but non-cultivable state: a strategy for Staphylococcus aureus survivable in dual-species biofilms with Pseudomonas aeruginosa?* Environ Microbiol, 2021. **23**(9): p. 5639-5649.
270. Chew, S.C., et al., *Matrix Polysaccharides and SiaD Diguanylate Cyclase Alter Community Structure and Competitiveness of Pseudomonas*

aeruginosa during Dual-Species Biofilm Development with Staphylococcus aureus. mBio, 2018. **9**(6): p. e00585-18.
271. Yang, L., et al., *Pattern differentiation in co-culture biofilms formed by Staphylococcus aureus and Pseudomonas aeruginosa.* FEMS Immunol Med Microbiol, 2011. **62**(3): p. 339-47.
272. Camus, L., et al., *How Bacterial Adaptation to Cystic Fibrosis Environment Shapes Interactions Between Pseudomonas aeruginosa and Staphylococcus aureus.* Front Microbiol, 2021. **12**: p. 617784.
273. Planet, P.J., *Adaptation and Evolution of Pathogens in the Cystic Fibrosis Lung.* J Pediatric Infect Dis Soc, 2022. **11**(Supplement_2): p. S23-S31.
274. Vyas, H.K.N., B. Xia, and A. Mai-Prochnow, *Clinically relevant in vitro biofilm models: A need to mimic and recapitulate the host environment.* Biofilm, 2022. **4**: p. 100069.
275. Diaz Iglesias, Y., et al., *Activity of Antibiotics against Staphylococcus aureus in an In Vitro Model of Biofilms in the Context of Cystic Fibrosis: Influence of the Culture Medium.* Antimicrob Agents Chemother, 2019. **63**(7): p. e00602-19.
276. Alves, P.M., et al., *Interaction between Staphylococcus aureus and Pseudomonas aeruginosa is beneficial for colonisation and pathogenicity in a mixed biofilm.* Pathog Dis, 2018. **76**(1): p. fty003.
277. Ruiz-Sorribas, A., et al., *In vitro polymicrobial inter-kingdom three-species biofilm model: influence of hyphae on biofilm formation and bacterial physiology.* Biofouling, 2021: p. 1-13.
278. Kempf, V.A., K. Trebesius, and I.B. Autenrieth, *Fluorescent in situ hybridization allows rapid identification of microorganisms in blood cultures.* Journal of clinical microbiology, 2000. **38**(2): p. 830-838.
279. Hogardt, M., et al., *Specific and rapid detection by fluorescent in situ hybridization of bacteria in clinical samples obtained from cystic fibrosis patients.* Journal of clinical microbiology, 2000. **38**(2): p. 818-825.
280. Livak, K.J. and T.D. Schmittgen, *Analysis of relative gene expression data using real-time quantitative PCR and the 2− ΔΔCT method.* methods, 2001. **25**(4): p. 402-408.
281. Neve, R.L., B.D. Carrillo, and V.V. Phelan, *Impact of Artificial Sputum Medium Formulation on Pseudomonas aeruginosa Secondary Metabolite Production.* J Bacteriol, 2021. **203**(21): p. e0025021.
282. Pluskal, T., et al., *MZmine 2: modular framework for processing, visualizing, and analyzing mass spectrometry-based molecular profile data.* BMC Bioinformatics, 2010. **11**: p. 395.
283. Sumner, L.W., et al., *Proposed minimum reporting standards for chemical analysis Chemical Analysis Working Group (CAWG) Metabolomics Standards Initiative (MSI).* Metabolomics, 2007. **3**(3): p. 211-221.

284. Moree, W.J., et al., *Interkingdom metabolic transformations captured by microbial imaging mass spectrometry.* Proc Natl Acad Sci U S A, 2012. **109**(34): p. 13811-6.
285. Lepine, F., et al., *Electrospray/mass spectrometric identification and analysis of 4-hydroxy-2-alkylquinolines (HAQs) produced by Pseudomonas aeruginosa.* J Am Soc Mass Spectrom, 2004. **15**(6): p. 862-9.
286. Wang, M., et al., *Sharing and community curation of mass spectrometry data with Global Natural Products Social Molecular Networking.* Nat Biotechnol, 2016. **34**(8): p. 828-837.
287. Petras, D., et al., *GNPS Dashboard: collaborative exploration of mass spectrometry data in the web browser.* Nat Methods, 2022. **19**(2): p. 134-136.
288. Xia, J., et al., *MetaboAnalyst: a web server for metabolomic data analysis and interpretation.* Nucleic Acids Res, 2009. **37**(Web Server issue): p. W652-60.
289. Diaz Iglesias, Y. and F. Van Bambeke, *Activity of Antibiotics against Pseudomonas aeruginosa in an In Vitro Model of Biofilms in the Context of Cystic Fibrosis: Influence of the Culture Medium.* Antimicrob Agents Chemother, 2020. **64**(4): p. e02204-19.
290. Imperi, F., et al., *New life for an old drug: the anthelmintic drug niclosamide inhibits Pseudomonas aeruginosa quorum sensing.* Antimicrob Agents Chemother, 2013. **57**(2): p. 996-1005.
291. Pollitt, E.J., S.A. Crusz, and S.P. Diggle, *Staphylococcus aureus forms spreading dendrites that have characteristics of active motility.* Sci Rep, 2015. **5**: p. 17698.
292. Noto, M.J., et al., *Mechanisms of Pyocyanin Toxicity and Genetic Determinants of Resistance in Staphylococcus aureus.* J Bacteriol, 2017. **199**(17): p. e00221-17.
293. Yehia, F.A.A., N. Yousef, and M. Askoura, *Celastrol mitigates staphyloxanthin biosynthesis and biofilm formation in Staphylococcus aureus via targeting key regulators of virulence; in vitro and in vivo approach.* BMC Microbiol, 2022. **22**(1): p. 106.
294. Buonocore, C., et al., *Evaluation of Antimicrobial Properties and Potential Applications of Pseudomonas gessardii M15 Rhamnolipids towards Multiresistant Staphylococcus aureus.* Pharmaceutics, 2023. **15**(2): p. 700.
295. Machan, Z.A., et al., *2-Heptyl-4-hydroxyquinoline N-oxide, an antistaphylococcal agent produced by Pseudomonas aeruginosa.* Journal of Antimicrobial Chemotherapy, 1992. **30**(5): p. 615-623.
296. Nguyen, A.T. and A.G. Oglesby-Sherrouse, *Interactions between Pseudomonas aeruginosa and Staphylococcus aureus during co-*

cultivations and polymicrobial infections. Appl Microbiol Biotechnol, 2016. **100**(14): p. 6141-6148.
297. Pollitt, E.J. and S.P. Diggle, *Defining motility in the Staphylococci.* Cellular and Molecular Life Sciences, 2017. **74**: p. 2943-2958.
298. Ammann, C.G., et al., *Pseudomonas aeruginosa outcompetes other bacteria in the manifestation and maintenance of a biofilm in polyvinylchloride tubing as used in dental devices.* Archives of Microbiology, 2016. **198**(4): p. 389-391.
299. Baldan, R., et al., *Adaptation of Pseudomonas aeruginosa in Cystic Fibrosis airways influences virulence of Staphylococcus aureus in vitro and murine models of co-infection.* PLoS One, 2014. **9**(3): p. e89614.
300. Pernet, E., et al., *Pseudomonas aeruginosa eradicates Staphylococcus aureus by manipulating the host immunity.* Nat Commun, 2014. **5**: p. 5105.
301. Cendra, M.d.M., et al., *Optimal environmental and culture conditions allow the in vitro coexistence of Pseudomonas aeruginosa and Staphylococcus aureus in stable biofilms.* Scientific reports, 2019. **9**(1): p. 1-17.
302. Tognon, M., et al., *Transcriptional profiling of Pseudomonas aeruginosa and Staphylococcus aureus during in vitro co-culture.* BMC Genomics, 2019. **20**(1): p. 30.
303. Limoli, D.H., et al., *Interspecies interactions induce exploratory motility in Pseudomonas aeruginosa.* Elife, 2019. **8**: p. e47365.
304. Kamer, A.M.A., et al., *Antibacterial, antibiofilm, and anti-quorum sensing activities of pyocyanin against methicillin-resistant Staphylococcus aureus: in vitro and in vivo study.* BMC Microbiol, 2023. **23**(1): p. 116.
305. Armbruster, C.R., et al., *Staphylococcus aureus protein A mediates interspecies interactions at the cell surface of Pseudomonas aeruginosa.* MBio, 2016. **7**(3): p. e00538-16.
306. Samad, T., et al., *Swimming bacteria promote dispersal of non-motile staphylococcal species.* Isme j, 2017. **11**(8): p. 1933-1937.
307. Worlitzsch, D., et al., *Reduced oxygen concentrations in airway mucus contribute to the early and late pathogenesis of Pseudomonas aeruginosa cystic fibrosis airway infection.* J Clin Invest, 2002. **109**: p. 317-325.
308. Vasiljevs, S., A. Gupta, and D. Baines, *Effect of glucose on growth and co-culture of Staphylococcus aureus and Pseudomonas aeruginosa in artificial sputum medium.* Heliyon, 2023. **9**(11): p. e21469.
309. Savli, H., et al., *Expression stability of six housekeeping genes: A proposal for resistance gene quantification studies of Pseudomonas aeruginosa by real-time quantitative RT-PCR.* J Med Microbiol, 2003. **52**(Pt 5): p. 403-408.
310. Camus, L., et al., *Trophic cooperation promotes bacterial survival of Staphylococcus aureus and Pseudomonas aeruginosa.* ISME J, 2020. **14**(12): p. 3093-3105.

311. Fu, T., et al., *ArcR contributes to tolerance to fluoroquinolone antibiotics by regulating katA in Staphylococcus aureus.* Front Microbiol, 2023. **14**: p. 1106340.
312. Chmiel, J.F. and P.B. Davis, *State of the art: why do the lungs of patients with cystic fibrosis become infected and why can't they clear the infection?* Respir Res, 2003. **4**(1): p. 8.
313. Donlan, R.M. and J.W. Costerton, *Biofilms: survival mechanisms of clinically relevant microorganisms.* Clin Microbiol Rev, 2002. **15**(2): p. 167-93.
314. Ciofu, O., et al., *Tolerance and resistance of microbial biofilms.* Nature Reviews Microbiology, 2022. **20**(10): p. 621-635.
315. Hunt, B.E., et al., *Macromolecular mechanisms of sputum inhibition of tobramycin activity.* Antimicrobial Agents and Chemotherapy, 1995. **39**(1): p. 34-39.
316. Wilton, M., et al., *Extracellular DNA Acidifies Biofilms and Induces Aminoglycoside Resistance in Pseudomonas aeruginosa.* Antimicrob Agents Chemother, 2016. **60**(1): p. 544-53.
317. Beaudoin, T., et al., *Staphylococcus aureus interaction with Pseudomonas aeruginosa biofilm enhances tobramycin resistance.* NPJ Biofilms Microbiomes, 2017. **3**: p. 25.
318. Wille, J. and T. Coenye, *Biofilm dispersion: The key to biofilm eradication or opening Pandora's box?* Biofilm, 2020. **2**: p. 100027.
319. Rouillard, K.R., et al., *Effects of Mucin and DNA Concentrations in Airway Mucus on Pseudomonas aeruginosa Biofilm Recalcitrance.* mSphere, 2022. **7**(4): p. e00291-22.
320. Mrsny, R.J., et al., *Addition of a bacterial alginate lyase to purulent CF sputum in vitro can result in the disruption of alginate and modification of sputum viscoelasticity.* Pulm Pharmacol, 1994. **7**(6): p. 357-66.
321. Yang, Y., et al., *Inhalable Antibiotic Delivery Using a Dry Powder Co-delivering Recombinant Deoxyribonuclease and Ciprofloxacin for Treatment of Cystic Fibrosis.* Pharmaceutical Research, 2010. **27**(1): p. 151-160.
322. Aitken, M.L., *Clinical trials of recombinant human DNase in cystic fibrosis patients.* Monaldi Arch Chest Dis, 1993. **48**(6): p. 653-6.
323. Okshevsky, M. and R.L. Meyer, *Evaluation of fluorescent stains for visualizing extracellular DNA in biofilms.* J Microbiol Methods, 2014. **105**: p. 102-4.
324. Peterson, B.W., et al., *Visualization of microbiological processes underlying stress relaxation in Pseudomonas aeruginosa biofilms.* Microsc Microanal, 2014. **20**(3): p. 912-5.

325. Guichard, M.J., et al., *Impact of PEGylation on the mucolytic activity of recombinant human deoxyribonuclease I in cystic fibrosis sputum.* Clin Sci (Lond), 2018. **132**(13): p. 1439-1452.
326. Das, T., et al., *Role of Pyocyanin and Extracellular DNA in Facilitating Pseudomonas aeruginosa Biofilm Formation*, in *Microbial Biofilms - Importance and Applications*. 2016.
327. Rouillard, K.R., et al., *Altering the viscoelastic properties of mucus-grown Pseudomonas aeruginosa biofilms affects antibiotic susceptibility.* Biofilm, 2023. **5**: p. 100104.
328. Serisier, D.J., et al., *Macrorheology of cystic fibrosis, chronic obstructive pulmonary disease & normal sputum.* Respir Res, 2009. **10**(1): p. 63.
329. Bos, A.C., et al., *Patient-specific modelling of regional tobramycin concentration levels in airways of patients with cystic fibrosis: can we dose once daily?* J Antimicrob Chemother, 2017. **72**(12): p. 3435-3442.
330. Fish, D.N. and T.J. Singletary, *Meropenem, a new carbapenem antibiotic.* Pharmacotherapy, 1997. **17**(4): p. 644-69.
331. Alkawash, M.A., J.S. Soothill, and N.L. Schiller, *Alginate lyase enhances antibiotic killing of mucoid Pseudomonas aeruginosa in biofilms.* APMIS, 2006. **114**(2): p. 131-8.
332. Kaplan, J.B., et al., *Recombinant human DNase I decreases biofilm and increases antimicrobial susceptibility in staphylococci.* J Antibiot (Tokyo), 2012. **65**(2): p. 73-7.
333. Bennett, W.D., *Controlled inhalation of aerosolised therapeutics.* Expert Opin Drug Deliv, 2005. **2**(4): p. 763-7.
334. Thornton, C.S. and M.D. Parkins, *Microbial Epidemiology of the Cystic Fibrosis Airways: Past, Present, and Future.* Semin Respir Crit Care Med, 2023. **44**(2): p. 269-286.
335. Saussereau, E., et al., *Effectiveness of bacteriophages in the sputum of cystic fibrosis patients.* Clin Microbiol Infect, 2014. **20**(12): p. O983-90.
336. Chang, R.Y.K., et al., *Bacteriophage PEV20 and Ciprofloxacin Combination Treatment Enhances Removal of Pseudomonas aeruginosa Biofilm Isolated from Cystic Fibrosis and Wound Patients.* AAPS J, 2019. **21**(3): p. 49.
337. Martin, I., et al., *Lytic Bacteriophage Is a Promising Adjunct to Common Antibiotics across Cystic Fibrosis Clinical Strains and Culture Models of Pseudomonas aeruginosa Infection.* Antibiotics (Basel), 2023. **12**(3): p. 593.
338. Ling, K.M., S.M. Stick, and A. Kicic, *Pulmonary bacteriophage and cystic fibrosis airway mucus: friends or foes?* Front Med (Lausanne), 2023. **10**: p. 1088494.

339. Vandersteegen, K., et al., *Microbiological and molecular assessment of bacteriophage ISP for the control of Staphylococcus aureus.* PLoS One, 2011. **6**(9): p. e24418.
340. De Soir, S., et al., *Exploiting phage-antibiotic synergies to disrupt Pseudomonas aeruginosa PAO1 biofilms in the context of orthopedic infections.* Microbiol Spectr, 2023: p. e0321923.
341. Vandersteegen, K., et al., *Romulus and Remus, two phage isolates representing a distinct clade within the Twortlikevirus genus, display suitable properties for phage therapy applications.* J Virol, 2013. **87**(6): p. 3237-47.
342. Van Nieuwenhuyse, B., et al., *A Case of In Situ Phage Therapy against Staphylococcus aureus in a Bone Allograft Polymicrobial Biofilm Infection: Outcomes and Phage-Antibiotic Interactions.* Viruses, 2021. **13**(10): p. 1898.
343. Uyttebroek, S., et al., *Stability of magistral phage preparations before therapeutic application in patients with chronic rhinosinusitis, sepsis, pulmonary, and musculoskeletal infections.* Microbiol Spectr, 2023. **11**(6): p. e0290723.
344. Henry, M., et al., *Development of a high throughput assay for indirectly measuring phage growth using the OmniLog(TM) system.* Bacteriophage, 2012. **2**(3): p. 159-167.
345. Trizna, E.Y., et al., *Bidirectional alterations in antibiotics susceptibility in Staphylococcus aureus-Pseudomonas aeruginosa dual-species biofilm.* Sci Rep, 2020. **10**(1): p. 14849.
346. Barr, J.J., et al., *Subdiffusive motion of bacteriophage in mucosal surfaces increases the frequency of bacterial encounters.* Proc Natl Acad Sci U S A, 2015. **112**(44): p. 13675-80.
347. Green, S.I., et al., *Targeting of Mammalian Glycans Enhances Phage Predation in the Gastrointestinal Tract.* mBio, 2021. **12**(1): p. e03474-20.
348. Shinde, P., N. Stamatos, and J.B. Doub, *Human Plasma Significantly Reduces Bacteriophage Infectivity Against Staphylococcus aureus Clinical Isolates.* Cureus, 2022. **14**(4): p. e23777.
349. Melo, L.D.R., et al., *The Protective Effect of Staphylococcus epidermidis Biofilm Matrix against Phage Predation.* Viruses, 2020. **12**(10): p. 1076.
350. Akturk, E., et al., *Combining phages and antibiotic to enhance antibiofilm efficacy against an in vitro dual species wound biofilm.* Biofilm, 2023. **6**: p. 100147.
351. Meneses, L., et al., *A systematic review of the use of bacteriophages for in vitro biofilm control.* Eur J Clin Microbiol Infect Dis, 2023. **42**(8): p. 919-928.
352. Suh, G.A., et al., *Considerations for the Use of Phage Therapy in Clinical Practice.* Antimicrob Agents Chemother, 2022. **66**(3): p. e0207121.

353. Lindgren, N.R., et al., *Nontypeable Haemophilus influenzae Infection Impedes Pseudomonas aeruginosa Colonization and Persistence in Mouse Respiratory Tract.* Infect Immun, 2022. **90**(2): p. e0056821.
354. Gannon, A.D. and S.E. Darch, *Same Game, Different Players: Emerging Pathogens of the CF Lung.* mBio, 2021. **12**(1): p. e01217-20.
355. Zhao, J. and W. Yu, *Interaction between Pseudomonas aeruginosa and Aspergillus fumigatus in cystic fibrosis.* PeerJ, 2018. **6**: p. e5931.
356. Song, B. and L.G. Leff, *Influence of magnesium ions on biofilm formation by Pseudomonas fluorescens.* Microbiol Res, 2006. **161**(4): p. 355-61.
357. Labrie, S.J., J.E. Samson, and S. Moineau, *Bacteriophage resistance mechanisms.* Nat Rev Microbiol, 2010. **8**(5): p. 317-27.
358. Aiyer, A. and J. Manos, *The Use of Artificial Sputum Media to Enhance Investigation and Subsequent Treatment of Cystic Fibrosis Bacterial Infections.* Microorganisms, 2022. **10**(7): p. 1269.
359. Lin, Q., J.M. Pilewski, and Y.P. Di, *Acidic Microenvironment Determines Antibiotic Susceptibility and Biofilm Formation of Pseudomonas aeruginosa.* Front Microbiol, 2021. **12**: p. 747834.
360. Schneider, E.L. and S.S. Shorr, *Alteration in cellular RNAs during the in vitro lifespan of cultured human diploid fibroblasts.* Cell, 1975. **6**(2): p. 179-84.
361. Borriello, G., et al., *Oxygen limitation contributes to antibiotic tolerance of Pseudomonas aeruginosa in biofilms.* Antimicrob Agents Chemother, 2004. **48**(7): p. 2659-64.
362. Pallett, R., et al., *Anaerobiosis influences virulence properties of Pseudomonas aeruginosa cystic fibrosis isolates and the interaction with Staphylococcus aureus.* Sci Rep, 2019. **9**(1): p. 6748.
363. Reigada, I., et al., *Surfaceome and Exoproteome Dynamics in Dual-Species Pseudomonas aeruginosa and Staphylococcus aureus Biofilms.* Front Microbiol, 2021. **12**: p. 672975.
364. Carroll, W., et al., *Detection of volatile compounds emitted by Pseudomonas aeruginosa using selected ion flow tube mass spectrometry.* Pediatr Pulmonol, 2005. **39**(5): p. 452-6.
365. Letoffe, S., et al., *Pseudomonas aeruginosa Production of Hydrogen Cyanide Leads to Airborne Control of Staphylococcus aureus Growth in Biofilm and In Vivo Lung Environments.* mBio, 2022. **13**(5): p. e0215422.
366. Smith, D., et al., *Hydrogen cyanide, a volatile biomarker of Pseudomonas aeruginosa infection.* J Breath Res, 2013. **7**(4): p. 044001.
367. Vandeplassche, E., T. Coenye, and A. Crabbe, *Developing selective media for quantification of multispecies biofilms following antibiotic treatment.* PLoS One, 2017. **12**(11): p. e0187540.

368. Moreau-Marquis, S., et al., *Co-culture models of Pseudomonas aeruginosa biofilms grown on live human airway cells.* J Vis Exp, 2010(44): p. 2186.
369. Anderson, G.G., et al., *In vitro analysis of tobramycin-treated Pseudomonas aeruginosa biofilms on cystic fibrosis-derived airway epithelial cells.* Infect Immun, 2008. **76**(4): p. 1423-33.
370. Kiedrowski, M.R., et al., *Staphylococcus aureus Biofilm Growth on Cystic Fibrosis Airway Epithelial Cells Is Enhanced during Respiratory Syncytial Virus Coinfection.* mSphere, 2018. **3**(4): p. e00341-18.
371. Wijers, C.D., R. Vagedes, and C. Weingart, *A novel method for investigating Burkholderia cenocepacia infections in patients with cystic fibrosis and other chronic diseases of the airways.* BMC Microbiol, 2016. **16**(1): p. 200.
372. Kirchner, S., et al., *Use of artificial sputum medium to test antibiotic efficacy against Pseudomonas aeruginosa in conditions more relevant to the cystic fibrosis lung.* J Vis Exp, 2012(64): p. e3857.
373. Abd-Allah, I.M., et al., *An Anti-MRSA Phage From Raw Fish Rinse: Stability Evaluation and Production Optimization.* Front Cell Infect Microbiol, 2022. **12**: p. 904531.
374. Kohler, T., et al., *Personalized aerosolised bacteriophage treatment of a chronic lung infection due to multidrug-resistant Pseudomonas aeruginosa.* Nat Commun, 2023. **14**(1): p. 3629.
375. Jorgensen, N.P., et al., *Rifampicin-containing combinations are superior to combinations of vancomycin, linezolid and daptomycin against Staphylococcus aureus biofilm infection in vivo and in vitro.* Pathog Dis, 2016. **74**(4): p. ftw019.
376. Kapoor, P. and P. Murphy, *Combination antibiotics against Pseudomonas aeruginosa, representing common and rare cystic fibrosis strains from different Irish clinics.* Heliyon, 2018. **4**(3): p. e00562.
377. Mugunthan, S., et al., *RNA is a key component of extracellular DNA networks in Pseudomonas aeruginosa biofilms.* Nat Commun, 2023. **14**(1): p. 7772.